

# **BENCH-SCALE TESTING OF THE MULTI-GRAVITY SEPARATOR IN COMBINATION WITH MICROCEL™**

## **FINAL REPORT**

Contract No.: DE-AC22-92PC92205

by

Gerald H. Luttrell, Parthasarathy Venkatraman, Dennis I. Phillips, and Roe-Hoan Yoon

Center for Coal and Minerals Processing  
Virginia Polytechnic Institute and State University  
146 Holden Hall  
Blacksburg, Virginia 24061-0258

Prepared for:

U.S. Department of Energy  
Pittsburgh Energy Technology Center  
P.O. Box 10940  
Pittsburgh, Pennsylvania 15236-0940

Contracting Officer's Representative: Carl Maronde

March 1995

U.S./DOE Patent Clearance is not required prior to the publication of this document. This report complies with the contract terms and conditions and fulfills the requirements thereof.



**CLEARED BY  
PATENT COUNSEL**

DOE/PC/92205--T7

## BENCH-SCALE TESTING OF THE MULTI-GRAVITY SEPARATOR IN COMBINATION WITH MICROCEL

Contract No: DE-AC22-92PC92205

### Final Report

#### Prime Contractor:

Center for Coal and Minerals Processing  
Virginia Polytechnic Institute and State University  
Blacksburg, Virginia 24061-0258

#### Subcontractors:

Carpco, Inc.  
Roberts & Schaefer Company  
Consolidation Coal Company  
Kerr-McGee Coal Corporation

#### Prepared for:

Pittsburgh Energy Technology Center  
U.S. Department of Energy  
P.O. Box 10940  
Pittsburgh, Pennsylvania 15236

March 1995

Contracting Officer's Representative: Carl Maronde

U.S./DOE Patent Clearance is not required prior to the publication of this document.  
This report complies with the contract terms and conditions and fulfills the requirements thereof.

DISTRIBUTION OF THIS DOCUMENT IS UNLIMITED

*nm*

MASTER

---

## **DISCLAIMER**

This report was prepared as an account of work sponsored by an agency of the United States Government. Neither the United States Government nor any agency thereof, nor any of their employees, makes any warranty, express or implied, or assumes any legal liability or responsibility for the accuracy, completeness, or usefulness or any information, apparatus, product or process disclosed, or represents that its use would not infringe privately owned rights. Reference herein to any specific commercial product, process, or service by trade name, trademark, manufacturer, or otherwise does not necessarily constitute or imply its endorsement, recommendation, or favoring by the United States Government or any agency thereof. The views and opinions of the authors expressed therein do not necessarily state or reflect those of the United States Government or any agency thereof.

---

## **DISCLAIMER**

**Portions of this document may be illegible  
in electronic image products. Images are  
produced from the best available original  
document.**

## EXECUTIVE SUMMARY

The costs of cleaning and dewatering fine coal are substantially higher than those of coarse coal. Because of this problem, many plants relegate the fines fraction and portions thereof to refuse or waste ponds. It is estimated that up to 2.8 billion tons of coal fines have been deposited in the ponds in the U.S. and 20 to 30 million tons of fresh refuse are still being discarded annually. This situation represents a significant loss of valuable national resources and loss of coals that have already been mined at high costs, and creates environmental problems. In order to address these problems, particularly concerning the difficulty in removing sulfur, the U.S. Department of Energy has sponsored the development of various advanced coal cleaning technologies, e.g., oil agglomeration, column flotation, chemical cleaning, microbial cleaning, etc., of which column flotation has been gaining acceptance in industry.

Column flotation is now in commercial use for removing ash-forming minerals from fine coal. However, this technology has difficulties in removing sulfur-containing minerals such as pyrite. According to the release analysis tests conducted on many high-sulfur coals, the sulfur rejection is substantially less than predicted by washability tests. It is generally believed that release analysis represents the best possible flotation results, while washability gives the best possible results obtainable by density-based separation. There are two reasons for the difficulty in removing pyritic sulfur from coal by flotation. First, middling particles containing both coal and pyrite show considerable floatability and report to froth products, resulting in the contamination of the clean coal products. Second, even the pyrite particles free of coal inclusions acquire hydrophobicity when superficially oxidized and, hence, report to the froth. Various reagents have been tested to solve these problems, but there have been no practicable solutions found to date. The difficulty in separating pyrite is not unique to flotation. Any other separation process exploiting the differences in the surface chemical properties of coal and pyrite face the same difficulty.

The fact that washability tests show better pyritic sulfur rejection potential than release analyses suggests that gravity separation should be better than flotation at rejecting pyritic sulfur. However, gravity separation is difficult with fine particles because of the very slow settling velocities and the wide range of particle sizes involved in usual flotation feeds. Nevertheless, there are new developments in the minerals industry where fine particle separation is enhanced by using strong centrifugal fields rather than the gravitational field alone. Several enhanced gravity separators are in commercial use in the minerals industry. These include, among others, the Multi-Gravity Separator (MGS), Falcon Concentrator, Knelson Concentrator, and Kelsey Jig. Laboratory-scale test work conducted on coal using some of these new devices showed promising results in removing pyrite; however, some are not as efficient as flotation in removing ash-forming minerals.

It was the purpose of this investigation to test a new fine coal cleaning system, in which a coal is cleaned first by column flotation to remove primarily ash-forming minerals and then by an enhanced gravity separation technique to remove the pyrite remaining in the flotation product. Of the various column flotation technologies developed under the auspices of the U.S. Department of Energy, the

Microcel™ flotation column was chosen because it is being used commercially in the U.S. coal industry, particularly by low-sulfur coal producers. Of the various enhanced gravity separation technologies used in minerals industry, MGS was chosen because it shows promise for pyrite rejection from fine coal streams containing a wide range of particle sizes. It is possible, however, that a combination of other column flotation and enhanced gravity separation devices can be used for the same purpose. Therefore, the use of Microcel™ and MGS in this project does not necessarily represent the best possible combination.

Two high-sulfur coals, namely Pittsburgh No. 8 and Illinois No. 6 seam coals, were tested at the bench scale at feed rates of 300 to 600 lb/hr. All the tests were conducted at the Coal Preparation Process Research Facility, Pittsburgh Energy Technology Center, U.S. Department of Energy. Run-of-mine (ROM) coal samples crushed to different sizes were used as feeds for the bench-scale tests. Effects of different circuit configurations, coal top size, feed rate, pulp density, and various other operating parameters were investigated.

The bench-scale tests were conducted using three different circuit configurations, i.e., i) Microcel™ column alone, ii) MGS alone, and iii) Microcel™ and MGS in series. In general, high ash-rejections were achieved using Microcel™ alone with both the Pittsburgh and Illinois No. 6 coals; however, this circuit produced poor sulfur rejections. On the other hand, the results obtained using MGS alone showed excellent pyritic sulfur rejections but with poor ash rejections. When using a Microcel™ column and an MGS unit in series, both the ash and pyritic sulfur rejections exceeded what can be achieved using either the Microcel™ column or the MGS unit alone, demonstrating a synergistic effect.

The test results obtained under various operating conditions were compared on the basis of separation efficiency. The best results were obtained using the combined Microcel™ column/MGS circuit. With the ROM Pittsburgh coal (-48 mesh) assaying 21.4% ash and 1.64% pyritic sulfur, a clean coal product with 5.6% ash and 0.41% pyritic sulfur was obtained. The combustible recovery was 89.2%, and the pyritic sulfur rejection was 81.4%. Using the Microcel™ column alone, the pyritic sulfur content was reduced to 0.78%, representing a 34.0% pyritic sulfur rejection. Thus, the pyritic sulfur rejection was improved by 139% due to the use of an enhanced gravity separator. With the MGS alone, the pyritic sulfur was reduced to 0.49%; however, the ash content was 14.3%, which was substantially higher than that (7.63%) obtained using the Microcel™ alone. Therefore, for the coal feeds having the characteristics of those used in these tests, it is necessary to use both column flotation and enhanced gravity separation in a single circuit in order to obtain clean coal products with low ash and low pyritic sulfur contents while maintaining high yields.

With the ROM Illinois coal (-48 mesh), the best results were also obtained using the Microcel™/MGS circuit. From the feed assaying 34.4% ash and 2.32% pyritic sulfur, a clean coal product with 8.0% ash and 0.57% pyritic sulfur was produced at 85.4% combustible recovery and 85.1% pyritic sulfur rejection. The pyritic sulfur content obtained using the Microcel™ alone was 1.7%, representing 60.0% pyritic sulfur rejection. Thus, the use of MGS in conjunction with

Microcel™ resulted in a 41.6% improvement in pyritic sulfur rejection. When using the MGS alone, the pyritic sulfur content was reduced to 0.68%; however, the ash content was as high as 23.7%. Thus, the results obtained with the Illinois coal also suggest that both column flotation and enhanced gravity separation are needed to produce low-ash, low-pyritic sulfur coals at high yields.

An economic analysis for cleaning the two high-sulfur coals using the combined Microcel™/MGS circuit has been carried out. The analysis is based on an assumption that Microcel™ and MGS units are added to an existing preparation plant to process the natural fines without further size reduction. For the Pittsburgh coal, the processing cost for the fine coal stream is estimated to be \$158/ton of SO<sub>2</sub> removed, while for the Illinois No. 6 coal it would be \$77/ton of SO<sub>2</sub> removed. These cost figures are substantially lower than those ( $\approx$ \$300-350/ton of SO<sub>2</sub> removed) obtained when the same coals were ground substantially finer than 200 mesh and then cleaned using either an advanced froth flotation process or an oil agglomeration process. Two main reasons may be given for the low estimated costs for using the combined Microcel™/MGS circuit. First, the circuit does not require the costly step of fine grinding. Second, because of the larger particle sizes in the feed stream, the cost of dewatering is substantially lower than is the case when coal is ground finer than 200 mesh before cleaning. The new coal cleaning concept tested in the present work also compares favorably with flue-gas scrubbing technologies, which have higher capital costs.

The synergistic effect of combining a flotation column and an enhanced gravity separator in a single coal cleaning circuit has been manifested in substantially improved pyritic sulfur rejection while meeting ash rejection specifications. The improved pyrite rejection process has an added benefit, that is, improved rejection of trace elements. Chemical analyses of the products obtained in the combined Microcel™/MGS circuit show that many of the 11 trace elements identified in Title III of the 1990 Clean Air Act Amendments (CAAA) are further removed beyond the level achieved using the Microcel™ flotation column alone. With the Pittsburgh coal, the incremental improvement in the removal of the 11 trace elements is 39% on average, while it is 27% with the Illinois No. 6 coal. Particularly significant improvements have been achieved with the removal of arsenic and mercury, which are predominantly associated with pyrite in coal. The average improvement achieved for these two elements is 125% for the Pittsburgh coal and 174% for the Illinois No. 6 coal. In view of the difficulties in removing mercury by electrostatic precipitators in coal-burning power plants, the new pre-combustion coal cleaning concept demonstrated in the present work should prove useful for meeting the 1990 CAAA in more ways than one.



**TABLE OF CONTENTS**

EXECUTIVE SUMMARY.....	i
TABLE OF CONTENTS.....	v
LIST OF FIGURES .....	ix
LIST OF TABLES.....	xiii
INTRODUCTION .....	1
1. Background.....	1
2. Description of the Proposed Investigation.....	6
3. Description of the Microcel and MGS Technologies .....	7
3.1 Description of the Multi-Gravity Separator (MGS) .....	7
3.2 Description of the Microcel Flotation Column.....	9
4. Objectives.....	11
5. Approach.....	12
PROJECT TASKS.....	16
Task 1 - Project Planning.....	16
1.1 Development of Project Work Plans.....	16
1.2 Project Reporting.....	17
Task 2 - CPPRF Modifications .....	17
2.1 Engineering and Design .....	17
2.2 Procurement and Fabrication.....	18
2.3 Construction.....	18
Task 3 - Sample Acquisition .....	18
3.1 Coal Selection.....	18
3.2 Bulk Sample Acquisition.....	19
Task 4 - Sample Characterization.....	19
4.1 Preliminary Characterization .....	19

4.2 Washability Characterization.....	23
4.3 Release Analysis Characterization .....	31
Task 5 - Flowsheet Development and Engineering Design.....	35
5.1 Flowsheet Development.....	35
5.2 Engineering Design.....	35
5.2.1 Flowsheet Design.....	36
5.2.2 Circuit Layout.....	38
5.2.3 Piping .....	40
5.2.4 Instrumentation and Electrical .....	40
5.3 Cost Analysis .....	42
5.4 ET Circuit Design Topical Report.....	42
Task 6 - Procurement and Fabrication.....	43
6.1 Bidding.....	43
6.2 Procurement/Fabrication.....	43
Task 7 - Process Module Installation .....	44
7.1 Installation/Construction .....	44
7.2 Safety Analysis/Review.....	44
Task 8 - Shakedown Testing.....	44
8.1 Start-Up .....	44
8.2 Exploratory Testing .....	45
Task 9 - MGS Scale-Up .....	45
9.1 Development of Scale-Up Criteria.....	45
9.1.1 Identification of Operating Parameters .....	46
9.1.2 Population Balance Model Development.....	47
9.1.3 Population Model Development .....	47
9.2 Scale-Up Validation.....	54
Task 10 - Detailed Testing.....	56
10.1 Microcel Parametric Testing .....	60

10.1.1 Testing of Pittsburgh No. 8 Coal .....	60
10.1.2 Testing of Illinois No. 6 Coal .....	65
10.2 MGS Parametric Testing.....	69
10.2.1 Testing of Pittsburgh No. 8 Coal .....	69
10.2.2 Testing of Illinois No. 6 Coal .....	76
10.3 Combined Microcel/MGS Parametric Testing .....	80
10.3.1 Testing of Pittsburgh No. 8 Coal .....	80
10.3.2 Testing of Illinois No. 6 Coal .....	87
10.4 Combined Microcel/MGS/WOC with WOC Testing .....	94
10.5 Long-Duration Testing.....	96
10.5.1 Testing of Pittsburgh No. 8 Coal .....	96
10.5.2 Testing of Illinois No. 6 Coal .....	102
10.5.3 Partition Curves for the MGS.....	108
10.6 Near-Term Applications.....	112
10.6.1 Testing of Pittsburgh No. 8 Coal .....	112
10.6.2 Testing of Illinois No. 6 Coal .....	114
Task 11 - Decommissioning.....	114
11.1 Circuit Decommissioning .....	114
11.2 Equipment Disposition.....	114
Task 12 - Sample Analysis.....	114
12.1 Standard Analyses.....	114
12.2 Specialty Analyses .....	115
12.3 Trace Element Analyses .....	116
Task 13 - Final Report.....	121
13.1 Technical Evaluation.....	121
13.2 Economic Evaluation .....	143
13.2.1 Estimation of Capital Costs .....	143
13.2.2 Estimation of Operating Costs.....	144

13.2.3 Cost-Benefit Analysis.....	144
13.3 Final Report.....	148
CONCLUSIONS .....	149

**LIST OF FIGURES**

Figure 1.	Comparison of centrifugal washability data with release analysis results for a 28 mesh x 0 Pittsburgh No. 8 seam coal.	4
Figure 2.	Comparison of centrifugal washability data with release analysis results for a 200 mesh x 0 Pittsburgh coal.	5
Figure 3.	Schematic drawing of the pilot-scale Mozley Multi-Gravity Separator (MGS).	8
Figure 4.	Schematic drawing of the Microcel flotation column.	10
Figure 5.	Project work breakdown structure showing required tasks and subtasks.	14
Figure 6.	Detailed project schedule by task and subtask.	15
Figure 7.	Comparison of release analysis and image analysis separation curves for pyrite obtained using a -28 mesh Illinois No. 6 coal.	25
Figure 8.	Comparison of release analysis and image analysis separation curves for mineral matter obtained using a -28 mesh Illinois No. 6 coal.	26
Figure 9.	Comparison of release analysis and image analysis separation curves for pyrite obtained using a -28 mesh Pittsburgh No. 8 coal.	27
Figure 10.	Comparison of release analysis and image analysis separation curves for mineral matter obtained using a -28 mesh Pittsburgh No. 8 coal.	28
Figure 11.	Weight percent pyrite containing carbonaceous inclusions finer than a given size obtained using a -28 mesh Illinois No. 6 coal.	29
Figure 12.	Weight percent pyrite containing carbonaceous inclusions finer than a given size obtained using a -28 mesh Pittsburgh No. 8 coal.	30
Figure 13.	Combustible recovery versus total ash rejection (top) and total sulfur rejection (bottom) obtained from replicate release analysis tests on -65 mesh Illinois No. 6 coal.	32
Figure 14.	Combustible recovery versus ash rejection (top) and total sulfur rejection (bottom) obtained from release analysis tests on -28 and -65 mesh Illinois No. 6 coal.	33
Figure 15.	Combustible recovery versus ash rejection (top) and total sulfur rejection (bottom) obtained from release analyses tests on -28, -65, and -200 mesh Pittsburgh No. 8 coal.	34
Figure 16.	Flow diagram for the testing of the Microcel, MGS, Microcel/MGS and Microcel/WOC/MGS circuits.	37
Figure 17.	Approximate MGS capacities for fine coal cleaning.	56
Figure 18.	Combustible recovery versus rejection plots for the parametric testing of the Pittsburgh No. 8 seam coal using the Microcel flotation column.	64
Figure 19.	Combustible recovery versus rejection plots for the parametric testing of the Illinois No. 6 seam coal using the Microcel flotation column.	68
Figure 20.	Combustible recovery versus rejection plots for the parametric testing of the Pittsburgh No. 8 seam coal using the MGS unit.	73

Figure 21.	Size-by-size analysis of MGS test data for a run-of-mine Pittsburgh No. 8 seam coal.....	76
Figure 22.	Combustible recovery versus rejection plots for the parametric testing of the Illinois No. 6 seam coal using the MGS unit.....	79
Figure 23.	Combustible recovery versus rejection plots obtained for the Microcel column during the parametric testing of the combined Microcel/MGS circuit using the Pittsburgh No. 8 seam coal.....	84
Figure 24.	Combustible recovery versus rejection plots obtained for the MGS unit during the parametric testing of the combined Microcel/MGS circuit using the Pittsburgh No. 8 seam coal.....	85
Figure 25.	Combustible recovery versus rejection plots obtained for the combined Microcel/MGS circuit during the parametric testing of the Pittsburgh No. 8 seam coal.....	86
Figure 26.	Combustible recovery versus rejection plots obtained for the Microcel column during the parametric testing of the combined Microcel/MGS circuit using the Illinois No. 6 seam coal.....	91
Figure 27.	Combustible recovery versus rejection plots obtained for the MGS unit during the parametric testing of the combined Microcel/MGS circuit using the Illinois No. 6 seam coal.....	92
Figure 28.	Combustible recovery versus rejection plots obtained for the combined Microcel/MGS circuit during the parametric testing of the Illinois No. 6 seam coal.....	93
Figure 29.	Combustible recovery versus rejection plots obtained for the Microcel column during the long-duration testing of the combined Microcel/MGS circuit using the Pittsburgh No. 8 seam coal.....	99
Figure 30.	Combustible recovery versus rejection plots obtained for the MGS unit during the long-duration testing of the combined Microcel/MGS circuit using the Pittsburgh No. 8 seam coal.....	100
Figure 31.	Combustible recovery versus rejection plots obtained for the combined Microcel/MGS circuit during the long-duration testing of the Pittsburgh No. 8 seam coal.....	101
Figure 32.	Long Duration results per hour during Pittsburgh #8 seam test.....	102
Figure 33.	Combustible recovery versus rejection plots obtained for the Microcel column during the long-duration testing of the combined Microcel/MGS circuit using the Illinois No. 6 seam coal.....	105
Figure 34.	Combustible recovery versus rejection plots obtained for the MGS unit during the long-duration testing of the combined Microcel/MGS circuit using the Illinois No. 6 seam coal.....	106
Figure 35.	Combustible recovery versus rejection plots obtained for the combined Microcel/MGS circuit during the long-duration testing of the Illinois No. 6 seam coal.....	107
Figure 36.	Long Duration results per hour during Illinois #6 seam test.....	108

Figure 37.	Effect of particle size on the partition curves for the MGS unit obtained during the long-duration testing of the Pittsburgh No. 8 seam coal.....	111
Figure 38.	Effect of particle size on the partition curves for the MGS unit obtained during the long-duration testing of the Illinois No. 6 seam coal.....	112
Figure 39.	Percent removals of trace elements after Microcel and MGS processing for the Pittsburgh No. 8 seam coal.....	120
Figure 40.	Percent removals of trace elements after Microcel and MGS processing for the Illinois No. 6 seam coal.....	121
Figure 41.	Combustible recovery versus ash rejection for run-of-mine Pittsburgh #8 seam coal.....	123
Figure 42.	Combustible recovery versus total sulfur rejection for run-of-mine Pittsburgh #8 seam coal.....	124
Figure 43.	Combustible recovery versus pyrite rejection for run-of-mine Pittsburgh #8 seam coal.....	125
Figure 44.	Combustible recovery versus ash rejection for each unit of the combined circuit.....	125
Figure 45.	Combustible recovery versus total sulfur rejection for each unit of the combined circuit.....	126
Figure 46.	Combustible recovery versus pyritic sulfur rejection for each unit of the combined circuit.....	127
Figure 47.	Combustible recovery versus ash rejection for each unit of the combined circuit during long duration testing.....	128
Figure 48.	Combustible recovery versus total sulfur rejection for each unit of the combined circuit during long duration testing.....	129
Figure 49.	Combustible recovery versus pyritic sulfur rejection for each unit of the combined circuit during long duration testing.....	130
Figure 50.	Combustible recovery versus ash rejection for run-of-mine Illinois #6 seam coal.....	131
Figure 51.	Combustible recovery versus total sulfur rejection for run-of-mine Illinois #6 seam coal.....	132
Figure 52.	Combustible recovery versus pyritic sulfur rejection for run-of-mine Illinois #6 seam coal.....	133
Figure 53.	Combustible recovery versus ash rejection for each unit of the combined circuit.....	134
Figure 54.	Combustible recovery versus total sulfur rejection for each unit of the combined circuit.....	135
Figure 55.	Combustible recovery versus pyritic sulfur rejection for each unit of the combined circuit.....	136
Figure 56.	Combustible recovery versus ash rejection for each unit of the combined circuit during long duration testing.....	137
Figure 57.	Combustible recovery versus total sulfur rejection for each unit of the combined circuit during long duration testing.....	138

Figure 58.	Combustible recovery versus pyritic sulfur rejection for each unit of the combined circuit during long duration testing. ....	139
Figure 59.	Concentrate sulfur versus ash content obtained during the parametric testing of the Pittsburgh No. 8 seam coal. ....	141
Figure 60.	Concentrate sulfur versus ash content obtained during the parametric testing of the Illinois No. 6 seam coal. ....	142
Figure 61.	Cost of SO <sub>2</sub> removed versus pyrite rejection for several traditional and advanced cleaning circuits. ....	148

**LIST OF TABLES**

Table 1.	Size-by-size ash and sulfur contents for the Illinois No. 6 seam coal .....	21
Table 2.	Size-by-size ash and sulfur contents for the Pittsburgh No. 8 seam coal .....	22
Table 3.	Complete listing of construction drawings provided to DOE for the ET circuit.....	39
Table 4.	Control Panel Instrumentation.....	41
Table 5.	Nomenclature used in the development of the population balance model for the MGS.....	48
Table 6.	Numbering system used for the detailed testing program .....	58
Table 7.	Performance expressions used in the present work .....	59
Table 8.	Parametric test matrix used to investigate the performance of the Microcel column for the Pittsburgh No. 8 seam coal .....	61
Table 9.	Correlation matrix for the testing of the Pittsburgh No. 8 seam coal using Microcel column flotation .....	64
Table 10.	Parametric test matrix used to investigate the performance of the Microcel column for the Illinois No. 6 seam coal.....	65
Table 11.	Correlation matrix for the testing of the Illinois No. 6 seam coal using Microcel column flotation.....	68
Table 12.	Parametric test matrix used to investigate the performance of the MGS unit for the Pittsburgh No. 8 seam coal .....	70
Table 13.	Correlation matrix for the testing of the Pittsburgh No. 8 seam coal using the MGS unit.....	73
Table 14.	Size-by-size analysis of MGS test data for a run-of-mine Pittsburgh No. 8 seam coal.....	74
Table 15.	Parametric test matrix used to investigate the performance of the MGS unit for the Illinois No. 6 seam coal .....	77
Table 16.	Correlation matrix for the testing of the Illinois No. 6 seam coal using the MGS unit.....	79
Table 17.	Parametric test matrix used to investigate the performance of the combined Microcel/MGS circuit for the Pittsburgh No. 8 seam coal.....	81
Table 18.	Correlation matrix for the testing of the Pittsburgh No. 8 seam coal using the combined Microcel/MGS circuit.....	86
Table 19.	Parametric test matrix used to investigate the performance of the combined Microcel/MGS circuit for the Illinois No. 6 seam coal .....	88
Table 20.	Correlation matrix for the testing of the Illinois No. 6 seam coal using the combined Microcel/MGS circuit.....	93
Table 21.	Results obtained from the testing of the combined Microcel/WOC/MGS circuit .....	95
Table 22.	Operating conditions examined in the long-duration testing of the Pittsburgh No. 8 seam coal .....	96

Table 23.	Operating conditions examined in the long-duration testing of the Illinois No. 6 seam coal .....	102
Table 24.	Overview of the MGS performance during the long-duration tests.....	109
Table 25.	Test results obtained during the near-term testing of the Pittsburgh No. 8 seam coal.....	113
Table 26.	Trace element analysis of the samples collected during the long-duration testing of the Pittsburgh No. 8 seam coal (material balanced data). ....	117
Table 27.	Trace element analysis of the samples collected during the long-duration testing of the Illinois No. 6 seam coal (material balanced data). ....	118
Table 28.	Cost-Benefit Analysis for the Pittsburgh No. 8 Seam Coal.....	147
Table 29.	Cost-Benefit Analysis for the Illinois No. 6 Seam Coal. ....	147

## INTRODUCTION

### 1. Background

The 1990 Revision of the Clean Air Act mandates that electric utilities reduce SO<sub>2</sub> emissions from 17.5 MM tons/year to 8.9 MM tons/year. This is to be accomplished in two phases. In Phase I, 111 plants representing about 261 units will be required to reduce their emissions to 2.5 lb SO<sub>2</sub>/MMBtu by 1995. In Phase II, these plants and almost all others must reduce their emission levels to below 1.2 lb SO<sub>2</sub>/MMBtu by year 2000.

It appears that the two most popular compliance options for the utilities are (i) scrubbing and (ii) coal switching. Installing wet-scrubbers may be a viable option for some of the large and relatively new power plants, while switching to low-sulfur coals may be a more realistic option for smaller and older power plants. However, even the larger power plants are cautious about installing scrubbers because of the high capital and O&M costs. For this reason and many others, coal switching seems to be gaining momentum among utilities (*Coal and Synfuels Technology*, Nov. 11, 1991). This will undoubtedly increase the future demand for compliance coals. In anticipation of this trend, many coal companies in the central Appalachian region have plans for building new preparation plants or for renovating old facilities. For example, one regional coal company anticipates that it will increase its low-sulfur coal production by approximately 50 MM tons/year when the Phase I program goes into effect (*Coal*, Oct., 1991). There is also considerable interest and activity in developing and demonstrating various beneficiation technologies for the western low-rank coals. It should be noted, however, that most of the upgrading technologies for the western low-rank coals may be uneconomical without the Oil Barrel Equivalent Tax Credit.

The new Clean Air Act imposes a ceiling on the total SO<sub>2</sub> emissions that can be allowed annually in the U.S. and permits trading of allowance credits among power plants and utility companies. This system provides flexibility for a company to over-comply in one plant using a high-efficiency scrubber, while burning high-sulfur coals in another. The allowance credit can also be traded to other companies who plan to build new power plants. Thus, while allowance trading offers provisions for continued utilization of high-sulfur coals, it also creates an incentive for precombustion removal of sulfur from high-sulfur coals beyond what can be normally achieved through conventional means. This incremental sulfur rejection creates a premium for the coal. For example, if allowance credits are traded at \$500/ton of SO<sub>2</sub> and the sulfur content of a coal is reduced from 2.5% to 2.0%, the coal immediately carries a \$5/ton premium (DOE, 1991).

To achieve the incremental sulfur rejection from high sulfur coals, some of the advanced coal cleaning technologies developed in recent years may be used. Of these, only the physical coal cleaning processes are likely to find commercial application in the near future. A common

feature of these processes is that the coal is pulverized to very fine sizes, often to micron-sizes, to liberate pyrite. In most of these processes, the liberated pyrite is then separated from the coal by exploiting the differences in the surface properties of coal and pyrite. Although advances have been made in improving the separation efficiencies in processing fine particles, the total processing costs may exceed the premium that can be gained from the incremental sulfur rejection when coal is pulverized to a micron-size. Economic analyses indicate that the major components of the processing costs are due to (i) pulverization of the coal to very fine sizes, (ii) downstream dewatering of the clean-coal concentrate and (iii) handling and transportation of the ultrafine coal.

Using the deep-cleaned coals as feed stocks for coal-water mixture (CWM) may obviate the dewatering cost, but a market for this technology has yet to be developed in the U.S., primarily due to the current low cost of oil and gas.

Therefore, it would be useful to develop a process of removing pyritic sulfur without micronizing the coal. It is very difficult, however, to remove more than 50% of the pyrite from a 65 mesh x 0 coal, which is the typical size treated by flotation in coal preparation plants today. Recent work at the Center for Coal and Minerals Processing (CCMP) at Virginia Tech has identified two major reasons why even the most advanced coal cleaning technologies (without fine grinding) fail to meet what is for most mineral systems a standard flotation separation, i.e., a 90-95% rejection. They are:

- 1) *superficial oxidation* of pyrite as an inadvertent corrosion-type process that occurs during mining, crushing and transportation, and
- 2) *incomplete liberation* of pyrite from coal such that a large fraction of the pyrite remains associated or locked with the coal as middlings (or composite particles).

The superficial oxidation of pyrite produces surface species, such as elemental sulfur or polysulfides, which are hydrophobic. When these surface species are formed, the separation becomes difficult since both coal and pyrite are hydrophobic. Fortunately, this problem can be minimized by controlling the electrochemical potentials of the system. This approach has been discussed extensively by Yoon et al. (*Processing and Utilization of High Sulfur Coals*, Idaho Falls, Idaho, Aug. 1991).

The problems created by the incomplete liberation of pyrite are more difficult to overcome. For the case of flotation, composite particles are recovered at a lower rate than well-liberated coal particles of the same size. Unfortunately, the flotation rate of a particle is controlled not only by its composition, but also by its size. Thus, it is possible for a composite particle of the optimum size to be floated more readily than a well-liberated coal particle of a different size. In fact, studies conducted at Virginia Tech indicate that large amounts of composite particles are often recovered during normal flotation separations. Furthermore, since

coal is strongly hydrophobic and flotation is a very surface-sensitive process, even the tiniest inclusions of coal in pyrite can make the particle readily floated.

One solution to the problem of recovering composite particles would be to employ the "split-feed flotation" technique. In this approach, the feed coal is carefully sized and the coarse and fine fractions are treated in separate flotation banks. However, it may be necessary to treat very narrow size fractions and have multitudes of split-feed flotation banks in order to achieve very efficient separations of the coal-pyrite composites. The high costs associated with this type of circuit make it impractical in today's coal industry. Another option would be to float for only a short period of time so that only the well-liberated, high-grade coal particles are recovered. This approach is known as the "grab-and-run" technique advocated by Professor Aplan of Penn State (*Coal Flotation*, Flotation - A.M. Gaudin Memorial Volume, Chpt. 45, 1976). The major problem is that low clean-coal yields are usually obtained when using this approach.

The most attractive method for separating composite particles from coal is to use separation processes which exploit bulk properties. For example, Figures 1 and 2 compare the washability data obtained for the Pittsburgh No. 8 coal using the centrifugal float-sink analysis and image analysis techniques. As the particle top-size is reduced from 28 to 200 mesh, a higher pyrite rejection can be achieved with a higher degree of combustible recovery. This is a result of improved liberation with decreasing particle size. The release analysis results, which represent the best possible flotation results, give pyritic sulfur rejections that are vastly inferior to those that can be expected from the washability analysis. In this case, release analysis shows that only 70% of the pyritic sulfur can be removed from the 200 mesh x 0 coal with 60% energy recovery, while the washability data show 90% pyritic sulfur rejection with 90% energy recovery. Thus, separation processes that exploit bulk properties appear to be a better choice for achieving high rejections of pyrite than separation processes which exploit surface properties.

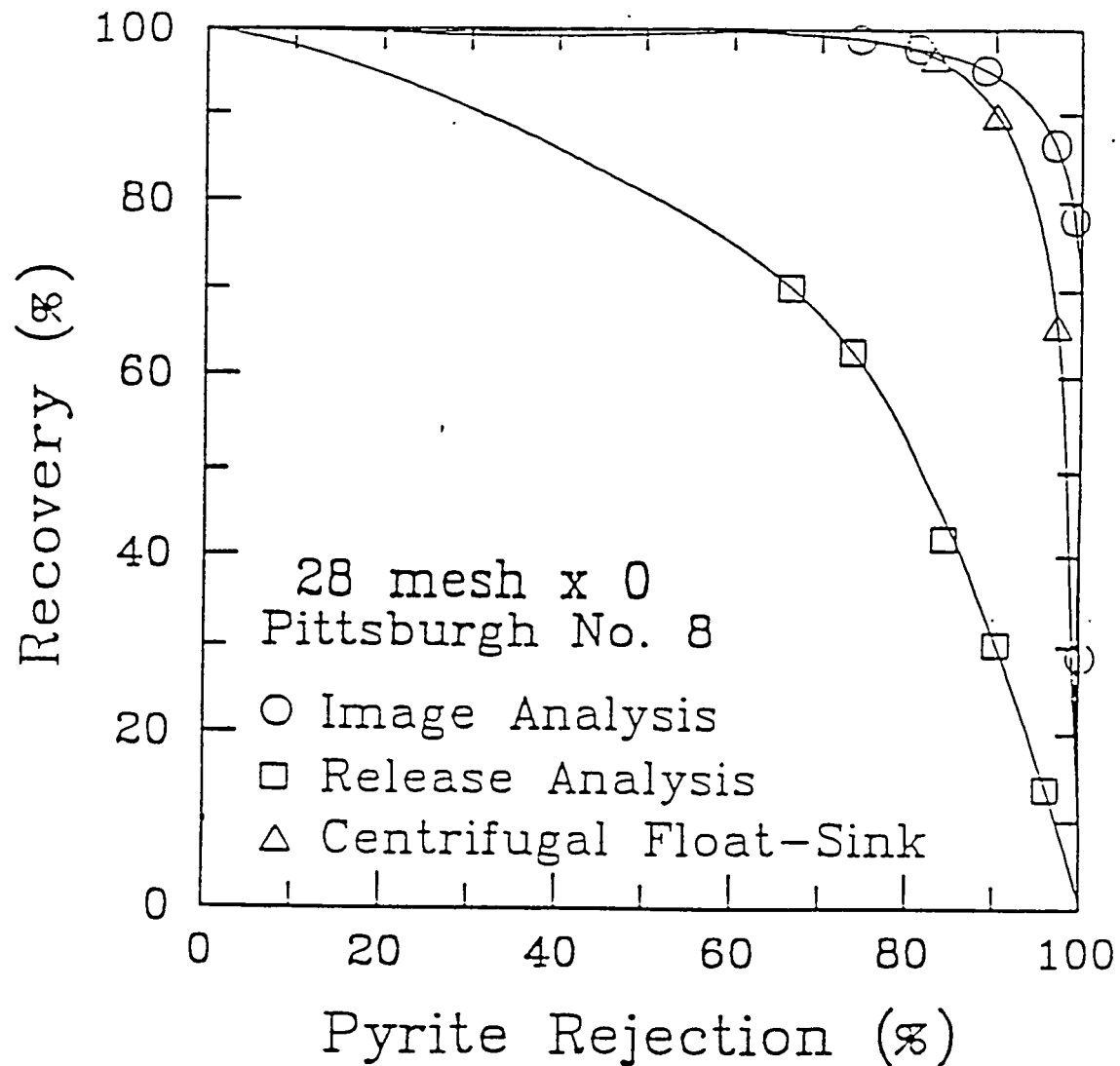


Figure 1. Comparison of centrifugal washability data with release analysis results for a 28 mesh x 0 Pittsburgh No. 8 seam coal.

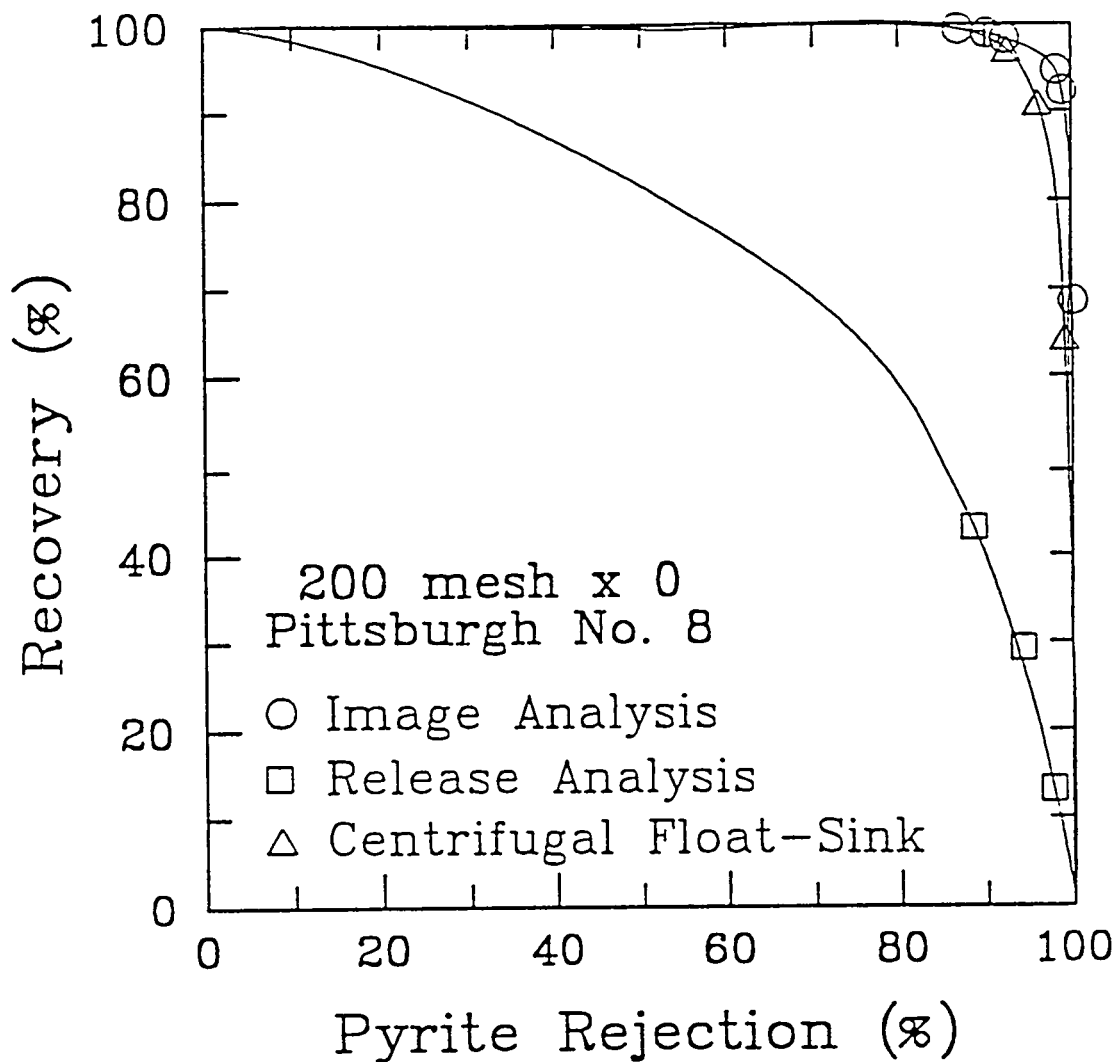


Figure 2. Comparison of centrifugal washability data with release analysis results for a 200 mesh x 0 Pittsburgh coal.

In light of the above discussion, both gravity and magnetic separation techniques would be attractive for coal cleaning since these techniques rely on the bulk properties of particles to create a separation. Magnetic separations are unlikely to find widespread application since the removal of paramagnetic particles such as pyrite from coal requires high-gradient magnetic separators (HGMS) which are energy-intensive and costly. Gravity separation techniques are much less costly, but all of the conventional gravity separation techniques currently used in the coal preparation industry are ineffective for upgrading flotation-size particles, e.g., 65 mesh x 0. Therefore, a new approach for fine-coal cleaning needs to be developed.

## 2. Description of the Proposed Investigation

The data shown above provide a tremendous incentive for using density-based separation techniques for fine-coal cleaning. In the past, this approach was considered to be impractical due to particle size limitations associated with conventional gravity separators. However, during the past several years a new generation of centrifugal fine-particle gravity concentrators have been developed in the minerals processing industry that are capable of treating flotation-size particles. One such unit is the Mozley Multi-Gravity Separator (MGS), which is currently marketed by Carpco of Jacksonville, Florida. In principle, the MGS is a flowing-film separator like shaking tables and spirals, except that particles are also subjected to centrifugal forces so that finer particles can be separated.

Previous studies conducted at Virginia Tech have shown that the MGS is very effective for sulfur reduction because of the large difference in specific gravity between coal and pyrite. However, it may be difficult to use the MGS, or any other fine-particle gravity concentrator, as a stand alone unit operation for fine-coal cleaning. For example, the separation of ash-forming minerals by the MGS is more difficult because of their lower specific gravity. Also, ultrafine clay "slimes" present in the feed coal often report to the clean-coal product by entrainment. Thus, the MGS is expected to be less efficient in removing ash-forming minerals such as clay than high-density particles such as pyrite.

To overcome the limitations associated with single-stage separation techniques, researchers at Virginia Tech have developed a two-stage coal cleaning process that combines centrifugal fine-particle gravity separation with advanced froth flotation. Froth flotation is used to reject ash-forming mineral matter such as clay, while the fine-particle gravity separator is used to reject coal-pyrite composites. In this way, these two technologies complement each other and compensate for each other's deficiencies.

The project described in this report was undertaken to provide the necessary research and development required to move this novel two-stage coal cleaning circuit toward commercialization.

### **3. Description of the Microcel and MGS Technologies**

This work involved the testing of the Multi-Gravity Separator (MGS) in conjunction with an advanced froth flotation technology developed at CCMP known as Microcel column flotation. Each of these technologies are described in the following sections.

#### **3.1 Description of the Multi-Gravity Separator (MGS)**

The Multi-Gravity Separator (MGS) was developed by Richard Mozley Limited, U.K., for the selective separation of fine particles based on differences in density. The MGS unit is distributed in North America by Carpco, Inc., of Jacksonville, Florida. A schematic of the pilot-scale version of this device is shown in Figure 3. The operating principle of MGS is similar to that of a conventional shaking table. However, by placing the table surface inside a rotating drum, it is possible to achieve many times the normal gravitational pull on the particles as they move across the table in a film of water flowing along the internal surface of the drum. The centrifugal field allows finer particles to be selectively separated than would be possible using conventional flowing-film separators.

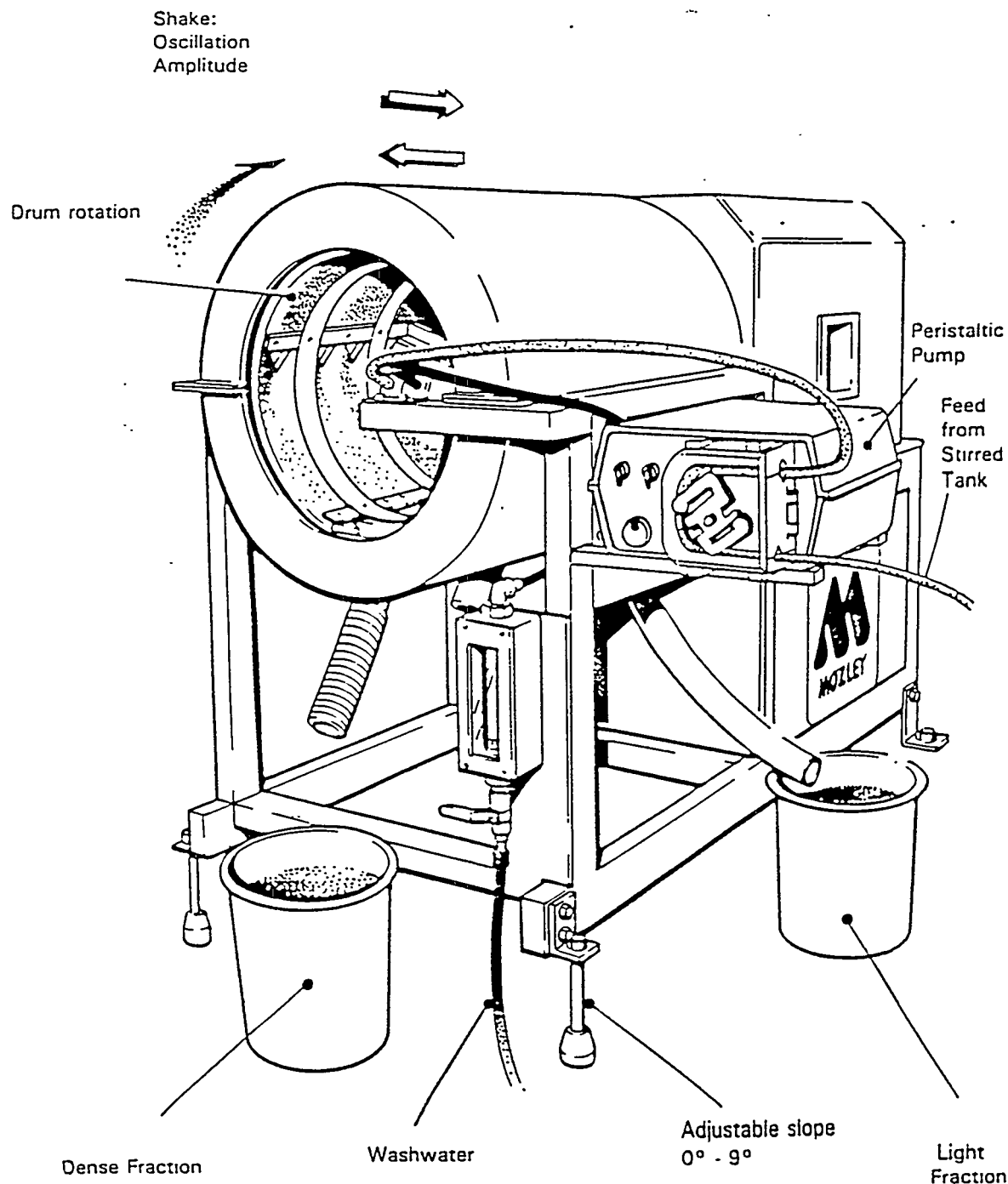


Figure 3. Schematic drawing of the pilot-scale Mozley Multi-Gravity Separator (MGS).

Successful applications of the MGS technology include the concentration of cassiterite, chromite, wolframite, graphite, mixed sulfides and gold. For these applications, MGS can treat particles in the range of 1-1000 mm with high separation efficiencies. The lower particle size limit is much smaller than can be achieved with any other commercially-viable gravity separation process. For example, shaking tables are generally effective over a particle size range of 200-1,200 mm. Tests conducted at Virginia Tech suggest that the MGS may be useful for processing fine coals below 30  $\mu\text{m}$  in diameter.

### 3.2 Description of the Microcel Flotation Column

The Microcel flotation column was developed in the early 1980's to take advantage of the benefits of using smaller air bubbles for flotation. Small air bubbles increase the rate of flotation and allow a higher throughput to be achieved at a given coal recovery (Yoon et al., *Coal Preparation*, Vol. 10, 1992). Also, like most other column flotation cells, Microcel is equipped with a wash water system that minimizes the entrainment of ultrafine mineral matter (such as clay) into the froth product. Because of these advantages, Microcel is capable of achieving better recoveries of coal and higher rejections of mineral matter than conventional flotation cells.

A schematic representation of a typical Microcel unit is shown in Figure 4. In this device, air bubbles in the range of 0.1-0.4 mm are generated by passing air and a portion of the flotation pulp through an in-line static mixer. The intense high-shear agitation provided by the in-line mixers generates smaller air bubbles than other commercially available air sparging systems. The Microcel bubble generators are not subject to plugging and can be serviced without column shutdown. The Microcel technology is marketed by ICF-Kaiser Engineers and Control International. More than a dozen full-scale units are already in commercial operation, and several other installations are currently planned or under consideration.

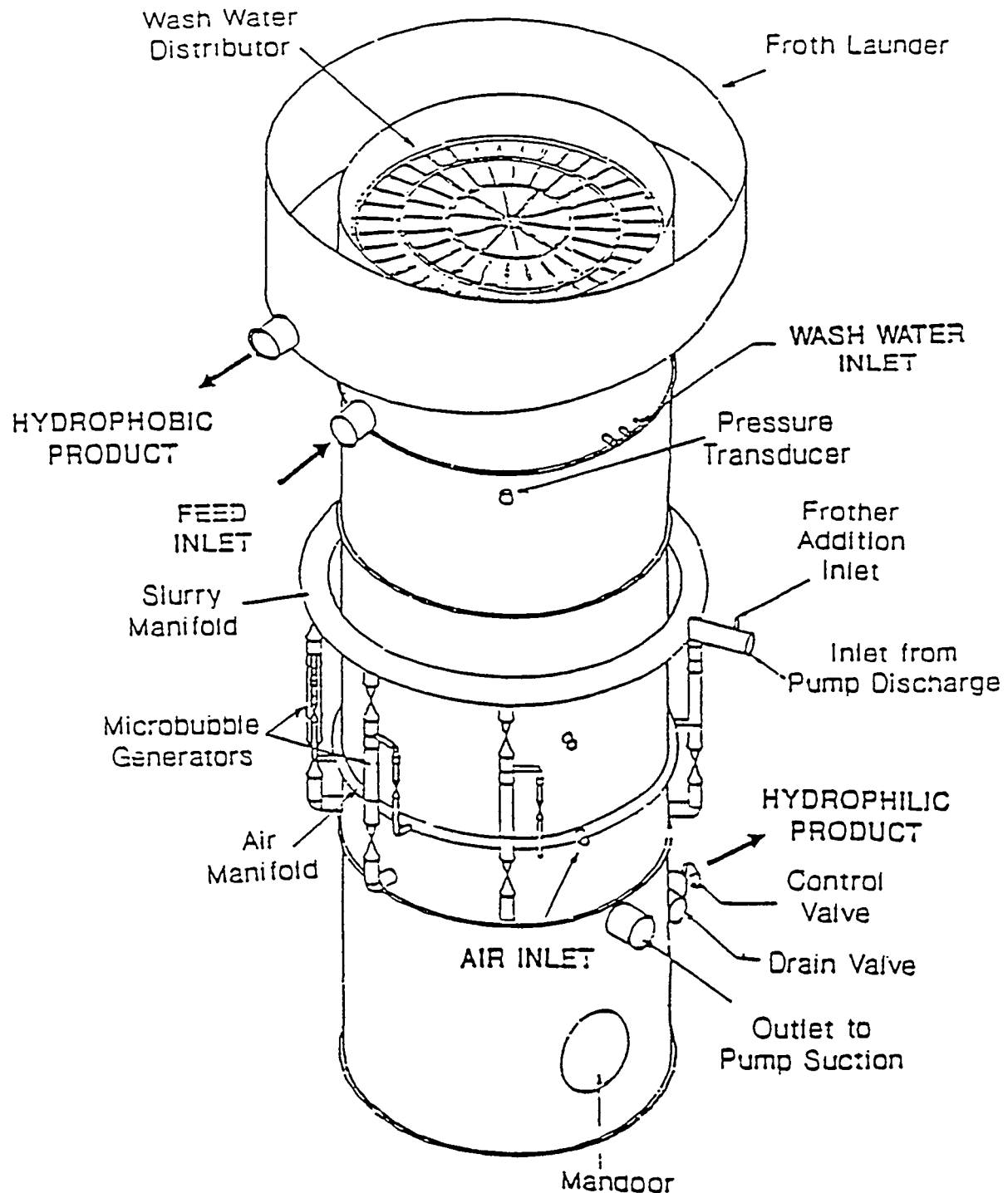


Figure 4. Schematic drawing of the Microcel flotation column.

#### 4. Objectives

The primary objective of this project was to design, install, and operate a continuous (300-500 lb/hr) advanced fine-coal processing circuit combining the Microcel and Multi-Gravity Separator (MGS) technologies. Both of these processes have specific advantages as stand-alone units. For example, the Microcel column effectively removes ash-bearing mineral matter, while the MGS efficiently removes coal-pyrite composites. By combining both unit operations into a single processing circuit, synergistic advantages can be gained. As a result, this circuit arrangement has the potential to improve coal quality beyond that achieved using the individual technologies.

In addition to the primary objective, secondary objectives of the test program included:

- *Circuit Optimization:* Evaluate and optimized the performance of each unit operation, individually and combined, by conducting parametric studies as a function of key operating variables. The goal of this work was to maximize the rejections of pyritic sulfur and ash while maintaining a high energy recovery.
- *Process Variability:* Evaluate the steady-state performance of the optimized processing circuit by (i) conducting several long-duration test runs and (ii) testing coal samples from other sources as specified by the participating coal companies.
- *Process Evaluation:* Conduct technical and economic evaluations to examine the feasibility of the proposed concept for fine-coal cleaning on an industrial scale. This evaluation includes a projected cost-benefit analysis and a review of all test data, engineering analyses, scale-up procedures, and process deficiencies.

The test work was conducted at the Pittsburgh Energy Technology Center's Coal Preparation Process Research Facility (CPPRF) located in Pittsburgh, Pennsylvania. The CPPRF is a state-of-the-art bench-scale testing facility for coal preparation research and development projects. The Emerging Technology (ET) section of the pilot plant was used for testing the combined Microcel and MGS circuit. The ET area, and subsequently installed mezzanine, is adjacent to the primary plant and was established for testing new and emerging technologies in coal preparation. This facility is ideally suited for bench-scale test work due to the availability of all necessary ancillary facilities (i.e., bulk solids handling, feed stock preparation, and waste disposal) and the ability to tightly control feed and operating conditions. The CPPRF is operated by Gilbert-Commonwealth for the Department of Energy.

## 5. Approach

The project objectives were met by testing two moderate-to-high sulfur coals in three different circuit configurations. The following configurations were evaluated:

- a single Microcel unit,
- a single MGS unit, and
- combined Microcel/MGS units.

In the combined circuit, the froth product from the Microcel was reprocessed by the MGS unit.

The successful completion of the project required the active participation of several different research, engineering, manufacturing and industrial organizations. These included:

- Virginia Center for Coal and Minerals Processing (CCMP)
- Roberts & Schaefer Company (R&S)
- Carpco, Inc.
- Consolidation Coal Company (Consol)
- Kerr-McGee Coal Company
- Rizzo & Sons, Inc.

The CCMP served as the prime contractor and provided the contractual management, technical guidance, and overall supervision necessary to complete the proposed work in a timely and orderly fashion. Technical personnel from CCMP also were primarily responsible for the flowsheet development, shakedown and testing of the proposed circuitry and was actively involved in the design and installation activities conducted by the various project participants. In addition, a variety of raw coal characterization studies and product sample analyses were conducted in the coal analysis laboratories at CCMP. R&S provided basic engineering services (which included such tasks as the layout of unit operations, specification of equipment/material requirements, selecting and monitoring the installation subcontractor, detailing of miscellaneous contractual services and on-site construction oversight). R&S also served as an external reviewer for the technical documents generated by the prime contractor. Carpco provided expertise related to the installation, shakedown and operation of the MGS circuit. This company also assisted in the analysis and interpretation of the experimental data collected using the MGS. Finally, the two

participating coal companies (Consol and Kerr-McGee) provided raw coal samples and miscellaneous technical services required to evaluate the overall success of the proposed work.

Figure 5 shows the work breakdown structure (WBS) for the project. In total, 13 different tasks and 36 different subtasks were required to carry out the proposed work. The project schedule for these work elements is shown in Figure 6. As shown, approximately 20 months were required to complete the proposed work. However, most of the work effort was concentrated during the six month period of activity at the CPPRF (July 1993 to January, 1994).

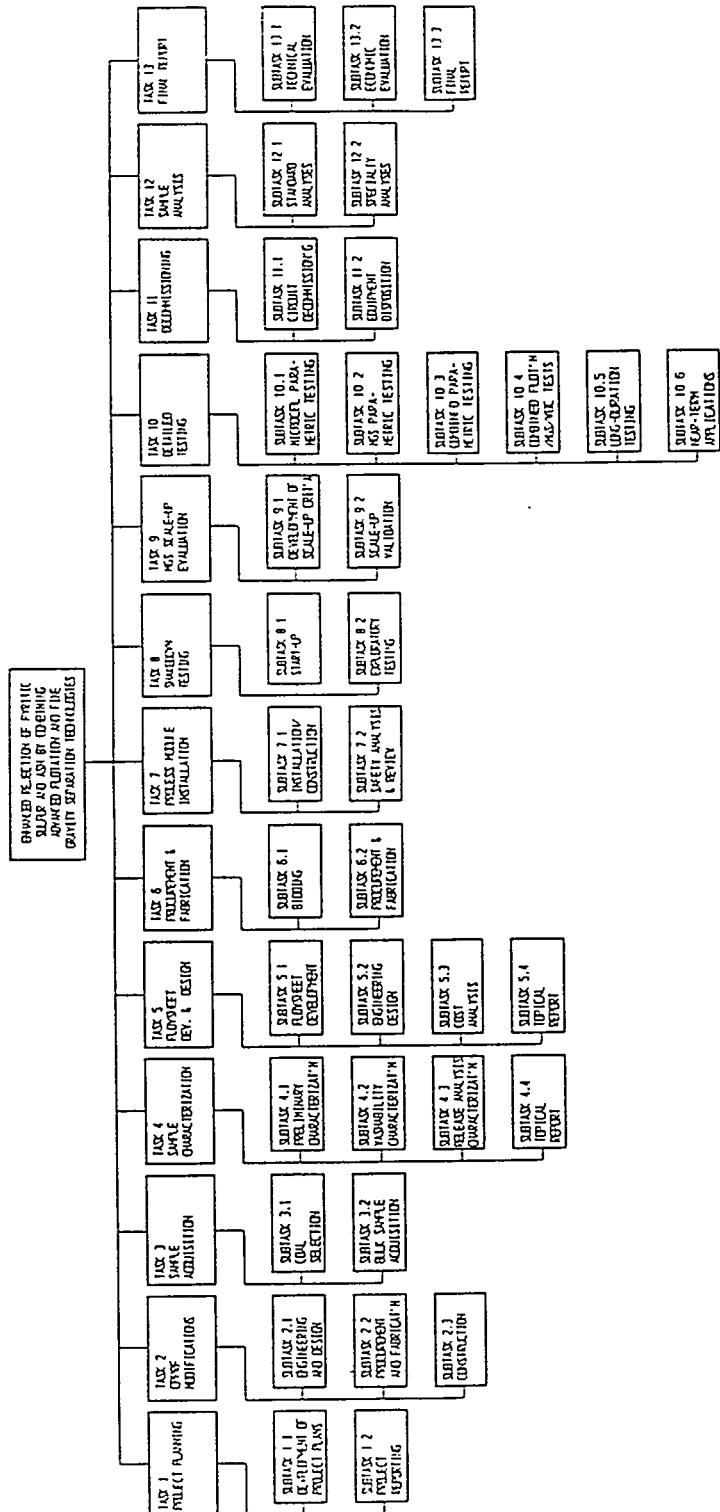


Figure 5. Project work breakdown structure showing required tasks and subtasks.

Detailed Project Schedule/Milestone Identification Chart

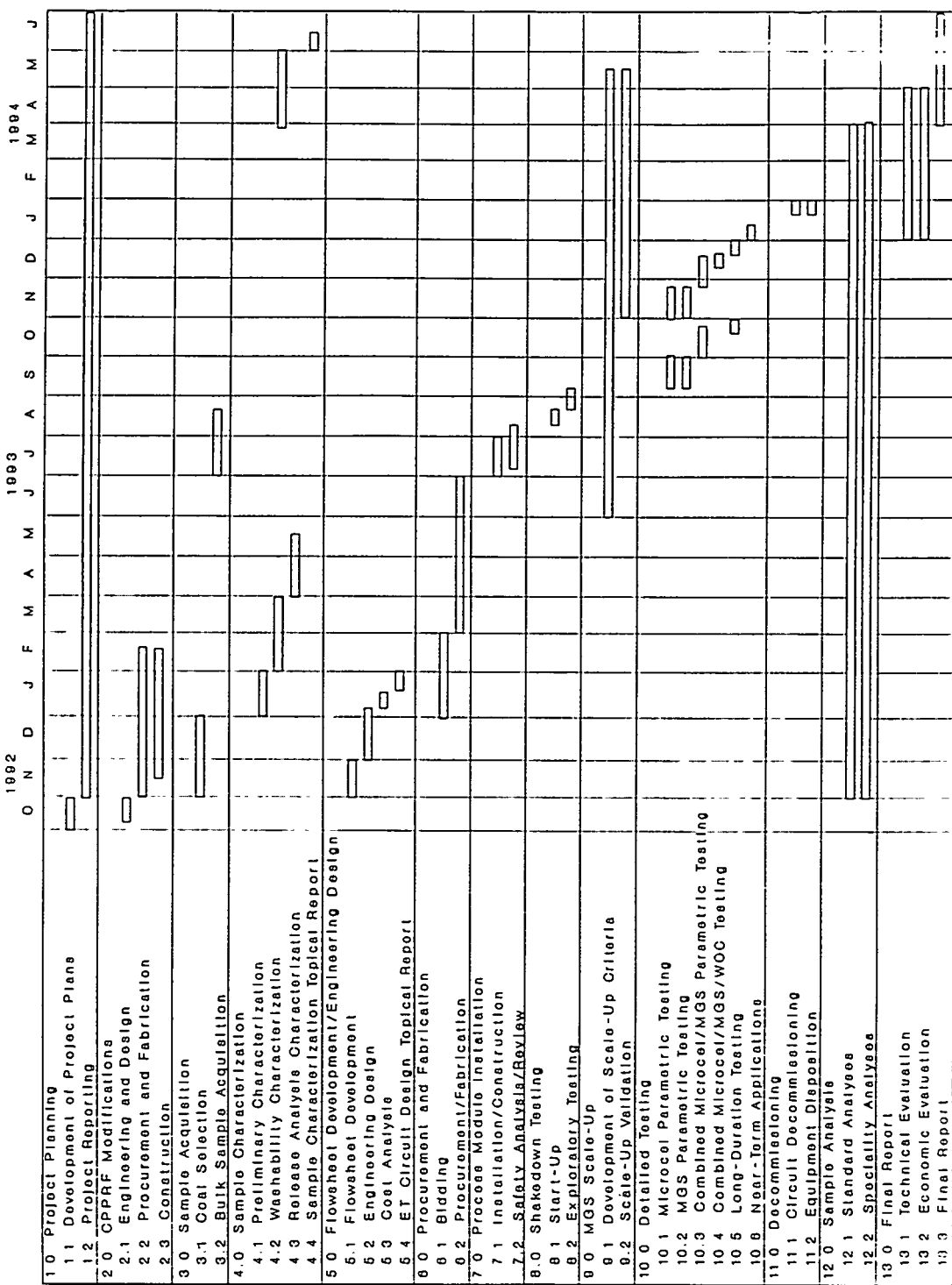


Figure 6. Detailed project schedule by task and subtask.

## PROJECT TASKS

### Task 1 - Project Planning

#### 1.1 Development of Project Work Plans

The first project activity was to prepare a detailed Project Work Plan. This document provided a detailed description of the test program, experimental procedures, analytical methods, and reporting guidelines for implementation and completion of the proposed work. The work plan detailed the assignment of project responsibilities for each participant involved in the project and clearly defined the lines of communication. Specific items provided in the Project Work Plan included:

- Work Breakdown Structure (WBS)
- Task Objectives/Anticipated Results
- Detailed Project Schedule
- Milestones Identification Schedule
- Quality Assurance/Quality Control (QA/QC) Plan
- Project Reporting Schedule
- Environmental, Safety, and Health (ES&H) Plan

Any revisions to the project work plan were discussed with the COR and submitted in writing to DOE for approval prior to implementation.

During this planning stage, preliminary drafts of several other technical/management project plans were also submitted with the Project Work Plan. These included:

- Test, Sampling and Analytical (TS&A) Plan
- Installation and Shakedown Plan
- Coal Procurement, Handling, and Logistics Plan
- Procurement and Fabrication Plan

- Decommissioning Plan
- ET Area Modification Design Plan
- Hazardous Substance Plan
- Project Management Plan
- Project Labor Plan
- Project Cost Plan

All project plans were developed by personnel from CCMP with assistance provided by Carpco, Roberts & Schaefer, Consolidation Coal and Kerr-McGee.

## 1.2 Project Reporting

The prime contractor (CCMP) was responsible for the timely submission of all weekly, monthly, quarterly, topical and final reports as specified by the DOE Reporting Requirements Distribution List and the Project Work Plan. The DOE Uniform Reporting System was used as the guide for preparing all project reports. CCMP coordinated preparation and dissemination of all technical reports and non-financial management reports. The Office of Sponsored Projects (OSP) at Virginia Tech prepared and certified all financial and property reports. Responsibility for the preparation of environmental and safety reports and documents, as required, rested with CCMP personnel and was submitted through OSP.

Reports were prepared by the various subcontractors and submitted directly to the CCMP Project Manager for incorporation into the required DOE report. To ensure that all project participants were fully aware of their reporting requirements, a separate reporting requirements schedule was prepared by CCMP and provided to each primary subcontractor. A project planning meeting was held shortly after project award to review these requirements.

## Task 2 - CPPRF Modifications

### 2.1 Engineering and Design

The prime contractor (CCMP) was responsible for completing several permanent modifications to the CPPRF to accommodate the installation and testing of this and other high efficiency preparation (HEP) projects. These modifications included:

- The addition of two (2) stories of open platform area extending along the north wall from the existing conventional precleaning and comminution structure to the east wall.

- The addition of a floor trench in the ET area.
- The upgrading of the raw coal receiving area.

The open platform area was necessary to allow access between the existing CPPRF structure and the circuitry to be installed as part of the proposed work and to provide additional space for installation of ET circuit equipment. The floor trench is used to contain accidental spills and to enable washdown of the test circuit area. The raw coal receiving area was upgraded with a truck ramp and a new hopper/screw conveyor to facilitate coal loading into the plant.

Engineering and design activities related to the CPPRF modifications were carried out by Roberts & Schaefer Company. This subtask included the development of engineering/fabrication/construction drawings and preparation of a detailed cost estimate. Specific details related to this work effort were provided in the ET Area Modification Design Plan.

## **2.2 Procurement and Fabrication**

Roberts & Schaefer performed the procurement and fabrication of all components and materials required to complete the CPPRF modifications. R&S prepared all bid specifications, bid solicitations, bid reviews, and awarded the subcontracts and purchase orders required to complete this effort. All procurement activities were to follow the guidelines established by the Department of Energy (DOE) and Virginia Tech. R&S periodically visited the selected fabrication shop(s) to inspect workmanship prior to shipping and installation.

## **2.3 Construction**

All on-site construction activities related to the CPPRF modifications were monitored by Roberts & Schaefer and coordinated with DOE and Gilbert-Commonwealth. R&S selected and monitored the various mechanical and electrical subcontractors that were necessary to complete the on-site installation and construction activities.

## **Task 3 - Sample Acquisition**

### **3.1 Coal Selection**

This subtask began immediately after approval of the Project Work Plan developed in Task 1 (Project Planning). Completion of this subtask was the responsibility of the prime contractor (CCMP) and the participating coal companies. Samples from several different U.S. coal seams having moderate-to-high sulfur contents were evaluated with two (2) seams being selected for testing in the CPPRF. These two coals were obtained from the Pittsburgh No. 8 and

Illinois No. 6 coal seams. These coals are well known for their large reserve base and relatively high pyritic sulfur content.

Prior to testing in the CPPRF, representative samples of each of the two base coal seams were collected, stored in an inert environment, and subjected to various laboratory characterization tests as outlined in Task 4 (Sample Characterization). Approximately one 55-gallon drum of representative sample was required for each seam. The characterization work was completed prior to the procurement and shipping of the bulk sample used in the CPPRF test work. This arrangement was necessary to minimize problems, i.e., oxidation and weathering, associated with the long-term storage of the bulk coal sample. In addition, this schedule allowed the potential cleanability of the selected feed coals to be evaluated prior to final selection and shipping of the CPPRF test coals.

### **3.2 Bulk Sample Acquisition**

Prior to the start of this subtask, the Coal Procurement, Handling, and Logistics Plan was finalized. This document provided detailed information related to the required tonnages and shipping/delivery dates for each of the two base coal samples. The CCMP and participating coal companies were responsible for the sampling campaign and safe transportation of the coal samples. To minimize problems associated with coal weathering, the bulk samples were procured and shipped to an off-site storage facility (Dillner Storage Company, West Elizabeth, Pennsylvania) just prior to start-up of the circuit.

Approximately 60-75 tons of each coal were required to complete the proposed test work. Each entire lot of coal was homogenized at the off-site storage facility and split into lots of 5-6 tons each for delivery to the CPPRF as needed. Once received, the raw coal was crushed to below 1/4-inch using the CPPRF coarse coal crushing circuit. The crushed coals were then stored in the 5-ton raw coal storage bins and inerted under nitrogen until needed in the testing program.

### **Task 4 - Sample Characterization**

A variety of laboratory characterization studies were undertaken in order to evaluate the potential cleanability of the base coal samples used in the present work, i.e., Pittsburgh No. 8 and Illinois No. 6 coal seams. The characterization effort was the sole responsibility of the prime contractor (CCMP). The characterization work began immediately after the acquisition of representative lots of each of the two base coal samples.

#### **4.1 Preliminary Characterization**

The first series of characterization studies were conducted to evaluate the overall quality of each run-of-mine sample. The samples were dry pulverized to two different topsizes (i.e., 28 and 65 mesh) using a laboratory hammer mill. The ground products were wet-screened, dried,

weighed and subjected to ash and sulfur analyses. The particle size distributions and size-by-size analyses are summarized in Tables 1 and 2.

The preliminary analyses indicate that a relatively large proportion of fines were generated by the grinding process. At the 65 mesh grind, more than half of the Illinois No. 6 coal and over one-third of the Pittsburgh No. 8 was found to be finer than 400 mesh. The high production of fines is typical of an impact-type crusher, such as a hammer mill. It is recommended that future grinding tests use a laboratory rod mill to minimize the production of excessive fines. The characterization data also indicate that the Illinois No. 6 seam coal possessed significantly higher ash and sulfur contents than the Pittsburgh No. 8 seam coal (i.e., 45% ash and 4.6% sulfur versus 18% ash and 3.6% sulfur). For both coals, the finer size fractions tended to yield lower ash and sulfur values than did the coarser fractions. The only exception to this trend was observed for the finest size fraction, i.e., 400 mesh x 0. In this case, the higher ash content can be largely attributed to the disproportionate amount of high-ash clay particles in the ultrafine size range.

Table 1. Size-by-size ash and sulfur contents for the Illinois No. 6 seam coal.

## Dry Pulverized to 28 Mesh Topsizer

Size Fraction (Mesh)	Individual			Cumulative		
	Weight (%)	Ash (%)	Sulfur (%)	Weight (%)	Ash (%)	Sulfur (%)
+28	0.71	51.72	3.25	0.71	51.72	3.25
28x35	4.91	44.70	4.91	5.62	45.59	4.70
35x48	6.16	46.75	4.00	11.78	46.20	4.33
48x65	11.64	46.50	5.77	23.42	46.35	5.05
65x100	8.18	33.79	4.36	31.60	43.10	4.87
100x150	11.02	33.88	5.01	42.62	40.71	4.91
150x200	8.62	30.64	4.85	51.24	39.02	4.90
200x270	5.62	33.20	5.75	56.86	38.44	4.98
270x400	8.24	32.80	5.84	65.10	37.73	5.09
-400	34.90	56.53	3.48	100.00	44.29	4.53
Feed	100.00	44.29	4.53			

## Dry Pulverized to 65 Mesh Topsizer

Size Fraction (Mesh)	Individual			Cumulative		
	Weight (%)	Ash (%)	Sulfur (%)	Weight (%)	Ash (%)	Sulfur (%)
+65	6.80	55.49	5.04	6.80	55.49	5.04
65x100	9.82	46.70	5.99	16.62	50.30	5.60
100x150	11.81	33.60	5.82	28.43	43.36	5.69
150x200	12.64	33.56	5.11	41.07	40.34	5.51
200x270	8.60	32.67	5.36	49.67	39.02	5.49
270x400	10.01	36.43	5.86	59.68	38.58	5.55
-400	40.32	56.53	3.52	100.00	45.82	4.73
Feed	100.00	45.82	4.73			

Table 2. Size-by-size ash and sulfur contents for the Pittsburgh No. 8 seam coal.

## Dry Pulverized to 28 Mesh Topsizer

Size Fraction (Mesh)	Individual			Cumulative		
	Weight (%)	Ash (%)	Sulfur (%)	Weight (%)	Ash (%)	Sulfur (%)
+28	0.00	0.00	0.00	0.00	0.00	0.00
28x35	28.06	29.71	3.64	28.06	29.71	3.64
35x48	19.17	14.07	3.47	47.23	23.36	3.57
48x65	14.34	13.33	4.13	61.57	21.03	3.70
65x100	9.91	14.10	4.07	71.48	20.07	3.75
100x150	9.09	13.93	4.03	80.57	19.37	3.78
150x200	5.25	8.99	3.52	85.82	18.74	3.77
200x270	3.85	13.73	4.96	89.67	18.52	3.82
270x400	2.71	12.93	4.40	92.38	18.36	3.84
-400	7.62	21.78	3.55	100.00	18.62	3.81
Feed	100.00	18.62	3.81			

## Dry Pulverized to 65 Mesh Topsizer

Size Fraction (Mesh)	Individual			Cumulative		
	Weight (%)	Ash (%)	Sulfur (%)	Weight (%)	Ash (%)	Sulfur (%)
+65	5.78	17.15	3.48	5.78	17.15	3.48
65x100	7.98	14.10	3.76	13.76	15.38	3.64
100x150	14.71	13.42	3.48	28.47	14.37	3.56
150x200	14.11	12.05	3.80	42.58	13.60	3.64
200x270	10.57	12.25	3.75	53.15	13.33	3.66
270x400	13.25	12.70	3.76	66.40	13.21	3.68
-400	33.60	27.52	2.93	100.00	18.02	3.43
Feed	100.00	18.02	3.43			

#### 4.2 Washability Characterization

In this subtask, standard and centrifugal float-sink tests were to be carried out using each of the two base coal samples. These analyses were performed at a 28 mesh topsize. The information collected from these tests allowed the degree of liberation to be estimated and provided a "yardstick" against which the performance of the density-based separator (i.e., MGS) could be evaluated. In selected tests, the clean-coal products were analyzed on a size-by-size basis so that any deficiencies in the rejection of mineral matter could be identified. All products were analyzed for ash, total sulfur, sulfur forms, and heating value.

The initial fine-coal washability tests were conducted using a Sharples high-G centrifuge. Aqueous solutions of zinc chloride were prepared to provide a wide range of heavy liquids for the float-sink tests. Zinc chloride solutions were selected over traditional organic heavy liquids because of lower costs and reduced health risks. In each test, a small amount of fine coal was suspended in the lowest SG zinc chloride solution and passed through the centrifuge. The light fraction was collected throughout the test period, while the heavy fraction was retained inside the bowl and collected after stopping the centrifuge. The heavy fraction was resuspended in the next highest SG solution and again passed through the centrifuge. This procedure was repeated until the desired range of float-sink products were collected for each coal.

The test results indicated that the fine-coal washability procedure employed at CCMP was unreliable. In fact, the test results obtained to date indicate that the fine-coal washability procedure used at CCMP gives a separation curve that is poorer than that obtained by flotation release analysis. This finding was considered to be highly unlikely (if not impossible), particularly for the rejection of pyritic sulfur. The difficulty in obtaining good fine-coal washability results was attributed to the poor dispersion of the ultrafine-coal particles suspended in the zinc chloride solutions. Although the use of chemical dispersants appeared to improve the reliability of the float-sink procedure, the data was not believed to be completely trustworthy.

For these reasons described above, the fine-coal centrifugal washability work was discontinued and an image analysis technique using a Scanning Electron Microscope Image Processing System (SEM-IPS) was substituted. The SEM-IPS provided a particle composition analysis by area resulting in the percent of carbonaceous material, mineral matter, and pyrite. An equivalent washability by density was then calculated (Adel et al., 1991). This technique is believed to be the most reliable method for determining fine-coal washability since it provides a direct measure of the various components contained in the coal sample and is not subject to problems related to coal dispersion.

Results of the SEM-IPS characterization tests conducted on the Pittsburgh No. 8 and Illinois No. 6 coal seams are presented in Figures 7-10. Because of the relatively high cost of the SEM-IPS work, only the 28 mesh x 0 grind was examined for each coal. In general, the image analysis data indicate that very high rejections of mineral matter and pyritic sulfur could be

obtained for each of the two base coal samples. For the Illinois No. 6 seam coal, mineral matter and pyrite rejections of approximately 85-90% could be achieved while maintaining coal recoveries approaching 90% (Figures 7-8). Similar reductions in mineral matter and pyritic sulfur could also be obtained for the Pittsburgh No. 8 seam coal (Figures 9-10).

The image analysis characterization data indicate that most of the pyrite which can be liberated is freed from the coal matrix at a relatively coarse size. This phenomenon is illustrated in Figures 11 and 12 which show the weight percent of pyrite containing carbonaceous inclusions finer than a specified size for each of the two base coals. For the Illinois No. 6 seam coal, only about 30% of the pyrite contains coal inclusions smaller than 10 microns. This value falls to approximately 20% for the Pittsburgh No. 8 seam coal. The data suggest that much of the pyrite which remains locked with the coal is very finely disseminated and cannot be completely liberated even at a 400 mesh x 0 grind size.

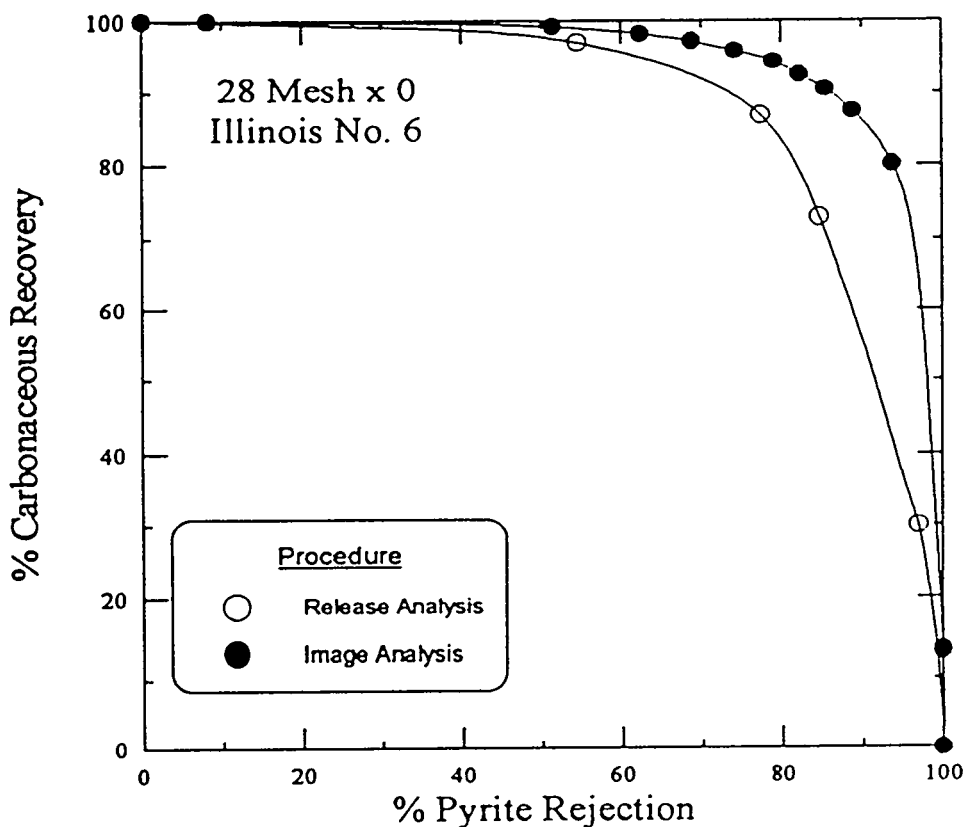


Figure 7. Comparison of release analysis and image analysis separation curves for pyrite obtained using a -28 mesh Illinois No. 6 coal.

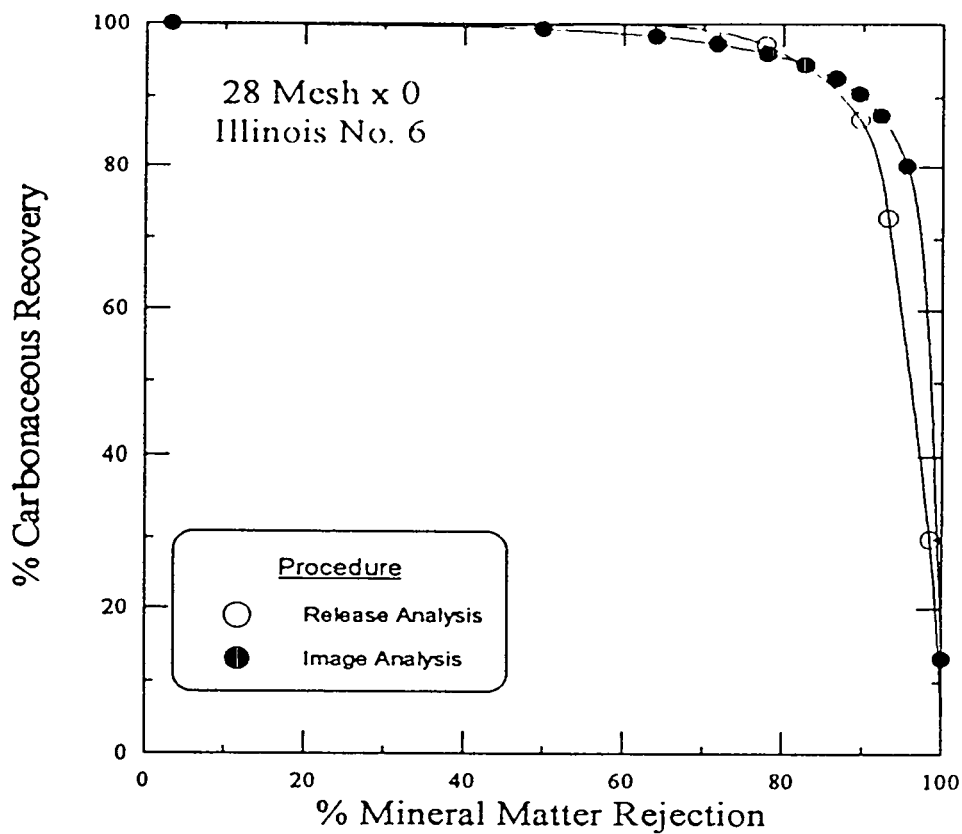


Figure 8. Comparison of release analysis and image analysis separation curves for mineral matter obtained using a -28 mesh Illinois No. 6 coal.

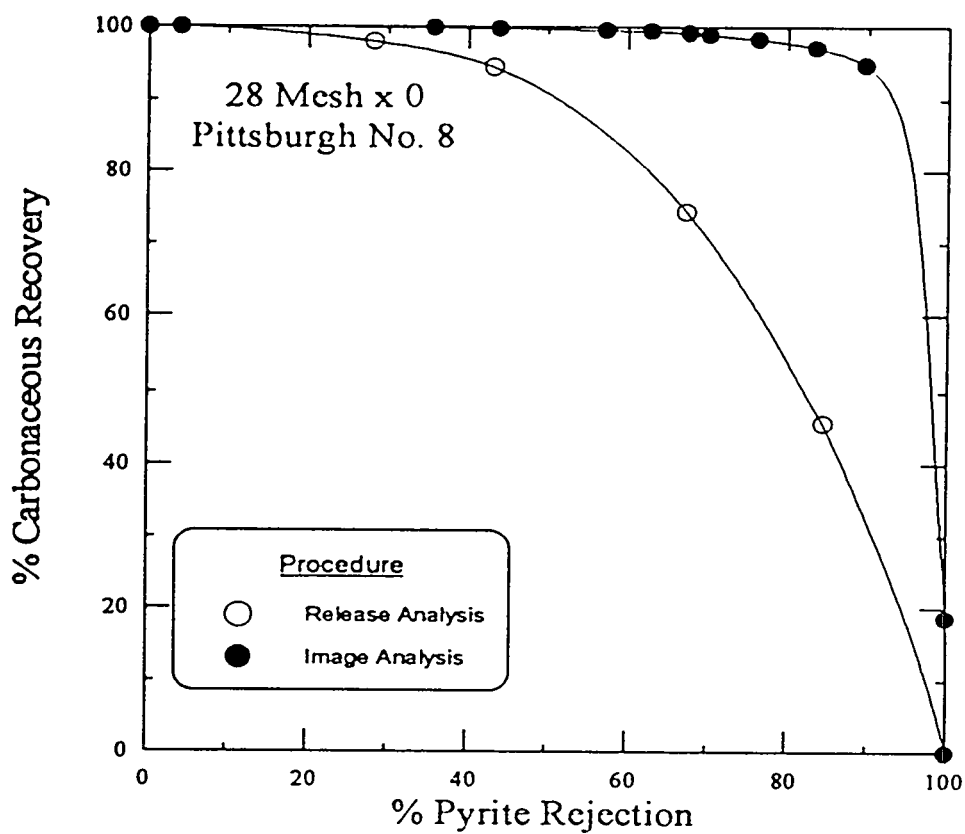


Figure 9. Comparison of release analysis and image analysis separation curves for pyrite obtained using a -28 mesh Pittsburgh No. 8 coal.

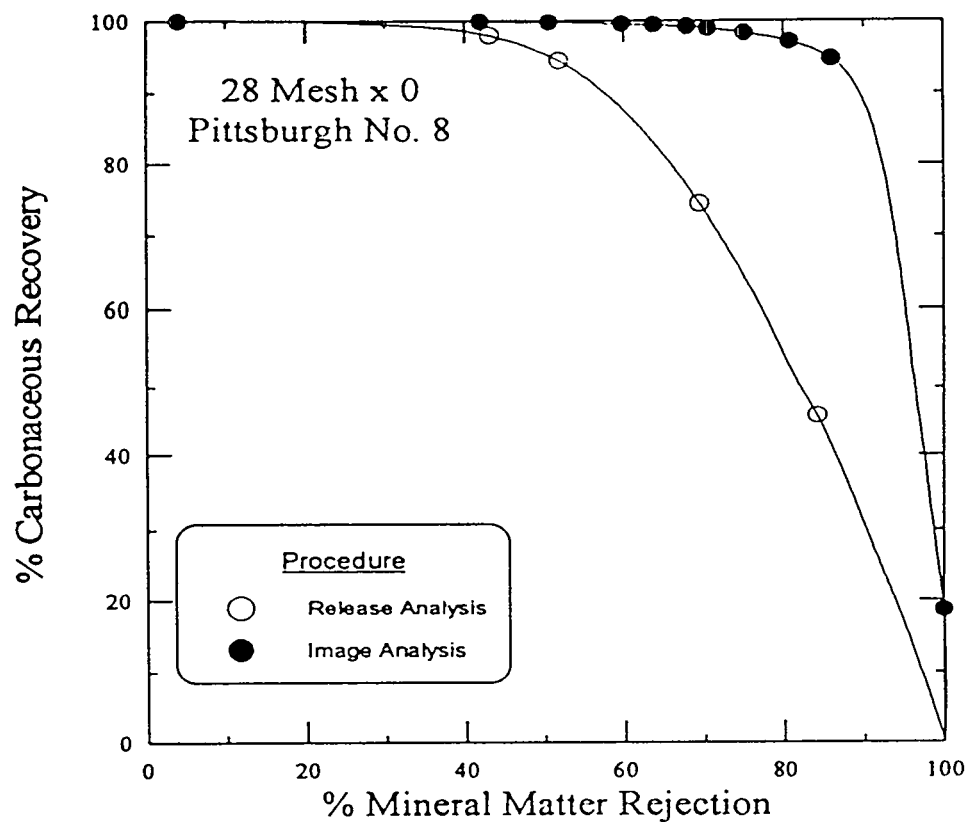


Figure 10. Comparison of release analysis and image analysis separation curves for mineral matter obtained using a -28 mesh Pittsburgh No. 8 coal.

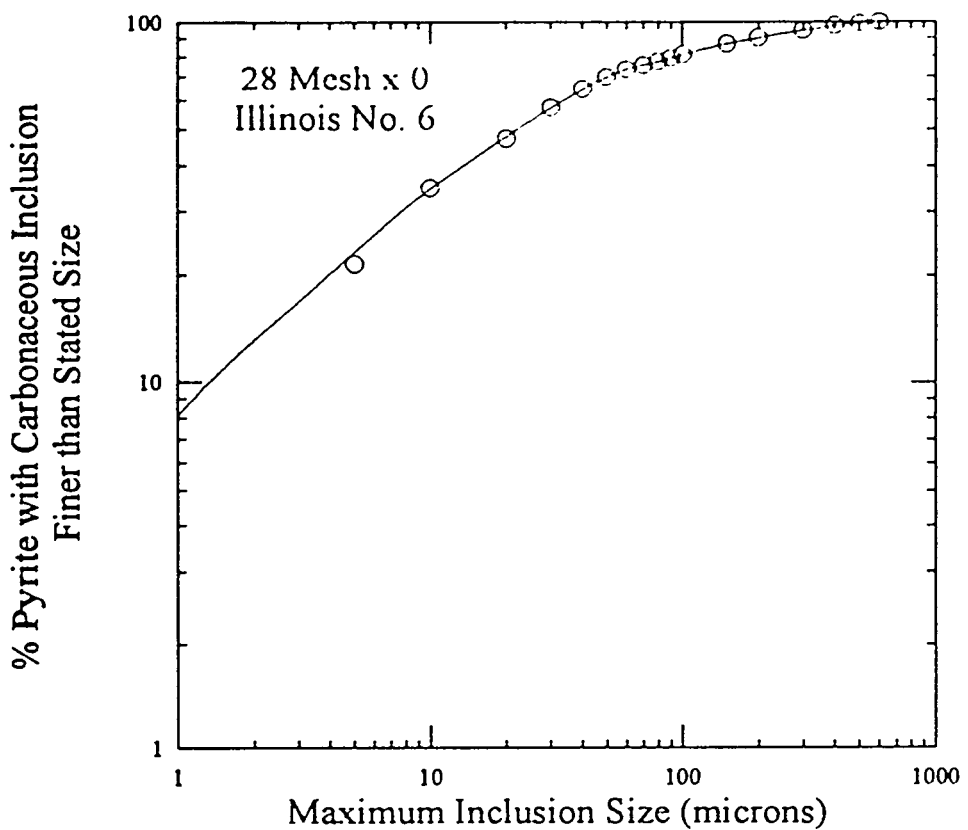


Figure 11. Weight percent pyrite containing carbonaceous inclusions finer than a given size obtained using a -28 mesh Illinois No. 6 coal.

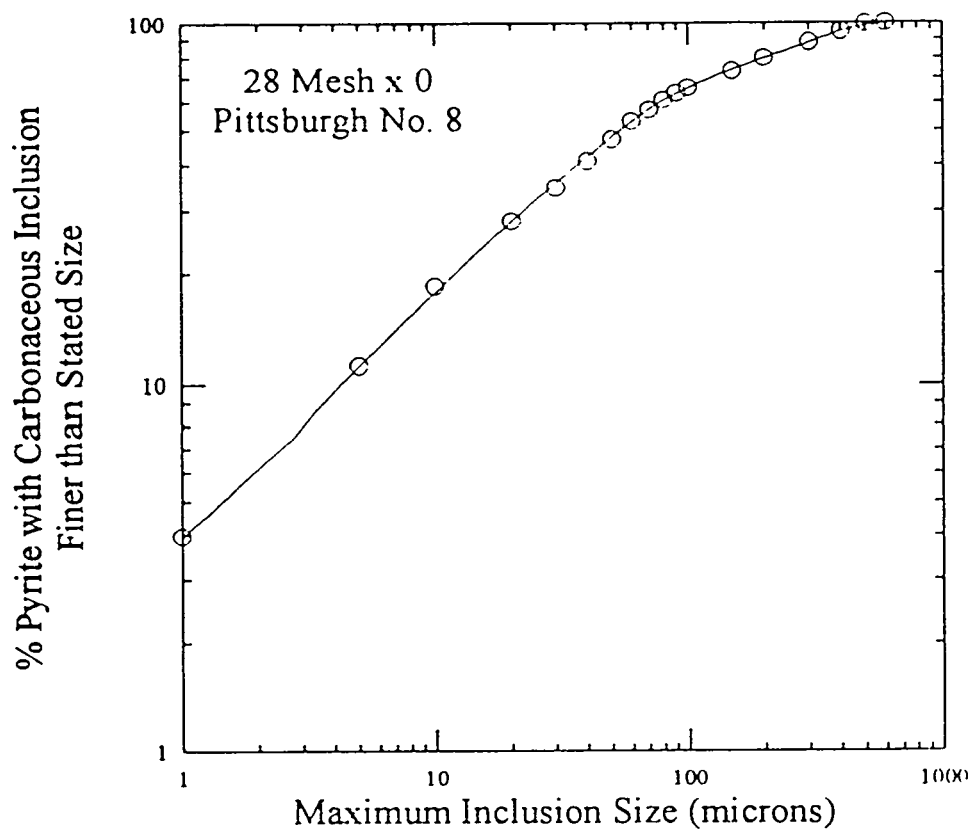


Figure 12. Weight percent pyrite containing carbonaceous inclusions finer than a given size obtained using a -28 mesh Pittsburgh No. 8 coal.

#### 4.3 Release Analysis Characterization

To characterize the potential performance of the flotation column in the ET Test Circuit, release analysis tests were conducted at several grind sizes for both the Pittsburgh No. 8 and Illinois No. 6 seam coals. The release analysis test provides an indication of the ultimate cleanability by flotation for a particular coal under a given set of reagent conditions. In the present work, the release analysis data provided a means by which the performance of the Microcel column could be evaluated. A Denver D-12 conventional flotation machine was used to conduct the release analysis tests. All products were analyzed for ash, total sulfur, sulfur forms, and heating value.

Each feed coal was pulverized in a laboratory hammer mill. Several different product size distributions similar to those used in the bench-scale circuit were used for the characterization work, i.e., 28 mesh x 0 and 65 mesh x 0. In addition, a 200 mesh x 0 grind size was examined for the Pittsburgh No. 8 seam coal. To determine the reliability of the release analysis test procedures, several duplicate tests were conducted on -65 mesh Illinois No. 6 seam coal. Results from these tests, shown in Figure 13, indicate that the release analysis procedure provides reproducible results. In this case, combustible recovery was plotted as a function of ash and sulfur rejection to normalize the effect of changes in feed quality.

Figure 14 shows the results of release analysis tests conducted on an Illinois No. 6 coal as a function of grind size (i.e., -28 and -65 mesh). As expected, an increase in product ash rejection is observed with a reduction in particle size; however, essentially no improvement was observed in sulfur rejection. This finding can be explained by either the inadequate liberation of pyritic sulfur, or the natural floatability of coal pyrite. The latter is the subject of an on-going DOE investigation (DE-AC22-92PC92246).

Figure 15 shows similar results for release analysis tests conducted on -28, -65 and -200 mesh Pittsburgh No. 8 seam coal. As shown, a slight improvement in product ash rejection occurs as the particle size is reduced. As with the Illinois No. 6 seam coal, particle size does not appear to dramatically impact the total sulfur rejection. These findings support the conclusion that a flotation-based separation process is acceptable for the rejection of ash-bearing minerals but is less effective for the removal of pyritic sulfur. As previously stated, a density-based separation would be more effective for the rejection of pyritic sulfur due to the large difference in specific gravities of coal and pyrite.

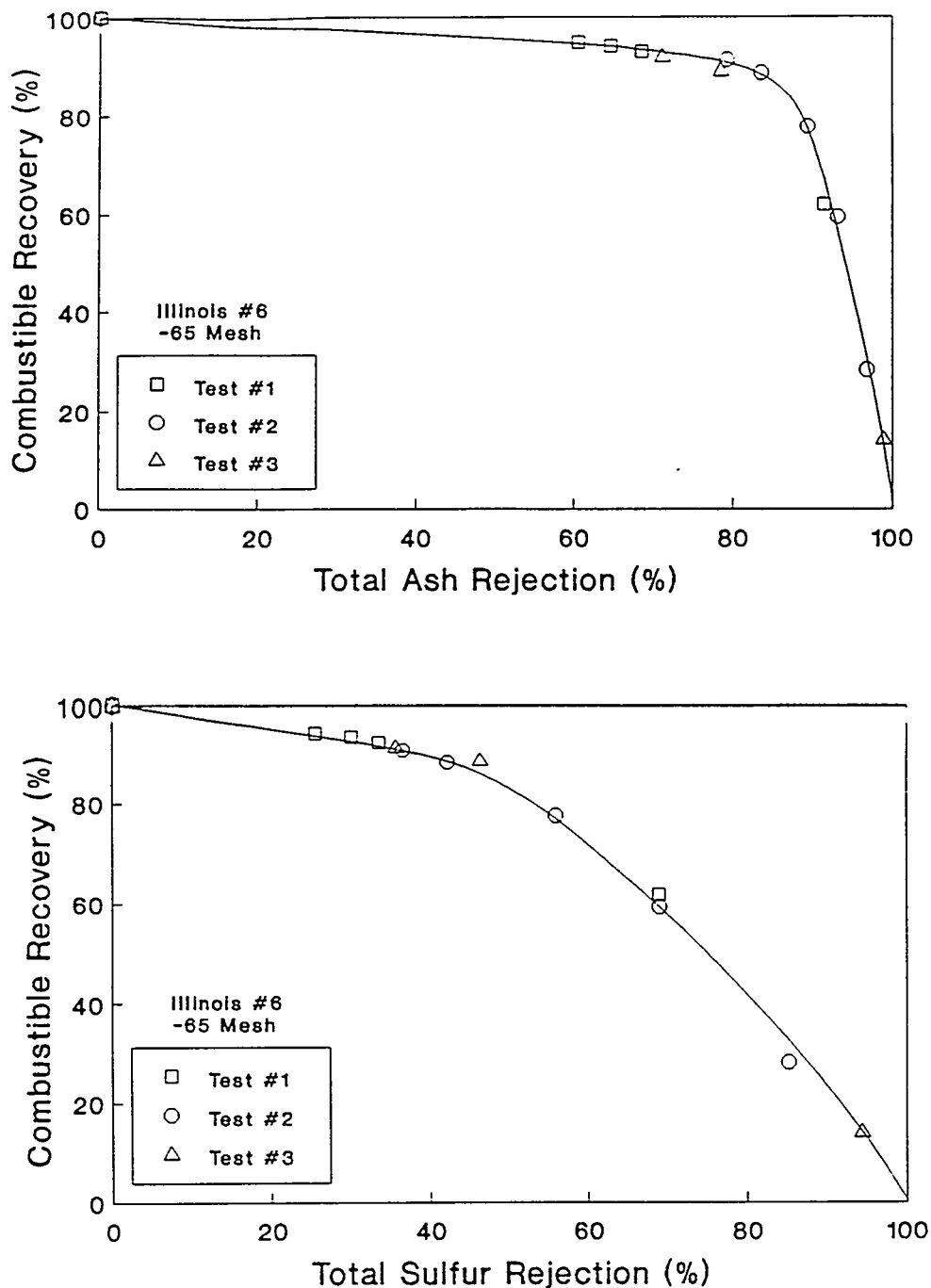


Figure 13. Combustible recovery versus total ash rejection (top) and total sulfur rejection (bottom) obtained from replicate release analysis tests on -65 mesh Illinois No. 6 coal.

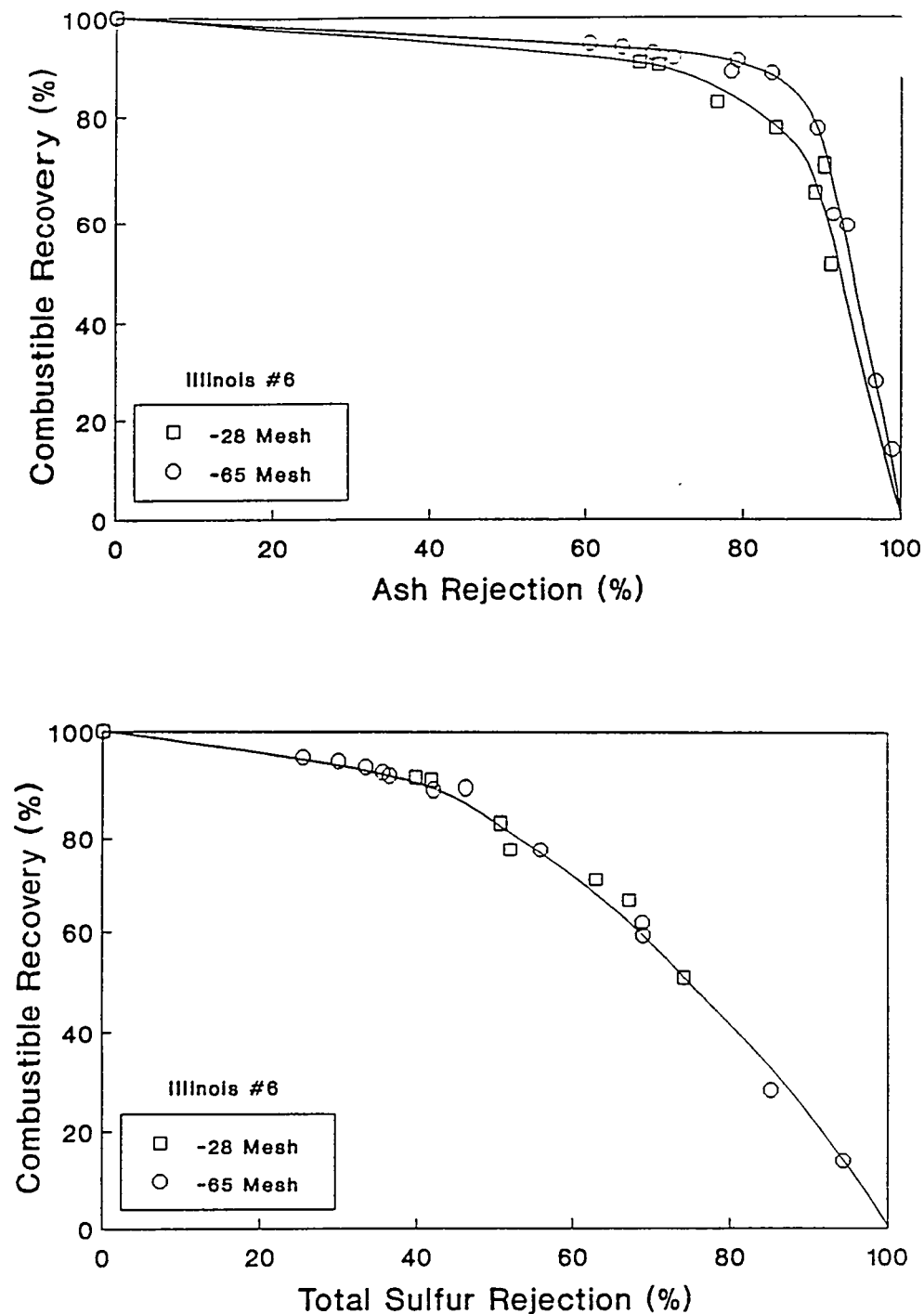


Figure 14. Combustible recovery versus ash rejection (top) and total sulfur rejection (bottom) obtained from release analysis tests on -28 and -65 mesh Illinois No. 6 coal.

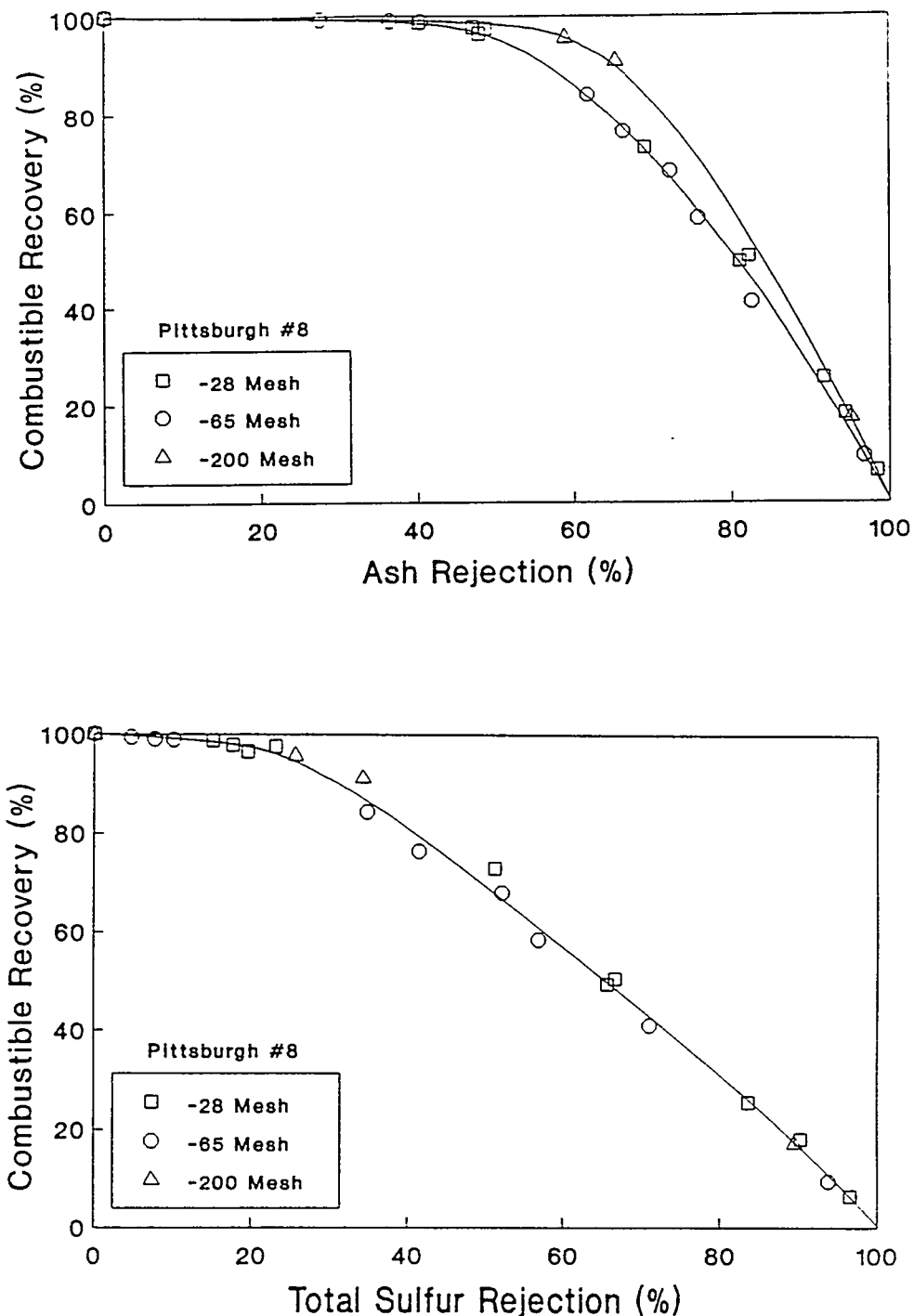


Figure 15. Combustible recovery versus ash rejection (top) and total sulfur rejection (bottom) obtained from release analyses tests on -28, -65, and -200 mesh Pittsburgh No. 8 coal.

## Task 5 - Flowsheet Development and Engineering Design

### 5.1 Flowsheet Development

This task began immediately after the approval of the project work plan. The work effort was shared by the prime contractor (CCMP) and the participating A&E firm (Roberts & Schaefer). Work elements completed in this subtask included:

- Calculations of mass and liquid flow rates based on particle size analyses and raw coal washability data currently available from the participating coal companies and other sources.
- Development of a flowsheet that summarizes the physical arrangement of the unit operations and connecting streams. Estimates of flow rates, solids contents, mean particle sizes, assays, etc., were provided on the basis of best available information.

The flowsheet was reviewed by the DOE COR and required modifications and revisions required to meet the project and environmental, safety and health (ES&H) objectives were incorporated prior to proceeding to subsequent design tasks.

### 5.2 Engineering Design

This subtask involved all activities related to the engineering design of the Microcel/MGS test circuit. This effort was primarily performed by Roberts & Schaefer. Work elements completed under this subtask included:

- Preparation of a detailed listing of required equipment including equipment type, unit size, throughput capacity, power requirements, air/water requirements, and operating limitations. Preliminary identification of potential vendors and suppliers were also made at this time.
- Development of an updated flowsheet that summarized the physical arrangement of all unit operations, connecting streams, valves, pumps, sampling points, process control instrumentation, etc. Complete material balances were projected for the entire circuit for each of the two base coals. The flowsheet specified expected flow rates, solids contents, mean particle sizes, assays, etc., for all streams.
- Development of engineering drawings detailing the construction, fabrication and installation of all components required to operate and evaluate the proposed unit operations and associated circuitry. These drawings unambiguously specified the spatial layout of equipment, location of electrical wiring, arrangement of piping and plumbing, and other pertinent electrical/mechanical requirements. These documents were of sufficient detail and quality to be utilized by the

mechanical/electrical subcontractor for the construction and assembly of the proposed circuitry.

- Preparation of an CPPRF Integration Plan/Schedule that outlined the specific requirements for integrating the proposed test circuit into the CPPRF.

Final approval of the proposed flowsheet, detailed engineering drawings, equipment specifications, plant layout, etc., were obtained from the DOE COR prior to the initiation of any additional work elements.

#### *5.2.1 Flowsheet Design*

The ET circuit was designed to allow for testing of the following four circuit configurations:

- Microcel only,
- Multi-Gravity Separator only,
- Microcel/Multi-Gravity Separator in combination, and
- Microcel/Water-Only Cyclone/Multi-Gravity Separator in combination.

The Microcel and MGS circuits were designed to allow for independent operation of each unit. This allows a direct comparison of the performance of each device to be obtained. The Microcel/MGS circuit will be used to determine the advantages of the combined processing scheme. In this circuit, the flotation product from the Microcel is de-aerated and fed directly to the MGS. The final circuit incorporates a water-only cyclone to remove a portion of clean-coal from the column product prior to feeding to the MGS. The intent of this circuit is to reduce the load to the MGS unit to provide a higher circuit throughput. The overall project test circuit is illustrated in Figure 16. The material-balanced flowsheets for each of the above described circuits are included in Appendix 1-A.

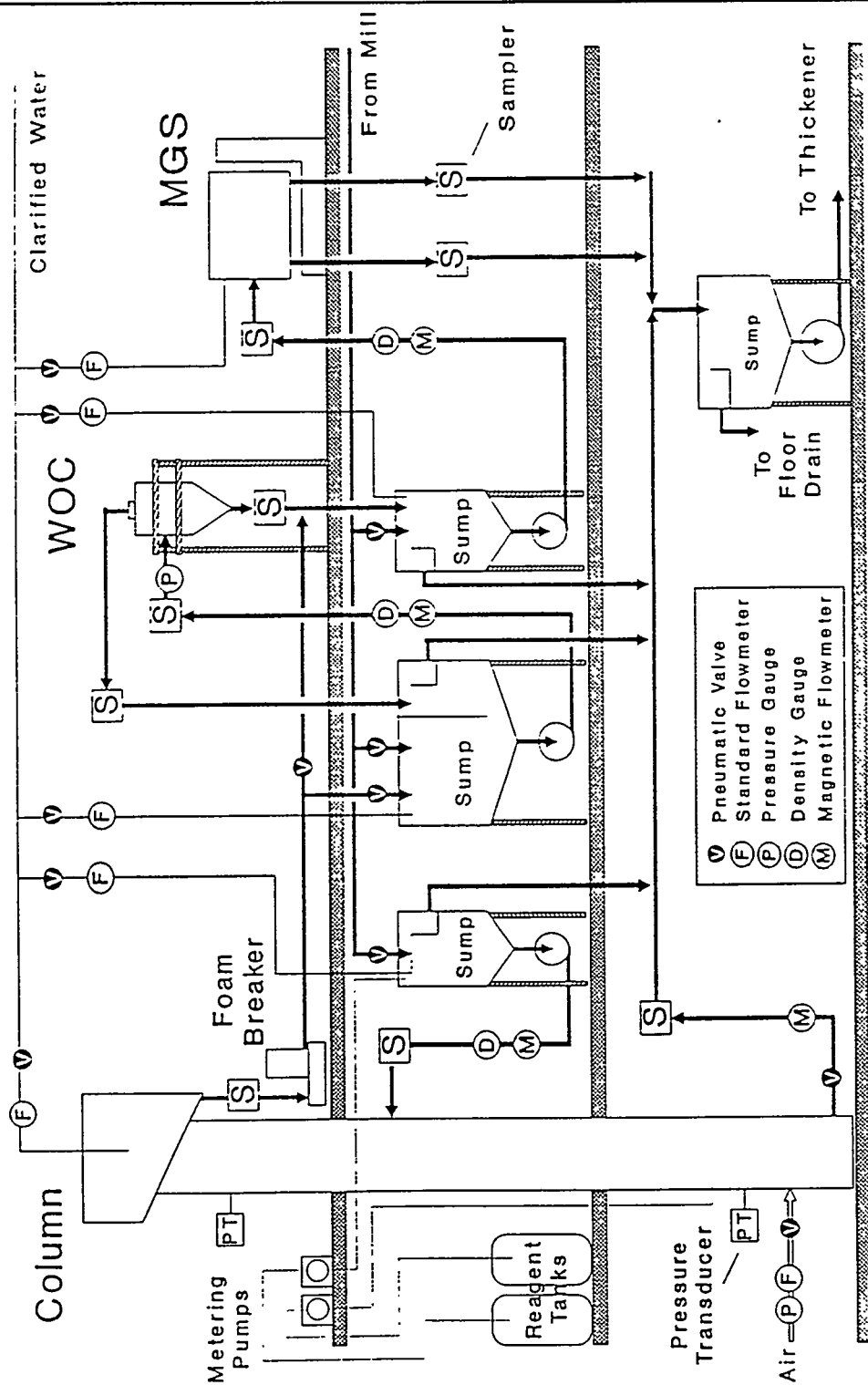


Figure 16. Flow diagram for the testing of the Microcel, MGS, Microcel/MGS and Microcel/WOC/MGS circuits.

Two different coal samples (Pittsburgh #8 and Illinois #6) were used for parametric testing in the various circuits. The bulk, run-of-mine samples were held at a nearby storage facility until required. This material was transferred by truck in 5-ton increments and off-loaded to the coarse coal storage bins at the CPPRF. The run-of-mine coal was fed from the storage silos to the CPPRF comminution circuit to produce feed slurries of various size consists for the ET circuit. Slurry entered the test circuit through a three-way automatic valve located above the CPPRF sludge storage tank, elev. 1106'-6". The automatic valve was configured to either send feed slurry to the ET circuit, or by-pass it into the sludge storage tank. From this point, the feed slurry could be directed to any of the three process feed sums (Unit No.'s 101, 102 and 103); thus allowing each circuit to be operated independently.

The process feed sums were arranged such that the Microcel, water-only cyclone or MGS could be independently operated. This approach allowed each device to be tested separately without being influenced by the performance of other unit operations. The process sums were equipped with side-mounted mixers to maintain the solids in a homogeneous suspension. In addition, the process sums have been designed with dish-shaped bottoms to facilitate mixing.

Each process sum was equipped with a variable speed (split sheave) pump to allow for variations in pressure and flow in each test circuit. Slurry from the pump discharge was circulated at relatively high velocities to the point of discharge and returned to the sum. This approach ensured that the solids remain in suspension throughout the circuit. Feed for each unit operation was bled-off the respective recirculation line through a pneumatic pinch valve. Feed rate to each unit operation was determined using mass flow sensors. Water addition lines were also provided for each sum to regulate the feed solids concentration solids. The flow rate of dilution water was regulated by pneumatic pinch valves.

Each sum/pump combination was equipped with a drain line and a constant head overflow box. These lines were directed to the ET waste sum located on ground floor (elev. 1086'-6"). In addition, the product and reject streams from all test circuits were discharged to the ET waste sum. Slurry from the waste sum was pumped either to the CPPRF thickener feed de-aeration tank or to the sludge tank. Emergency overflow lines from the waste sum were directed to the CPPRF's existing ground floor trenches and sent to the thickener via ground floor sum pumps.

### 5.2.2 Circuit Layout

The column/MGS circuit was planned for installation in the newly constructed mezzanine area adjacent to the ET test area and the temporary module stack previously installed and used by Process Technology, Inc. (PTI), for an earlier project. Detailed plan and elevation drawings

showing the equipment, instrumentation, piping and electrical layouts were previously provided to DOE and are included in Appendix 10. A complete listing of these drawings are given in Table 3.

Table 3. Complete listing of construction drawings provided to DOE for the ET circuit.

#### MECHANICAL - ET CIRCUIT

<u>R &amp; S Drawing No.</u>	<u>Title</u>
9234-L1	Layout - Plan Views
9234-L2	Layout - Elevation Sections
9234-L1A	Layout - Plan Views
9234-L2A	Layout - Elevation Sections
9234-P1	Piping - Plan Views
9234-P2	Piping - Elevation Sections
9234-P3	Piping - Typical Details

#### MECHANICAL - RAW COAL RECEIVING AREA

<u>R &amp; S Drawing No.</u>	<u>Title</u>
9234-L3	Layout of Plant Feed
9234-C1	Plant Feed Truck Ramp
9234-C2	Plant Feed Truck Ramp - Details
9234-PW1	18" Screw Feeder Receiving Hopper
9234-PW2	18" Screw Feeder Discharge Chute & Supports

#### ELECTRICAL

<u>R &amp; S Drawing No.</u>	<u>Title</u>
9234-E0	Motor Data Chart
9234-E1	Control Panel Layout
9234-E2	MCC Panel Layout
9234-E3	MCC Single Line
9234-E4	Instrumentation & Control Panel Wiring
9234-E5	MCC Panel Wiring
9234-E6	MCC Panel Wiring
9234-E7	Instrumentation & Control Panel Wiring
9234-E8	Instrumentation & Control Panel Wiring
9234-E9	Nuclear Density Unit Wiring Diagram
9234-PID	P&I Diagram

The construction drawings specified that the process waste sump/pump circuit be located on the ground floor (elev. 1086'-6). This allowed for gravity transport of slurry from all sump overflows, drain lines and unit operations. The process feed sums and Microcel base were to be located on the first mezzanine level (elev. 1096'-6). The MGS and cyclone feed sump/pumps were to be located on the existing PTI structure and the column feed sump/pump on the west side of the existing sludge storage tank. The latter was necessary to provide sufficient access around all process equipment. The Microcel base is located on elevation 1086'-6 and passes through the 1096'-6 elevation. The water-only cyclone was mounted directly to the cyclone feed sump. The column overflow weir, reagent feeders and MGS will be located on the second mezzanine level (elev. 11106'-6). The MGS was to be placed on the PTI structure, while the reagent feeders were located against the north wall of the facility.

The above described circuit layout was selected to minimize piping runs and installation costs and to maximize spacing between adjacent process equipment. The latter is necessary to allow for equipment maintenance and to ensure safe working conditions. In addition, this circuit layout provided an opportunity to reuse existing mechanical systems already installed by PTI.

#### *5.2.3 Piping*

The system utilities (i.e. compressed air, clarified water, and process water) were provided by DOE/PETC. Tie-in points to the CPPRF utility circuits were arranged with and approved by DOE/PETC prior to installation. Maximum anticipated utility consumption were determined as follows:

- Process Water - 50 gpm
- Air - 25 scfm @ 80 psi (process)  
10 scfm @ 80 psi (instrument)

All incoming utility piping was equipped with manual shut-off valves located at the tie-in points to completely isolate the test circuit if necessary. Water/slurry lines and pneumatic lines were constructed of CPVC (80 psi minimum rating) and schedule 40 steel (150 psi minimum rating), respectively. Diagrams showing the proposed piping layout were provided to DOE in the detailed construction diagrams.

#### *5.2.4 Instrumentation and Electrical*

Several different types of remote sensors were used in the ET test circuit. These include the following:

- Venturi Flow Meters,
- Magnetic Flow Meters,
- Nuclear Density Gauges,
- Paddlewheel Flow Meters,
- DP Cells, and
- Hi/Lo Level Indicators.

The venturi flow meter was used to meter air to the Microcel flotation column. A magnetic flowmeter and nuclear density gauge was used on the Microcel and MGS sump/pump recirculation systems to monitor mass flow rates. Paddlewheel flow meters were used exclusively for water flow measurement. The DP cells and High/Low level indicators were used for level detection in the Microcel and waste sump, respectively. All instrumentation will be equipped with a remote 4-20 mA signal output. In addition, a number of pneumatically-actuated control valves was used to regulate process liquid and slurry flow rates.

The ET circuit control panel was located on the second mezzanine level (elev. 1106'-6) next to the sludge storage tank. The control panel housed all of the necessary electrical and pneumatic instrumentation interfaces shown in Table 4.

Table 4. Control Panel Instrumentation

LED Displays	All water and slurry flow meters
	All density meters
	All pressure sensors
	Column air flow measurement
PID Controller for column level control	
Pressure regulators/gauges for pneumatic valve control	
Start/stop switches	All motor drives
Emergency stop button	

The bulk of the above described instrumentation and controls are provided for on-line sensing and operation. However, two stabilizing control loops were also installed in the ET circuit. The first is for control of column level. In this loop, a pressure reading provided by a DP cell was used to control the column tailings discharge rate which, in turn, was regulated by a pneumatic pinch valve. Valve response was controlled by a stand-alone PID controller. The fractional air hold-up was determined from differential pressure measurements in the column collection zone. Finally, a Hi/Lo sump level controller was installed on the ET circuit waste sump as a safety precaution. This controller prevented overflow and/or dry pumping conditions within the waste sump.

All power to the ET test circuit was supplied from a central motor control center (MCC) located on the east side of the sludge storage tank on elevation 1106'-6. A single supply line was connected to the ET MCC from the existing CPPRF MCC to power the test circuit. All equipment in the ET circuit was powered by the local MCC. This approach minimized the impact to the existing CPPRF MCC and facilitated installation of the test circuit. All electrical services had a Class II, Division II, Group F and a NEMA 4 rating and were not be interlocked to any existing CPPRF equipment.

### **5.3 Cost Analysis**

In this subtask, a detailed analysis was performed to provide an updated cost estimate for the proposed test circuit. The analysis included all capital expenditures as well as the cost of miscellaneous supplies, contractual labor, rental fees, etc. This subtask was carried out in conjunction with Subtask 5.2. A detailed listing of all major equipment was provided in Appendix 1-B. This listing provides unit dimensions, capacities and requirements for air, water and power for all of the unit operations included in the ET circuit.

### **5.4 ET Circuit Design Topical Report**

An ET Circuit Design Topical Report was prepared by CCMP and R&S after completing all work elements associated with the flowsheet development, engineering design, and cost analysis. This document provided all relevant material balance calculations, flow diagrams, engineering analyses, equipment specifications, cost analyses, estimation procedures, and construction/fabrication drawings.

In addition to the above, an Operation, Maintenance and Safety Manual was prepared for each of the key unit operations to be installed in the CPPRF. This document provided a brief technical description of the equipment, start-up and shutdown procedures, and recommended guidelines for safe operation.

As part of PETC's extensive EH&S program, two EH&S permits were required prior to the initiation of operations for this project. One was for the operation of the circuit and one was for the installation and operation of two nuclear density gauges. The first step toward acquiring the permit for the operation of the circuit was to conduct a system safety analysis (SSA) on the design of the circuit, prior to finalization of the design. This provided an opportunity to correct any design-related EH&S concerns at an early date when changes could easily and inexpensively be made. PETC EH&S specialists reviewed the required documents and provided detailed comments on the design and proposed operation. The design was then finalized based on this input. The second and final step for obtaining the EH&S permit for operation of the circuit as well as the EH&S permit for the nuclear sources was conducted when the installation of the circuit was nearly complete.

## Task 6 - Procurement and Fabrication

### 6.1 Bidding

The procurement and fabrication of all key components of the proposed circuitry began immediately upon approval of engineering drawings and specifications developed in Task 5. The prime contractor (CCMP) was responsible for directing the work conducted under this subtask, although some technical assistance was provided by the participating A&E firm (Roberts & Schaefer). The work elements undertaken in this subtask include:

- Preparation and solicitation of competitive bid packages for major purchases of equipment, materials, fabricated components, and services necessary to complete the installation of the proposed circuitry in the CPPRF.
- Review of bid packages and selection of appropriate vendors based on quoted cost, availability and suitability.

All bidding for services and high-value equipment was performed by R&S with input (e.g., bid specification, source identification, and bid review) from CCMP and Carpco.

### 6.2 Procurement/Fabrication

After appropriate vendors were selected on the basis of the competitive bidding process, the following work elements were initiated:

- Request to the DOE COR for the approval of purchases of equipment, supplies and contractual services.
- Prepare and issue all required purchase orders and requests for services.
- Procure and ship major equipment, fabricated components, materials, supplies, etc., to the test facility.
- Inspection of all purchased equipment, materials, and fabricated components to ensure that they are of suitable workmanship, and are structurally, mechanically and/or electrically operational.

Roberts & Schaefer performed much of the work in this subtask with the exception of procurement associated with the major equipment items (e.g., MGS and Microcel). However, all procurement actions were reviewed by CCMP to ensure that appropriate state and federal guidelines were followed.

## Task 7 - Process Module Installation

### 7.1 Installation/Construction

This work effort was jointly shared by the prime contractor (CCMP) and the participating A&E firm (Roberts & Schaefer). The preliminary draft of the Installation and Shakedown Plan was updated on the basis of information gathered since its original submission. After final approval of this plan, the work elements to be completed under this subtask were then initiated. A regional subcontractor, i.e., Rizzo & Sons, was competitively selected to perform the on-site construction activities. This effort involved the positioning of all major unit operations and associated installation of piping, electrical wiring, instrumentation, etc., as designated in the flowsheet developed in Task 5 (Flowsheet Development and Engineering Design). During the installation of the proposed test circuit, all pertinent local, state and federal regulations were followed by all participating subcontractors. A brief Schedule/Status Sheet was prepared weekly and provided to the DOE COR during the entire duration of this subtask. This document summarized the previous week's accomplishments and presented the planned work and objectives for the upcoming week.

### 7.2 Safety Analysis/Review

At the completion of on-site construction and prior to operation of the circuit, a final Safety Analysis and Review was performed. The System Safety Analysis conducted in Task 5 for the process circuit was revised and submitted to DOE along with standard operating methods and emergency shutdown procedures. These documents were used by DOE to ensure that all EH&S concerns were adequately addressed prior to issuing EH&S Permit for circuit operation and installing/operating the nuclear sources.

## Task 8 - Shakedown Testing

### 8.1 Start-Up

After completing Task 7 (Process Installation), shakedown tests were conducted to get the various unit operations up and running. Prior to the initiation of this effort, operator training was provided to ensure that all parties were familiar with standard operating procedures and emergency shutdown procedures. Several "dry" runs were conducted to evaluate the electrical and mechanical integrity of the test circuit. Water was then passed through the circuit for leak testing and establishing operating pressures. In addition, preliminary tests were performed to determine whether the pumping capacities, pipe sizes, electrical supplies, instrumentation/control systems, etc., were adequate. A complete and detailed listing of the activities to be carried out under this subtask were provided in the Installation and Shakedown Plan.

## **8.2 Exploratory Testing**

After completing the preliminary shakedown, a variety of exploratory test runs were undertaken. These tests were necessary in order to:

- evaluate the performance of the CPPRF grinding circuit in terms of capacity and product consistency,
- provide "hands-on" operator training prior to detailed testing,
- validate the design capacities for the various unit operations included in the test circuit,
- establish appropriate operating levels for the various process variables associated with the Microcel and MGS test units, and
- identify key operating parameters to be examined in the detailed testing program (Task 10).

During the exploratory tests, the Test, Sampling and Analytical Plan was updated and submitted to the DOE COR. This document specified the frequency, duration and types of test runs to be conducted using the Microcel and MGS units. The plan provided an overall sampling plan that specified the location of sampling points, frequency of sampling, sampling procedures, data logging requirements, and analytical techniques and procedures.

Because of the cooperative teaming arrangements required by this project, several different participants were on-site during a substantial portion of the shakedown testing. These included various technical personnel from CCMP, Carpco, and R&S. Personnel from CCMP were responsible for the start-up, operation and fine-tuning of the Microcel unit. Carpco provided the staffing and expertise necessary to properly start-up and operate the MGS unit. Preliminary tests were conducted on the MGS at the CCMP pilot plant to train operating personnel. Other components in the fine-coal circuitry, including additional pumps, sumps, screens, head tanks, reagent feeders, storage tanks, sampling devices, miscellaneous instrumentation, etc., were jointly operated and monitored by personnel from CCMP and R&S. Specific details related to this work are provided in the Installation and Shakedown Plan.

## **Task 9 - MGS Scale-Up**

### **9.1 Development of Scale-Up Criteria**

Reliable scale-up criteria have been developed for the Microcel column as a result of the work conducted in a previous DOE project (U.S. DOE DE-AC2289PC89909). This scale-up procedure has been successfully validated using Microcel columns from 2-inch to 10-foot in diameter. In addition, a

computer simulator has been developed at Virginia Tech which is capable of predicting the separation performance of the Microcel column for different feed coals. Unfortunately, much less is known about the scale-up of the MGS unit, particularly for applications involving the cleaning of fine coal. To overcome this problem, a simulation program has been developed in the present work (i) to identify the most desirable operating conditions for MGS and (ii) to assist in the sizing of the MGS for full-scale commercial applications.

#### *9.1.1 Identification of Operating Parameters*

Development of a process model for the MGS requires identification of the operating parameters which affect performance. A series of tests have been conducted at the CCMP to identify these parameters. The following key operating parameters have been identified: feed flow rate, feed solids content, wash water flow rate, drum rotation speed, tilt angle and shake amplitude.

The feed flow rate to the MGS affects both mass loading and retention time. As with most continuous processes, an increase in feed rate would increase the mass loading and decrease the retention time. This should lead to an overall decrease in coal recovery. This operating parameter is strongly dependent on the feed solids content. At a fixed volume feed rate, an increase in percent solids increases the mass loading within the unit. However, the overall retention time does not change. Thus, higher solids contents should allow higher capacities to be achieved without a reduction in capacity. Conversely, for a fixed mass feed rate of solids to the unit, an increase in percent solids should lower the volume flow rate and increase the retention time. This would lead to an increase in recovery.

Another important operating variable is wash water flow rate. Wash water is added at the lip of the drum to prevent low-density particles from discharging with the high-density fraction. This mechanism parallels the cross-flow of wash water used on conventional shaking tables for recovery of the coarse particles. This parameter is somewhat related to shake intensity/amplitude and tilt angle. The tilt angle represents the angle of decline of the drum axis towards the low-density product discharge end (typically 2-8 degrees). Tilt angle predominantly controls the rate at which material progresses through the drum. As a result, this parameter also influences the particle retention time. The shake intensity and amplitude are complementary in nature. Shake is applied in the axial direction with a sinusoidal wave form. The shaking action imparts an additional shearing action on the particles that aids in the particle stratification process.

Although many factors influence the overall performance of the MGS, the most important operating variable is the drum rotation speed. A higher drum speed increases the centrifugal field within the separator. The required drum speed is a function of the size and density of particles to be separated, i.e., finer particles typically require higher rotational speeds.

### *9.1.2 Population Balance Model Development*

In the present work, a microscopic population balance model was developed to describe the separation process in the MGS under steady-state operating conditions. Basically, the MGS unit can be divided into four zones along its axial length. There are two main zones in which the separation takes place. The primary concentration takes place in zone III (rougher zone) and the final concentration takes place in zone II (cleaner zone). In one cycle, high-density particles along with entrapped low-density particles settle down in the low-velocity region of the flowing film. The scraper imparts a counter-current movement, transporting the settled particles upstream towards the high-density discharge lip. However, the movement of the scraper not only causes transport towards the high-density discharge, but also brings the settled particles into the high-velocity region of the flowing film. This sequence of settling and scraping enhances the separation of low-density particles from high-density particles. In zones I and IV, the transport of the concentrate and waste particles takes place.

Model equations representing the particles in terms of size and specific gravity have been developed by conducting a volume balance around each zone in the MGS. Each equation considers terms that describe the movement of the solid particles due to fluid flow, buoyancy or gravity, as well as the scraping action. The operating and design variables are incorporated in the model with an aim to predict the performance of the unit and aid in scale-up.

### *9.1.3 Population Model Development*

The separation of high-density particles from low-density particles in a MGS is dependent on the settling velocity of the particles, flow rate of the slurry and scraping/ploughing rate. In modeling the MGS, the separation can be described in terms of the flow pattern along the axial length of the rotating drum (x-direction) and also along the thickness of the flowing film (z-direction). Although there are two main zones of separation, the only difference in the two zones is the flow rate of the slurry. The flow rate in the rougher zone (zone III) is higher than that of the flow rate in the cleaner zone (zone II). To model these zones, a generalized microscopic population balance model can be written based on simple volume balances. In the present work, it is assumed that the slurry leaving zone II reports to the high-density product and the slurry leaving zone III reports to low-density product. A list of symbols used in the model derivation are given in Table 5.

Table 5. Nomenclature used in the development of the population balance model for the MGS.

A	=	cross-sectional area of the MGS
$Q_f$	=	total volumetric flow rate of feed pulp
$Q_w$	=	total volumetric wash water flow rate
$Q_l$	=	total volumetric flow rate reporting to lights
$Q_b$	=	total volumetric flow rate reporting to heavies
$Q_{d2}$	=	upward flow rate from zone III to zone II
$k_1$	=	scraping distance
$s_w$	=	scraper width
$F_1$	=	percent solids content in the z-direction
$\Phi$	=	volume fraction solids
$v_t(\psi)$	=	terminal settling velocity of the particle
$\delta$	=	average particle diameter
$\theta$	=	flowing film thickness in the z-direction at L
$F_c$	=	centrifugal force acting on a particle
$m$	=	particle mass
$r$	=	drum radius
$\omega^2$	=	drum angular velocity
D	=	drum diameter
N	=	drum rotational speed (rpm)
$\rho$	=	particle specific gravity
W	=	volumetric fluid flow per unit time and unit depth
$\Delta$	=	specific gravity of the slurry
$\alpha$	=	angle of drum tilt
$\psi(\text{feed})$	=	number concentration in the feed
$\psi(\delta, \rho, x, z)$	=	number concentration of particle size, $\delta$ , of the specific gravity class, $\rho$ , at the position $x$ and $z$
$\psi_h$	=	number concentration in the heavies
$\psi_l$	=	number concentration in the lights

The generalized microscopic population balance model can be expressed by:

$$\frac{d\psi}{dt} + \frac{d}{dx}(\nu_x \psi) + \frac{d}{dy}(\nu_y \psi) + \frac{d}{dz}(\nu_z \psi) + \sum_{i=1}^j \frac{d}{d\xi_i}(\nu_j \psi) + \dot{D} + \dot{A} = 0$$

Terms      I       $\rightarrow$       II       $\leftarrow$       III      IV

In this model, the properties of interest are size ( $\delta$ ) and specific gravity ( $\rho$ ). It is inherently assumed that there are no continuous or discrete changes in particle size within the separator. Also, the system is assumed to be operating under steady-state conditions. For simplicity, the system has been assumed to be operated under plug-flow conditions in the x- and z- directions and is completely mixed in the y-direction. Based on these restrictions, the various terms in the population balance model can be derived as follows.

$$\text{Term I} = 0$$

$$\text{Term II} = \frac{d}{dx}(\nu_x \psi)$$

$$= \frac{d}{dz}(\nu_z \psi)$$

$$\text{and } \frac{d}{dy}(\nu_y \psi) = 0$$

$$\text{Term III} = 0$$

$$\text{Term IV} = 0$$

Thus, the overall model equation simplifies to:

$$\frac{d}{dx} (v_x \psi) + \frac{d}{dz} (v_z \psi) = 0$$

$$v_x \frac{d\psi}{dx} + \psi \frac{dv_x}{dx} + v_z \frac{d\psi}{dz} + \psi \frac{dv_z}{dz} = 0$$

The velocity along the axial length ( $v_x$ ) consists of two components; (i) a flow component in the positive x-direction towards the low-density end of the drum,  $v_f = f(x)$ , and a scraping component in the negative x-direction,  $v_{sc} = f(x)$ . The flow component,  $v_f$ , can be determined by calculating the volumetric flow passing through each zone of the MGS. A total volumetric flow balance around the MGS gives:

$$Q_f + Q_w = Q_l + Q_h$$

Since the main purpose of adding wash water is to prevent the entrainment of low-density particles, it is logical to assume that all of the wash water added in zone II would report to zone III. There is an internal flow from zone III to zone II and vice versa. The net flow ( $Q_{\Omega}$ ) would be in the negative x-direction flowing from zone III towards zone II. The flow component  $v_f$  in zone II and III can be written as follows:

For  $0 \leq x \leq L$ :

$$v_f = -\frac{Q_{\Omega} + Q_w}{A}$$

For  $L \leq x \leq M$ :

$$v_f = \frac{Q_f + Q_w - Q_{\Omega}}{A}$$

The scraping component ( $v_{sr}$ ) can be determined from the pitch of the scraper and the thickness of the bottom layer of the flowing film. The scraper is pivoted towards the scraper arm. The position of the scraper is dependent on the radial speed of the arm. The scraper arm rotates at a 5% higher speed than the drum. Hence, the pitch of the scraper is a function of the drum speed. The thickness of the bottom layer of the flowing film depends on the settling rate. The thickness of the bottom layer can either be expressed in terms of percent solids in the z-direction or determined from the force balance on the particles at different positions in the z-direction. This dictates that:

$$v_{sr} = kI * FI$$

where,

$$kI = \frac{2\pi r}{4 * sw} * 1.05 * sw$$

$$sw = f(\text{drumspeed})$$

$$FI = f(\text{ploughing action, feed \% solids, settling rate})$$

Therefore, the velocity component in the x direction can be written as:

$$v_x = v_f - v_{sr}$$

For  $0 \leq x \leq L$ :

$$v_x = -\frac{Q_p + Q_w}{A} - (kI * FI)$$

For  $L \leq x \leq M$ :

$$v_x = \frac{\rho_f + \rho_w - \rho_p}{A} - (kI * FI)$$

The velocity along the thickness of the flowing film ( $v_z$ ) consists of two components; a settling component in the negative  $z$ -direction towards the bottom of the drum),  $v_s = f(z)$  and a ploughing action component in the positive  $z$ -direction,  $v_p = f(z)$ . The settling component,  $v_s$ , is a function of particle size, specific gravity and the flow characteristics, i.e.:

$$v_s(\psi) = v_t(\psi) * (1 - \phi)^{3.65}$$

The Richardson & Zaki equation has been used to represent the hindered settling of the particles within the settled bed, i.e.:

$$v_s(\psi) = v_t(\psi) * (1 - k_v \int_0^a \delta^3 \psi d\delta)^{3.65}$$

The ploughing action,  $v_p$ , brings the settled particles into the high-velocity region of the flowing film. This action can be described by:

$$v_p = kI * \Theta$$

where,

$$\Theta = \left[ \frac{3\mu * W}{\Delta g \sin \alpha} \right]^{1/3}$$

Therefore, the velocity component in the  $z$ -direction can be written as:

$$v_z = v_p - v_s$$

$$v_z = (kI * \Theta) - (v_t(\psi) * (1 - k_v \int_0^a \delta^3 \psi d\delta)^{3.65})$$

Using all of the aforementioned mathematical expressions, the final modeling expression for the MGS can be rewritten as:

For  $0 \leq x \leq L$ :

$$\begin{aligned}
 & I \\
 & \left[ \left( \frac{Q_p + Q_w}{A} \right) \right] \frac{d\psi}{dx} + \psi \frac{d}{dx} (-kI * fI) \\
 & + \left[ (kI * \Theta) - \left[ v_t(\psi) * (1 - k_v \int_0^x \delta^3 \psi d\delta)^{3.65} \right] \right] \frac{d\Psi}{dz} \\
 & + \psi \frac{d}{dz} \left[ \left[ (kI * \Theta) - \left[ v_t(\psi) * (1 - k_v \int_0^x \delta^3 \psi d\delta)^{3.65} \right] \right] \right] = 0
 \end{aligned}$$

For  $L \leq x \leq M$ :

$$\begin{aligned}
 & II \\
 & \left[ \left( \frac{Q_p + Q_w}{A} \right) - (kI * fI) \right] \frac{d\psi}{dx} + \psi \frac{d}{dx} (-kI * fI) \\
 & + \left[ (kI * \Theta) - \left[ v_t(\psi) * (1 - k_v \int_0^x \delta^3 \psi d\delta)^{3.65} \right] \right] \frac{d\Psi}{dz} \\
 & + \psi \frac{d}{dz} \left[ \left[ (kI * \Theta) - \left[ v_t(\psi) * (1 - k_v \int_0^x \delta^3 \psi d\delta)^{3.65} \right] \right] \right] = 0
 \end{aligned}$$

Boundary conditions for the model include:

$$x = L; z = \theta; \quad \psi = \psi_f \text{ (Feed)}$$

$$x = 0; \quad \psi = \psi_h \text{ (I) High-Density Component}$$

$$x = M; \quad \psi = \psi_l \text{ (II) Low-Density}$$

The model derived in the present work assumes that the separation process in the MGS takes place due to particle transport. Thus, the final model equation is written in terms of velocity

distributions in the x- and z-directions. Unfortunately, there are certain terms in the model which are yet to be completely defined. The internal net flow ( $Q_\Omega$ ) from zone III to zone II has to be evaluated. The volume of the material in the bottom layer of the flowing film that is being transported upstream by the scraper is presently assumed to be a function of the solids content in the z-direction. A mathematical relationship between this parameter and the operating and design variables has not yet been derived.

## 9.2 Scale-Up Validation

Because of limitations associated with the identification of unknown modeling terms in the population balance model, an overall scale-up model for the MGS could not be completed under the allotted project schedule. However, the data collected to date indicates that the unit capacity of the MGS is proportional to the square of drum diameter and directly proportional to drum speed. Based on this observation, a preliminary scale-up plot has been constructed based on the test data obtained using the Pittsburgh No. 8 and Illinois No. 6 coal seams. This plot, which is shown in Figure 17, suggests that a full-scale, twin-drum MGS unit would be capable of processing approximately 25 tph of fine coal. Validation of these assumptions through additional testing at various feed flow rates using units of different diameters is recommended for future research and development projects.

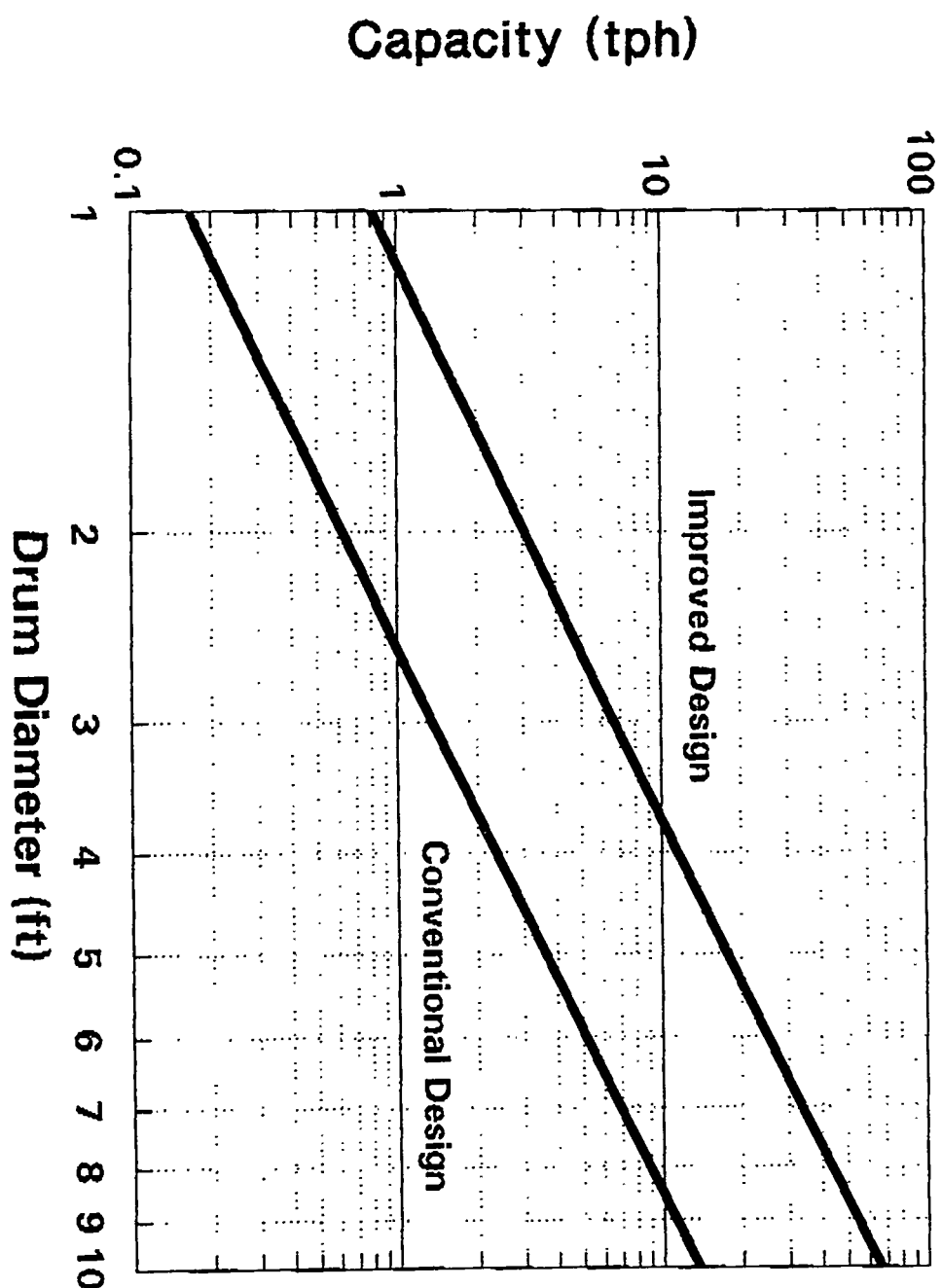


Figure 17. Approximate MGS capacities for fine coal cleaning.

### Task 10 - Detailed Testing

Detailed testing of the proposed circuitry was initiated after the successful completion of shakedown and exploratory testing. The primary objective of this work was to investigate the effects of various operating parameters on the performance of the Microcel, MGS, combined Microcel/MGS, and combined Microcel/MGS/WOC circuits. Test runs were carried out in accordance with Test, Sampling and Analytical Test Plan approved by the DOE COR. Statistically designed sets of experiments were used throughout the detailed testing program. The emphasis of the parametric testing was to characterize and optimize the performance of the MGS unit both with and without the precleaning operations (i.e., Microcel column and water-only cyclone).

Personnel from the prime contractor (CCMP) and Carpco were on-site for most of the duration of the detailed test work. These participants were responsible for the day-to-day operation of the proposed circuitry, implementation of the test program, analysis of test samples, and interpretation of the test data. Periodic assistance in operating the circuit was also provided by personnel from R&S. The participating coal companies provided advice for formulating the test program and assistance in the interpretation of the experimental data as it became available. Brief weekly Schedule/Status Reports were prepared and submitted to the DOE COR throughout the duration of this task to assist in on-site monitoring of project progress.

The first series of tests were carried out using only the Microcel flotation column. These tests examined the effects of reagent dosage, feed size and feed rate on column performance. In each test run, the flow rates of feed slurry, air, water and reagents were set at the predetermined levels established by the test plan. The column was allowed to operate at these settings until steady-state conditions were reached. This normally required about 30-45 minutes of uninterrupted operation (i.e., 2-3 slurry retention times). During steady-state operation, representative samples of the feed, clean-coal and reject streams were collected using standard sampling techniques, dried and subjected to ash, total sulfur, pyritic sulfur and heating value analyses.

The second series of tests were conducted using only the MGS unit. A much broader test program was undertaken for the MGS due to the lack of acceptable operating guidelines for coal cleaning applications. Operating parameters examined for the MGS included feed size, drum speed, wash water rate, feed solids content and feed rate. After setting these parameters at the predetermined levels established by the test plan, the MGS was allowed to operate for a period of time sufficient to reach steady-state conditions. Incremental sampling during several test runs at the CPPRF indicated that steady-state conditions were normally reached after about 45-60 minutes of uninterrupted operation. After this period of time, representative samples of the feed, clean-coal and reject streams were collected using standard sampling techniques, dried and subjected to ash, total sulfur, pyritic sulfur and heating value analyses.

After identifying the key operating parameters for the Microcel and MGS units, testing began on the combined circuit in which the Microcel froth product was recleaned by the MGS unit. Parameters examined in this series of tests included Microcel feed rate, MGS feed rate, MGS drum speed, MGS wash water rate and MGS shake amplitude. As before, the circuit was operated for a period of time sufficient to ensure that steady-state conditions had been achieved. The optimum operating settings identified in the combined Microcel/MGS tests were then used for a long-duration run of the combined circuit.

Two different feed coals, i.e., Pittsburgh No. 8 and Illinois No. 6, were used in each series of parametric tests. The chronological order of testing for the Pittsburgh No. 8 seam coal was as follows: (i) parametric testing of the independent Microcel and MGS units, (ii) parametric testing of the combined Microcel/MGS circuit, and (iii) long-duration testing of the combined Microcel/MGS circuit. An identical sequence of unit testing was then repeated for the Illinois No. 6 seam coal. Table 6 summarizes the systematic approach that was used in assigning test run identification numbers throughout the detailed test program.

The effectiveness of each coal cleaning unit was quantified using a variety of performance indicators. These included clean-coal yield, combustible recovery, energy recovery, ash rejection, total sulfur rejection, pyritic sulfur rejection and separation efficiency. In all cases, these values were calculated from the assay values obtained from samples of the clean coal, tailings and feed streams. A complete listing of the calculation formula used in the present work are provided in Table 7. A commercially available mass-balancing program (BILMAT) was used to adjust all of the assay values so that a self-consistent set of experimental data was obtained in each test run. Assay values which did not balance well were considered to be unreliable and were eliminated from the data set.

Table 6. Numbering system used for the detailed testing program.

TEST NUMBER RANGES	CIRCUIT	COAL SEAM
101-199	Microcel Only	Pittsburgh #8
201-299	MGS Only	Pittsburgh #8
301-399	Microcel Conc. to MGS	Pittsburgh #8
PITT-LD	Microcel Conc. to MGS	Pittsburgh #8
401-499	Microcel Only	Illinois #6
501-599	MGS Only	Illinois #6
601-699	Microcel Conc. to MGS	Illinois #6
ILL-LD	Microcel Conc. to MGS	Illinois #6

Table 7. Performance expressions used in the present work.

Performance Indicator	Calculation Formula
Clean Coal Yield (%)	$Y_p = 100 \frac{(A_f - A_t)}{(A_p - A_t)}$
Combustible Recovery (%)	$R_{comb} = 100 Y_p \frac{(100 - A_p)}{(100 - A_f)}$
Energy Recovery (%)	$R_{BTU} = 100 Y_p \frac{BTU_p}{BTU_f}$
Ash Rejection (%)	$J_{ash} = (100 - Y_p) \frac{A_t}{A_f}$
Sulfur Rejection (%)	$J_{sulfur} = (100 - Y_p) \frac{S_t}{S_f}$
Pyritic Rejection (%)	$J_{pyritic} = (100 - Y_p) \frac{P_t}{P_f}$
Ash Separation Efficiency (%)	$SE_{ash} = R_{BTU} - (100 - J_{ash})$
Sulfur Separation Efficiency (%)	$SE_{sulfur} = R_{BTU} - (100 - J_{sulfur})$
Pyritic Separation Efficiency (%)	$SE_{pyritic} = R_{BTU} - (100 - J_{pyritic})$

Nomenclature:

$A_p$ ,  $A_t$ ,  $A_f$  = Ash contents of the coal product, tailings and feed streams.

$BTU_p$ ,  $BTU_t$ ,  $BTU_f$  = Energy contents of the coal product, tailings and feed streams.

$S_p$ ,  $S_t$ ,  $S_f$  = Total sulfur contents of the coal product, tailings and feed streams.

$P_p$ ,  $P_t$ ,  $P_f$  = Pyritic sulfur contents of the coal product, tailings and feed streams.

After completing each set of parametric tests, statistical analyses of the experimental test data were carried out using a commercially available software package from the Stat-Ease Corporation known as Design-Expert. The program was used to create the test matrices and to perform all required statistical computations and regression analyses. The first step in the statistical analysis involved the determination of influence of each test variable on circuit performance. This was carried out by fitting the test data using a linear regression model. In general, a large coefficient in the linear regression model indicates that the given variable has a

large influence on the response in question. The second step in the statistical analysis involved the development of empirical models for each test circuit. These models are capable of predicting circuit response (e.g., energy recovery, ash rejection, separation efficiency, etc.) as a function of various operational settings (e.g., feed rate, drum speed, frother dosage, etc.). In each case, data fitting was performed using a standard quadratic regression model. Although cubic models typically provided a better overall fit, quadratic models were preferred since they provided reasonably good correlations, minimized model complexity, and reduced aliasing of the model coefficients. The data fitting procedure was an iterative process since, in most cases, several analyses were required in order to obtain a suitable relationship between the operating variables and circuit performance. After selecting an appropriate model (i.e., linear, quadratic or cubic), a variety of statistical routines were executed to identify the goodness-of-fit. For all runs, the values of regression coefficients, standard errors, variances, t-tests, etc., were determined as a means of quantifying the statistical significance of each of the coefficients in the model. In general, good correlations were obtained between the model predictions and experimental results.

After acceptable empirical models were developed for each series of test runs, the resultant mathematical relationships were plotted using a three-dimensional graphics routine. The response surface plots allow the joint influence of the various operating parameters on circuit response to be readily visualized. In the present work, response surface plots were developed for combustible recovery, energy recovery, ash rejection, total sulfur rejection, pyritic sulfur rejection, separation efficiency, and weight of sulfur dioxide per unit heating value.

## 10.1 Microcel Parametric Testing

In this subtask, the key operating parameters associated with the operation of the Microcel column were examined using a statistically designed set of experiments for each coal. The results of these tests are discussed in the following sections.

### 10.1.1 *Testing of Pittsburgh No. 8 Coal*

A three-level Box-Behnken experimental design was used to evaluate the performance of the Microcel flotation column for upgrading a run-of-mine sample of Pittsburgh No. 8 seam coal. Parameters examined in this series of tests included grind size, feed flow rate and frother dosage. The test matrix for the parametric study is provided in Table 8. A summary of the test results and performance calculations is provided in Appendix 2-A.

Table 8. Parametric test matrix used to investigate the performance of the Microcel column for the Pittsburgh No. 8 seam coal.

#### Microcel Conditions Held Constant

Collector Dosage (lbs/ton):	1
Wash Water (lpm):	40.13
Percent Solids (w/w):	11-12
Air Flow Rate (SCFM):	9.01

#### Microcel Variables

Test Number	Feed Size (microns)	Feed Rate (lbs/hr)	Frother Dosage (ml/min)
101	300	300	1.00
102	300	400	0.50
103	300	500	1.00
104	300	400	1.50
105	200	400	1.00
106	200	500	0.50
107	200	500	1.50
108	200	400	1.00
109	100	300	1.00
110	100	400	0.50
111	100	500	1.00
113	200	300	1.50
114	200	400	1.00
116	200	300	1.50
117	200	400	1.00

Figure 18 shows the combustible recovery obtained from the Box-Behnken tests as a function of the rejections of ash, total sulfur and pyritic sulfur. Although the flotation tests were conducted over a wide range of operating conditions, most of the experimental data points fell along distinct recovery-rejection curves. Although not shown, the test results generally fell just below the performance curve established by release analysis. The "knee" or "elbow" in each separation curve was found to correspond to the point of maximum separation efficiency. The test data suggest that a 90% energy recovery would provide an ash rejection of nearly 70%. At the same energy recovery, a total sulfur rejection of approximately 25% and pyritic sulfur rejection of 65% would be achieved using the Microcel column. It is also interesting to note that the Box-Behnken test data indicate that several different combinations of operating parameters can be used to achieve the same level of separation performance. This implies that other factors (e.g., column capacity, operating cost, maintenance considerations, etc.) should be used to select the preferred column operating point.

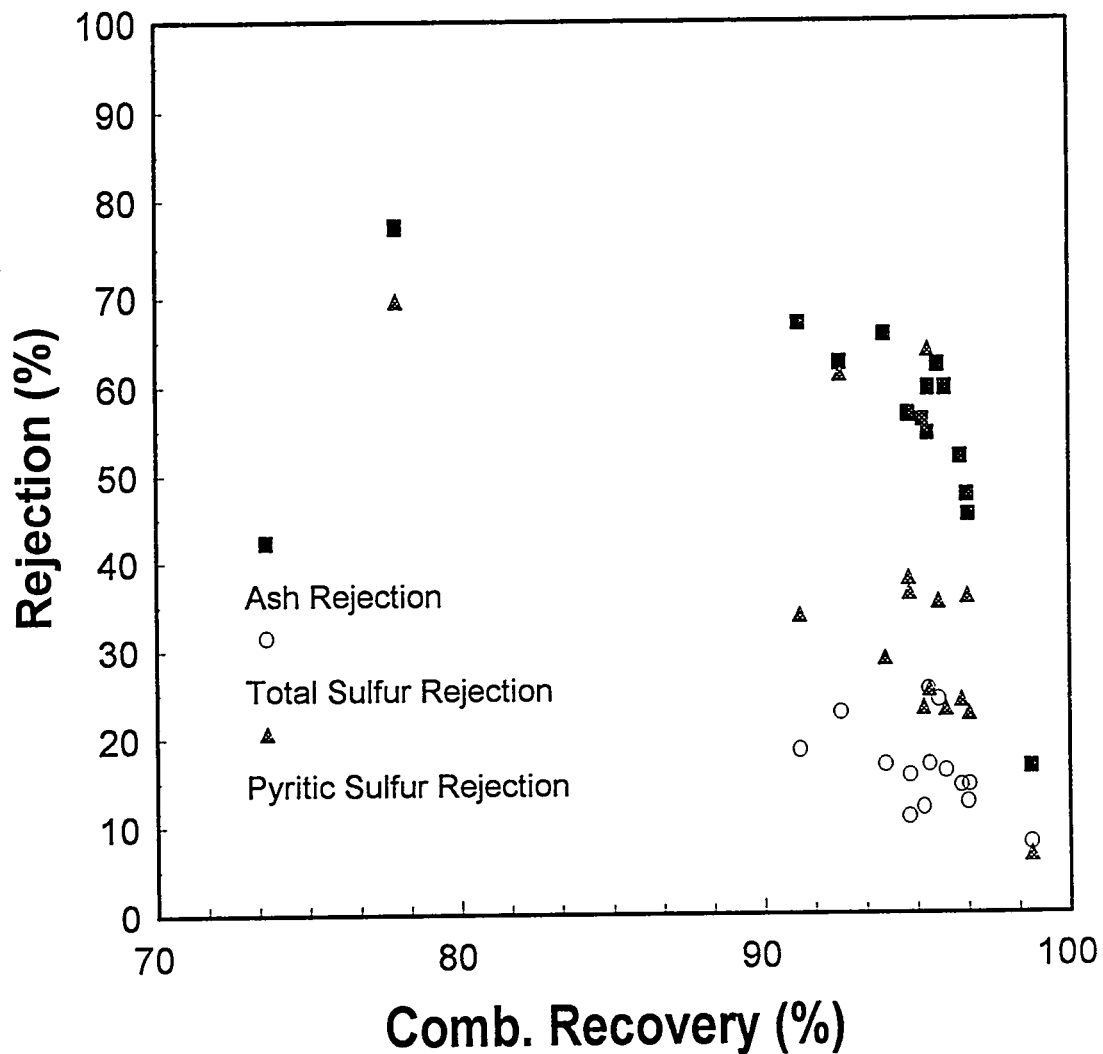


Figure 18. Combustible recovery versus rejection plots for the parametric testing of the Pittsburgh No. 8 seam coal using the Microcel flotation column.

The statistical analyses for the testing of the Pittsburgh No. 8 seam coal by Microcel column flotation is provided in Appendix 3-A. The correlation matrix, which shows the correlation between each of the operating variables and column performance, is given in Table 9. The test data indicate that higher frother dosages produced a very large increase in coal recovery. The higher dosage of frother produced smaller air bubbles which increased recovery by improving both the flotation kinetics and froth carrying capacity. An increase in particle size or feed flow rate resulted in a lower coal recovery, although the impact of these parameters were small compared to that obtained by varying frother dosage.

Table 9. Correlation matrix for the testing of the Pittsburgh No. 8 seam coal using Microcel column flotation.

Process Response	Process Variable		
	Increasing Particle Size	Increasing Feed Rate	Increasing Frother Dosage
Comb. Recovery	S↓	M↓	L↑
Energy Recovery	S↓	S↓	L↑
Ash Rejection	S↑	L↑	L↓
Sulfur Rejection	S↓	L↑	L↓
Pyritic Rejection	L↓	L↑	L↓
Efficiency lb SO <sub>2</sub> /MM Btu	S↑ L↑	L↑ M↓	M↓ L↑

Correlation: L=Large, M=Medium, S=Small

Table 9 shows that both feed rate and frother dosage had a large impact on the rejections of ash, total sulfur and pyritic sulfur. In general, higher frother dosages decreased rejection, while higher feed rates increased rejection. The improvement in rejection can be attributed to a decrease in the recovery of middlings particles at the lower frother dosages and higher feed flow rates. These trends are in good agreement with the overall concept of a fixed column performance curve, i.e., recovery and rejection are inversely related. In contrast, an increase in grind size was found to decrease both the coal recovery and the rejection of sulfur. The decreased recovery can be explained by an increase in particle detachment at the coarser grind size, while the lower sulfur rejection can be attributed to poorer liberation of pyrite. However, one would assume that the liberation of ash-containing minerals was more complete since ash rejection did not diminish at the coarser grind sizes.

The response surface plots and calculations for the Microcel tests conducted using the Pittsburgh No. 8 seam coal are provided in Appendix 4-A. Unfortunately, the limited data set allowed unique fits to be obtained only for the linear regression model. Therefore, no information was generated concerning possible interactions between the various operating parameters.

#### 10.1.2 Testing of Illinois No. 6 Coal

The test matrix for the testing of the Illinois No. 6 seam coal using the Microcel flotation column is provided in Table 10. This series of experiments required nine test runs in which the collector and frother dosages were varied. A summary of the test results and performance calculations are provided in Appendix 2-B.

Table 10. Parametric test matrix used to investigate the performance of the Microcel column for the Illinois No. 6 seam coal.

#### Microcel Conditions Held Constant

Feed Rate (lbs/ton):	500
Wash Water (lpm):	40.1
Percent Solids (w/w):	11-12
Grind Size (d <sub>80</sub> (microns)): 200	200
Air Flow Rate (SCFM):	8.89

#### Microcel Collector and Frother Dosages

Test Number	Collector Dosage lbs/ton	Frother Dosage ml/min
401	2.00	2.00
402	2.00	1.00
403	3.00	3.00
404	2.00	3.00
405	1.00	3.00
406	1.00	2.00
407	3.00	1.00
408	3.00	2.00
409	1.00	1.00

Figure 19 shows the combustible recovery obtained in this series of tests versus the rejections of ash, total sulfur and pyritic sulfur. In general, the results of all nine tests were very similar with the optimums having combustible recoveries in the mid-to-high 80's, ash rejections in the low 80's, and pyritic sulfur rejections in the low 60's.

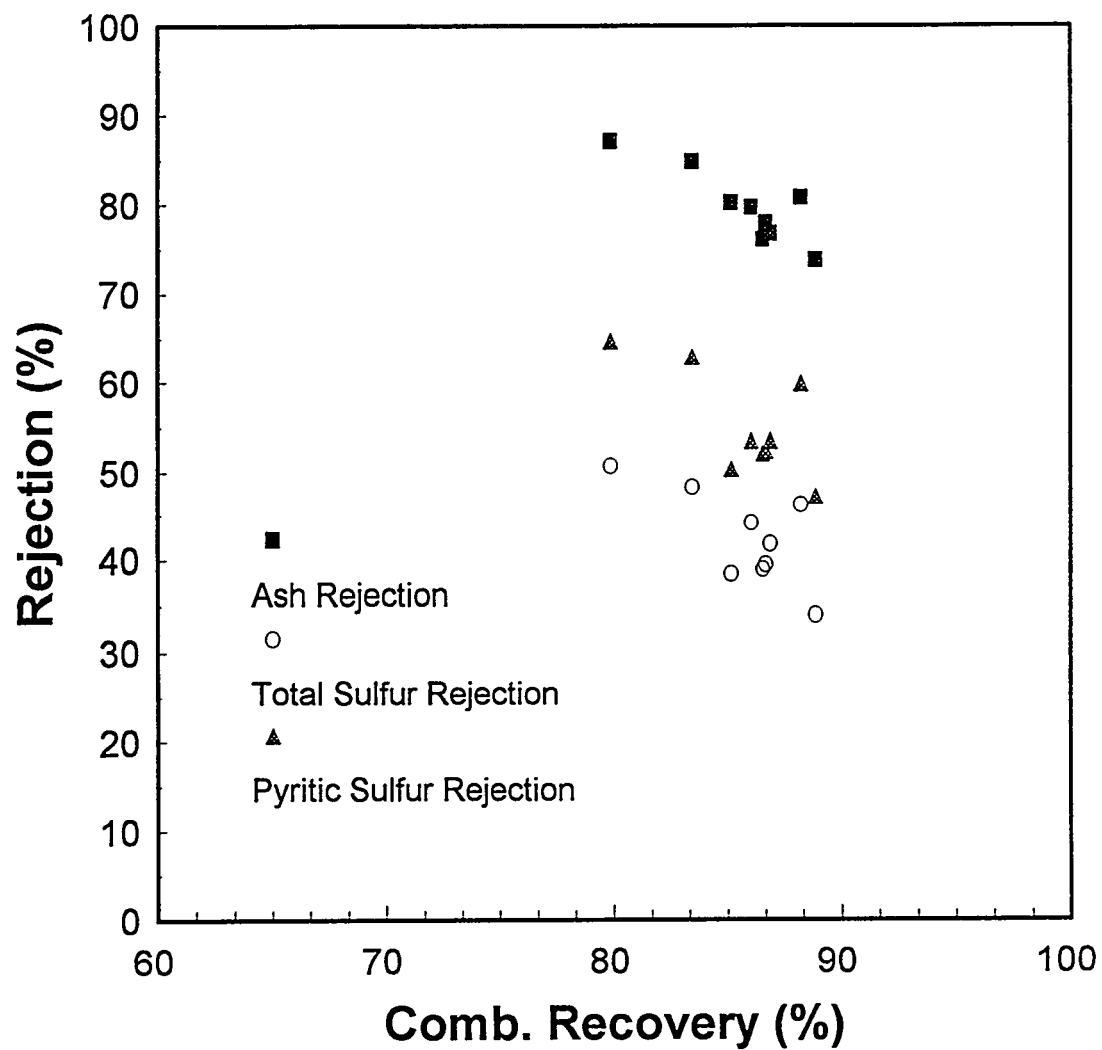


Figure 19. Combustible recovery versus rejection plots for the parametric testing of the Illinois No. 6 seam coal using the Microcel flotation column.

The statistical analyses for the testing of the Illinois No. 6 seam coal by Microcel column flotation is provided in Appendix 3-B. The correlation matrix, given in Table 11, indicates that higher reagent dosages generally increased coal recovery and decreased the rejection of mineral matter (as would be expected from the recovery-rejection curve). The only exception to this trend was ash rejection, which actually increased with increasing collector dosage. This finding agrees with previous work conducted at Virginia Tech which indicates that traditional hydrocarbon-based coal collectors (i.e., kerosene, fuel oil, diesel fuel, etc.) increase the hydrophobicities of coal and pyrite while having essentially no effect on ash-forming mineral matter. Table 11 also indicates that frother dosage has a much greater impact on column performance than collector dosage. The importance of frother dosage can probably be attributed to its effect on bubble size.

Table 11. Correlation matrix for the testing of the Illinois No. 6 seam coal using Microcel column flotation.

Process Response	Process Variable	
	Increasing Collector Dosage	Increasing Frother Dosage
Comb. Recovery	S↑	L↑
Energy Recovery	S↑	L↑
Ash Rejection	S↑	L↓
Sulfur Rejection	S↓	L↓
Pyritic Rejection	S↓	L↓
Efficiency	M↑	L↓
lb SO <sub>2</sub> /MM Btu	L↑	M↑

Correlation: L=Large, M=Medium, S=Small

Appendix 4-B provides the response surface plots and calculations for the Microcel tests conducted using the Illinois No. 6 seam coal. The interaction between collector and frother dosage was evaluated by examining the joint coefficient for these parameters in the quadratic regression model for each response. These analyses indicate that there is a strong interaction between collector and frother dosage for the case of pyrite rejection. All other performance indicators (i.e., ash rejection, energy recovery, etc.) showed this interaction to be of only minor importance.

## 10.2 MGS Parametric Testing

In this subtask, the key operating parameters associated with the MGS were examined using a statistically designed set of experiments. The operating variables examined in this phase of the work included feed flow rate, wash water rate, rotation speed, feed solids content and grind size. The results obtained from this test work are discussed in the following sections.

### *10.2.1 Testing of Pittsburgh No. 8 Coal*

A run-of-mine sample of Pittsburgh No. 8 seam coal was used as feed material for the independent MGS tests. The test program examined the effects of grind size, drum speed, wash water, percent solids feed, and feed rate on separation performance. The specific test matrix for this series of tests is shown in Table 12. Testing these five variables over three ranges required that 43 individual test runs be performed (which including several replicate tests). The test data and performance calculations are summarized in Appendix 2-C.

Table 12. Parametric test matrix used to investigate the performance of the MGS unit for the Pittsburgh No. 8 seam coal.

MGS Conditions Held Constant

Shake Amplitude (mm): 15  
 Shake Frequency (cps): 5  
 Tilt Angle (degrees): 6

MGS Variables

Test Number	Grind Size (microns)	Drum Speed rpm	Wash Water lpm	Percent Feed Solids w/w	Feed Rate lbs/hr
201	200	280	1.02	35	110
202	200	280	1.02	35	235
203	200	241	1.48	26	169
204	200	280	0.53	25	273
205	200	240	0.53	25	159
206	200	280	0.53	25	100
207	200	280	0.95	26	200
208	200	321	1.10	15	173
209	200	280	0.91	16	261
210	300	281	0.95	35	216
211	300	280	0.98	25	260
212	300	280	1.51	26	215
213	300	280	0.91	25	110
214	300	321	0.95	25	217
215	300	281	0.45	26	215
216	300	241	1.02	25	217
217	300	280	1.02	14	239
218	200	282	0.49	35	210
219	200	280	1.51	35	216
220	200	320	0.98	25	334
221	200	240	0.98	24	347
222	200	280	0.98	26	164
223	200	240	0.98	26	137
224	200	281	1.51	25	313
225	200	281	1.48	16	200
226	200	242	0.98	15	212
227	100	284	0.98	36	197
228	100	282	0.91	25	100
229	100	280	0.98	26	321
230	100	320	0.98	26	198
231	100	280	0.49	25	204
232	100	240	0.98	25	208
233	100	280	1.48	26	200
234	100	280	0.98	15	205
235	200	320	0.95	35	208
236	200	241	0.95	35	223
237	200	320	0.98	25	128
238	200	280	0.98	26	176
239	200	321	0.53	26	186
240	200	321	1.51	25	146
241	200	280	1.59	25	103
242	200	260	0.42	15	236
243	200	250	0.91	16	119

Figure 20 graphically illustrates the effects the various operating parameters on the relationship between combustible recovery and the rejections of ash, total sulfur and pyritic sulfur. Figure 20 shows that the MGS was very effective in rejecting pyrite, but less effective in rejecting ash-containing mineral matter. This is opposite to the trends observed previous in Figure 18 for the Microcel flotation test results. In any case, the MGS achieved recoveries in excess of 90% at ash rejections up to 50%, total sulfur rejections up to 50% and pyritic sulfur rejections up to 75%.

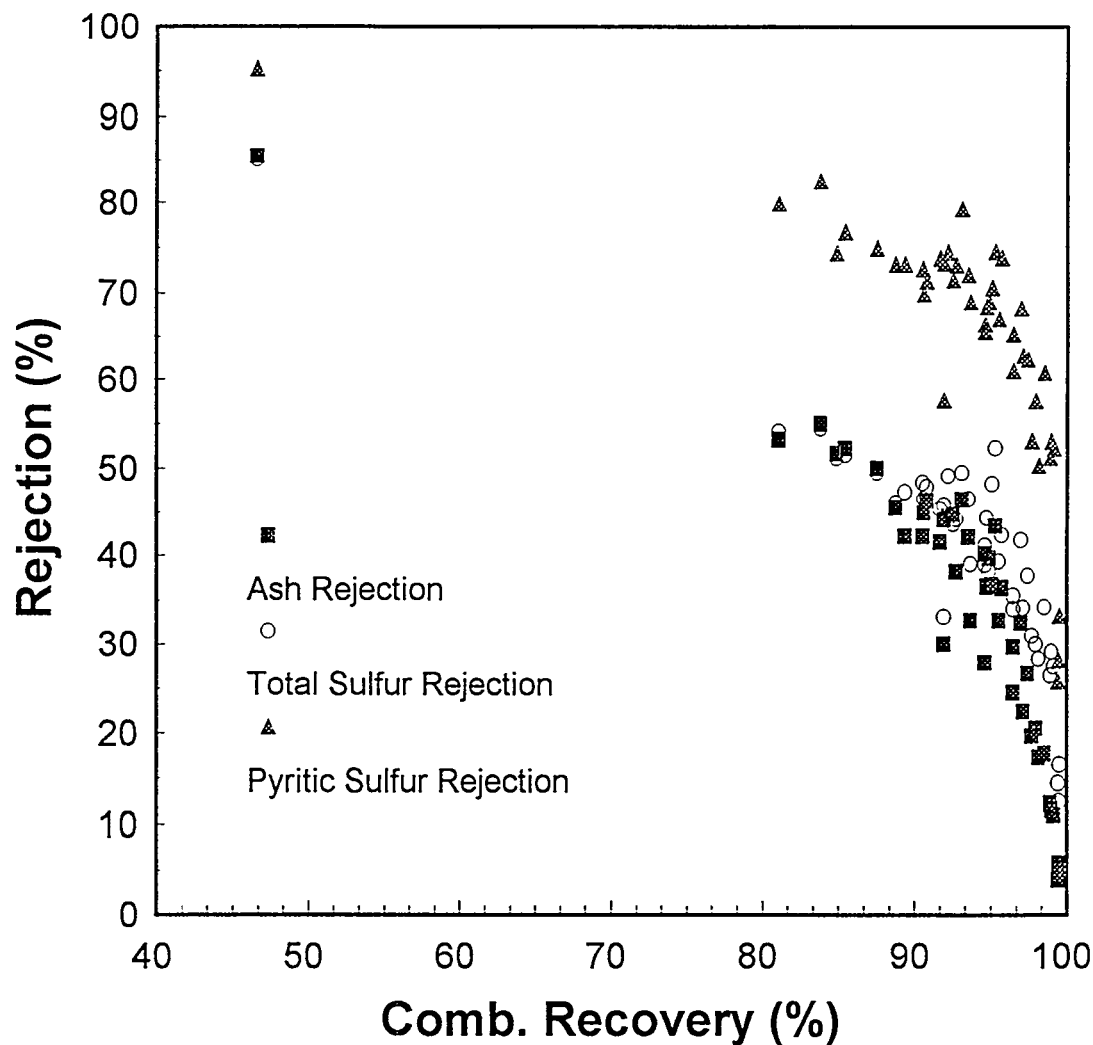


Figure 20. Combustible recovery versus rejection plots for the parametric testing of the Pittsburgh No. 8 seam coal using the MGS unit.

The statistical analyses for the testing of the Pittsburgh No. 8 seam coal by the MGS is provided in Appendix 3-C. Table 13 provides the correlation matrix for this series of tests. As shown, drum speed was found to be the most important variable in controlling the performance of the MGS unit. In general, an increase in drum speed produced a large decrease in coal recovery and a large increase in the rejections of ash, total sulfur and pyritic sulfur. This finding was expected since higher speeds increase the centrifugal force which pins particles to the drum surface. These particles are eventually carried into the reject launder by the rotating scrapers. Likewise, an increase in feed solids content decreased coal recovery by reducing the velocity of the flowing film which carries particles into the coal product. However, as shown in Table 13, drum speed was found to have a much more dramatic impact on MGS performance than feed solids content. Grind size, feed rate and wash water rate were found to have only a small influence on separator performance. In general, a change in any of these operating parameters which improved coal recovery resulted in a corresponding decrease in the rejection of mineral matter. This implies that changes in the various operating conditions simply varied the amounts of middlings particles reporting to either the clean-coal or reject streams. The one notable exception to this rule was found for the effect of grind size on pyrite rejection. In this case, both the coal recovery and pyrite rejection decreased (albeit small) as the grind size became coarser. This phenomenon can be explained by a decrease in pyrite liberation at the coarser grind sizes.

Table 13. Correlation matrix for the testing of the Pittsburgh No. 8 seam coal using the MGS unit.

Process Response	Process Variable				
	Increasing Grind Size	Increasing Feed Rate	Increasing Drum Speed	Increasing Wash Water	Increasing Feed Solids
Comb. Recovery	S↓	S↓	L↓	S↑	M↓
Energy Recovery	S↓	S↓	L↓	S↑	M↓
Ash Rejection	S↑	S↑	L↑	S↓	M↑
Sulfur Rejection	S↑	S↑	L↑	S↓	L↑
Pyritic Rejection	S↓	S↑	L↑	S↓	M↑
Efficiency lb SO <sub>2</sub> /MM Btu	S↓ M↑	M↓ S↑	L↑ L↓	S↓ S↑	L↑ L↓

Correlation: L=Large, M=Medium, S=Small

Appendix 4-C provides the response surface plots and calculations for the MGS tests conducted using the Pittsburgh No. 8 seam coal. The most important interactions were found to occur between drum speed and feed solids content. In order to maintain the same level of performance, higher drum speeds were required as the solids content of the feed slurry decreased. The higher drum speed is necessary to overcome the increased drag force imparted by the higher velocity of the flowing film when the feed rate was increased.

The parametric test data obtained under this subtask suggests that the MGS is very effective in separating high-density pyrite from low-density coal. On the other hand, the unit appears to be less efficient in rejecting ash-forming mineral matter. The poor ash rejection can be largely attributed to ultrafine clay slimes which are too small to be pinned to the drum wall and report to the clean-coal product by entrainment in the process water. To test this hypothesis, a sample of Pittsburgh No. 8 seam coal was processed using the MGS and the resultant products were analyzed on a size-by-size basis. This series of tests utilized a slightly coarser grind-size than that previously employed for the parametric tests. The size-by-size test results, which are summarized in Table 14 and Figure 21, show that the best overall separation was obtained for particles in the 100 x 325 mesh size class. In this size range, ash and pyritic rejections of 75-80% were obtained at a combustible recovery of 85%. As expected, the finest size fraction (325 mesh x 0) gave worst results in terms of ash rejection, although the rejection of pyritic sulfur was still quite good, i.e., 72.6%. It is also interesting to note that the performance of the MGS also drops when treating particles larger than 48 mesh. Particles in this size range have sufficient mass to be pinned to the drum, but the physical size of the particle places it in the high-velocity region of the flowing film. As a result, the pinning force is incapable of preventing the particle from being carried along with the flowing-film into the clean coal product. Additional tests are needed to establish the full range of particle sizes which can be effectively treated by the MGS.

Table 14. Size-by-size analysis of MGS test data for a run-of-mine Pittsburgh No. 8 seam coal.

Particle Size (Mesh)	Weight Yield (%)	Comb. Recovery (%)	Ash Rejection (%)	Sulfur Rejection (%)	Pyritic Rejection (%)
+48	92.12	97.22	46.51	17.39	35.04
48 x 100	75.10	87.20	69.25	55.39	68.10
100 x 200	70.42	83.00	78.74	70.47	81.04
200 x 325	78.69	87.79	71.28	67.67	83.52
-325	91.29	95.35	13.64	44.71	72.61
Total	86.14	93.39	43.53	41.12	63.20

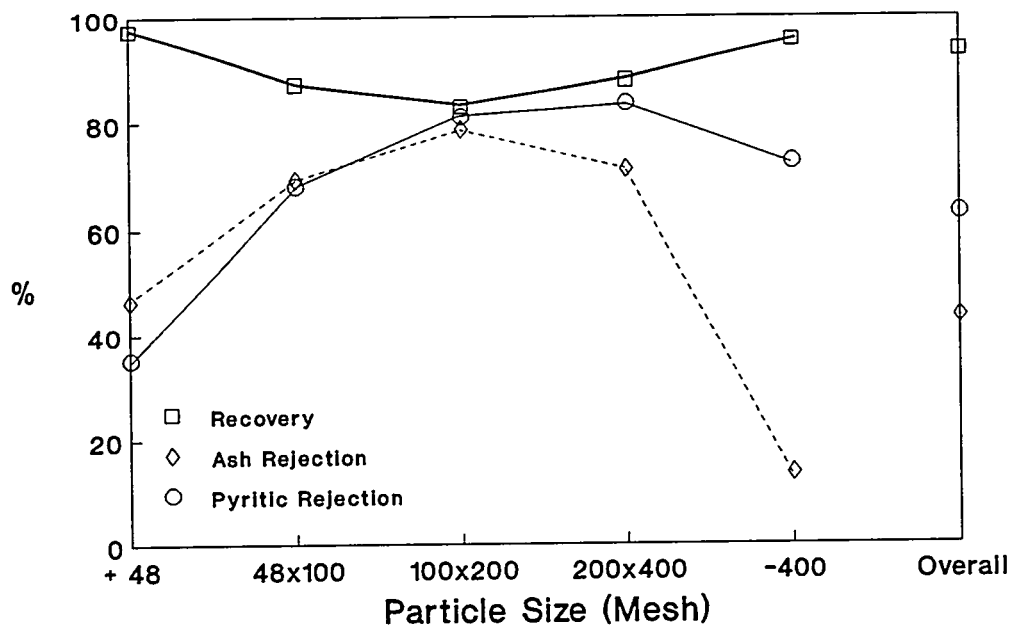


Figure 21. Size-by-size analysis of MGS test data for a run-of-mine Pittsburgh No. 8 seam coal.

### *10.2.2 Testing of Illinois No. 6 Coal*

The MGS testing of the Illinois No. 6 seam coal involved a four parameter test matrix in which drum speed, wash water, feed solids content and feed rate were varied. As shown in Table 15, 27 individual test runs were necessary in order to complete the specified Box-Behnken test matrix. The performance calculations for this series of tests are provided in Appendix 2-D.

Figure 22 shows the recovery-rejection curves obtained from the parametric study conducted using the MGS unit. As shown, the MGS achieved better rejections of pyritic sulfur than ash. This data is in good agreement with those obtained previously using the Pittsburgh No. 8 seam coal.

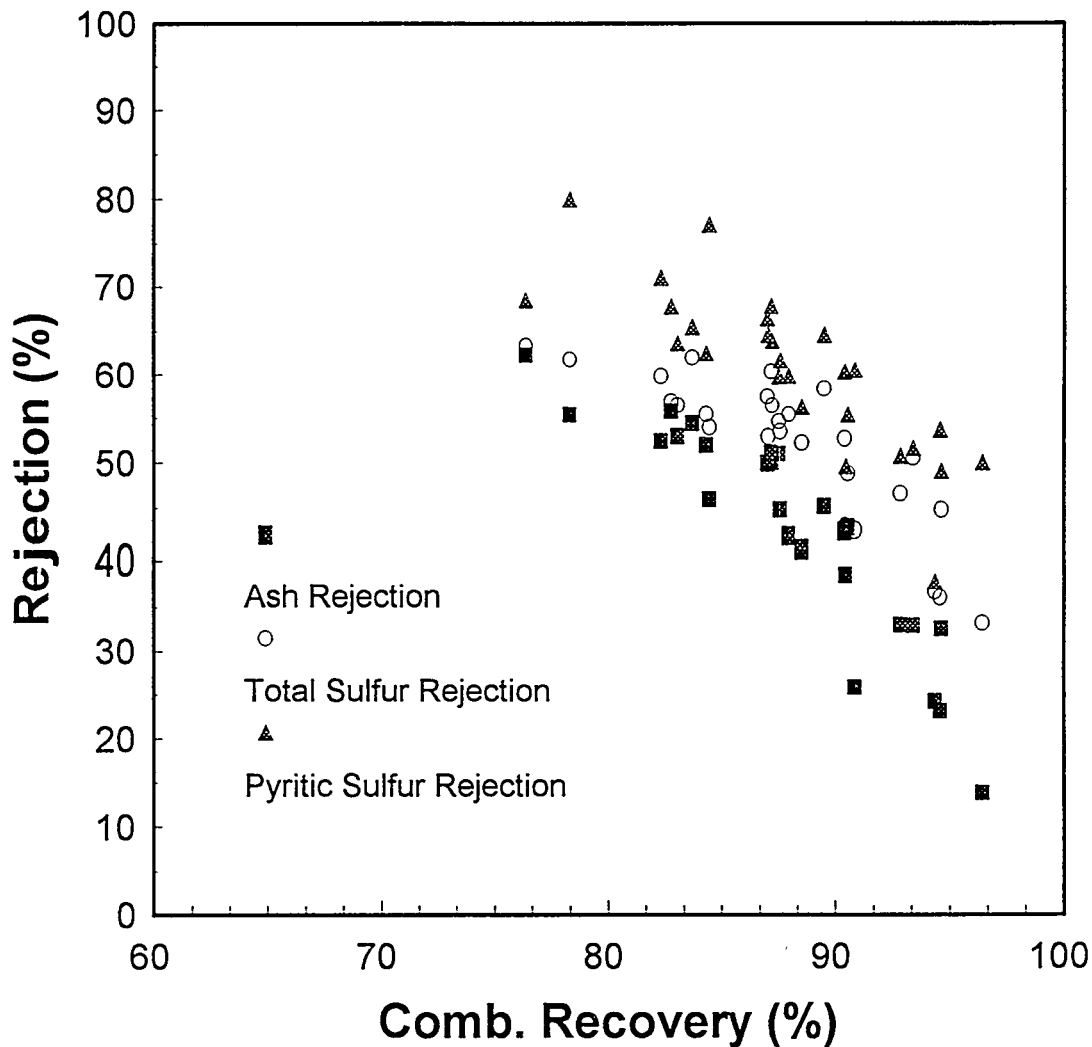
Table 15. Parametric test matrix used to investigate the performance of the MGS unit for the Illinois No. 6 seam coal.

**MGS Conditions Held Constant**

Shake Amplitude (mm):	15
Shake Frequency (cps):	5
Tilt Angle (degrees):	6
Grind Size (d80 (microns)): 200	

**MGS Variables**

Test Number	Drum Speed rpm	Wash Water lpm	Percent Feed Solids w/w	Feed Rate lbs/hr
501	280	0.76	30.71	345.21
502	280	0.76	24.16	198.64
503	281	1.63	34.63	199.60
504	321	1.51	25.81	212.36
505	280	0.00	18.95	234.40
506	280	0.76	17.14	306.22
507	281	0.80	29.60	241.91
508	283	1.51	24.46	272.41
509	280	0.00	26.32	293.41
510	281	0.83	33.89	140.90
511	283	0.68	25.56	210.43
512	320	0.83	17.06	206.79
513	241	1.55	26.40	216.30
514	320	0.76	28.13	141.23
515	320	0.80	37.77	229.75
516	240	0.76	24.36	267.37
517	280	0.00	30.11	154.62
518	241	0.80	37.18	225.19
519	320	0.76	25.38	279.12
520	281	0.83	18.24	135.93
521	280	1.59	28.63	148.15
522	240	0.80	29.61	153.00
523	241	0.83	17.22	209.50
524	281	1.59	17.30	213.91
525	322	0.00	25.72	216.83
526	241	0.00	26.20	226.57
527	281	0.00	37.75	260.03



I\_MGS\_REJ

Figure 22. Combustible recovery versus rejection plots for the parametric testing of the Illinois No. 6 seam coal using the MGS unit.

Appendix 3-D summarizes the statistical analyses performed for the testing of the Illinois No. 6 seam coal by the MGS unit. Table 16 provides the correlation matrix for this series of tests. As with the Pittsburgh No. 8 seam coal, drum speed was found to be the most important operating parameter for the MGS. Higher speeds tended to decrease coal recovery and increase the rejections of ash, total sulfur and pyritic sulfur. The influence of feed solids content was also found to be very similar. However, unlike the results obtained using the Pittsburgh No. 8 seam coal, both the wash water rate and feed rate were found to have a significant impact on the performance of the MGS when treating the Illinois No. 6 seam coal. For example, higher wash water rates were found to produce a large increase in coal recovery and pyritic sulfur rejection. One explanation for the increased significance of wash water can be attributed to the larger range of values examined in this series of tests (i.e., 0.5-1.5 lpm for the Pittsburgh No. 8 seam coal versus 0-1.5 lpm for the Illinois No. 6 seam coal). However, this possibility cannot be used to explain the increased importance of feed rate, as a smaller range of feed rates was examined for the Illinois No. 6 seam coal. Therefore, a more plausible explanation for the increased significance of these operating parameters may be the increased population of middlings particles present in the Illinois No. 6 seam coal.

Table 16. Correlation matrix for the testing of the Illinois No. 6 seam coal using the MGS unit.

Process Response	Process Variable			
	Increasing Drum Speed	Increasing Feed Solids	Increasing Wash Water	Increasing Feed Rate
Comb. Recovery	L↓	M↓	L↑	M↑
Energy Recovery	L↓	M↓	L↑	M↑
Ash Rejection	L↑	M↑	S↓	M↓
Sulfur Rejection	L↑	L↑	M↓	L↓
Pyritic Rejection	L↑	L↑	L↓	L↓
Efficiency lb SO <sub>2</sub> /MM Btu	M↑ L↓	L↑ M↓	M↓ S↑	L↓ S↓

Correlation: L=Large, M=Medium, S=Small

The response surface plots and calculations for the MGS tests conducted using the Illinois No. 6 seam coal are provided in Appendix 4-D. As with the Pittsburgh No. 8 seam coal, the most important interactions were found to occur between drum speed and feed solids content. Thus, higher drum speeds are required as the solids content of the feed slurry decreases in order to maintain the same level of separation performance.

### **10.3 Combined Microcel/MGS Parametric Testing**

After completing the tests for the individual units, a statistically designed set of experiments was developed to examine the effects of key operating parameters on the performance of the combined Microcel/MGS circuit. In each of these tests, the run-of-mine coal was processed by Microcel column flotation followed by recleaning of the froth concentrate by the MGS. The results of this test work are discussed in the following sections.

#### *10.3.1 Testing of Pittsburgh No. 8 Coal*

A four-parameter Box-Behnken test matrix was used in the testing program for the Pittsburgh No. 8 seam coal. Column feed rate was the only variable examined for the Microcel column, while variables examined for the MGS unit included drum speed, wash water and feed rate. The specific operating conditions for this series of tests are summarized in Table 17. Samples were taken independently around both the Microcel and MGS units, which allowed for complete evaluation of each unit as well as the total circuit. A summary of the individual and combined test results are provided in Appendix 2-E.

Table 17. Parametric test matrix used to investigate the performance of the combined Microcel/MGS circuit for the Pittsburgh No. 8 seam coal.

**Microcel**

Wash Water (lpm):	40.12
Percent Solids (w/w):	14.5 - 15.5
Grind Size (d80 (microns)):	200
Air Flow Rate (SCFM):	8.89
Diesel dosage (lbs/ton):	1
Frother Dosage (ml/min):	1

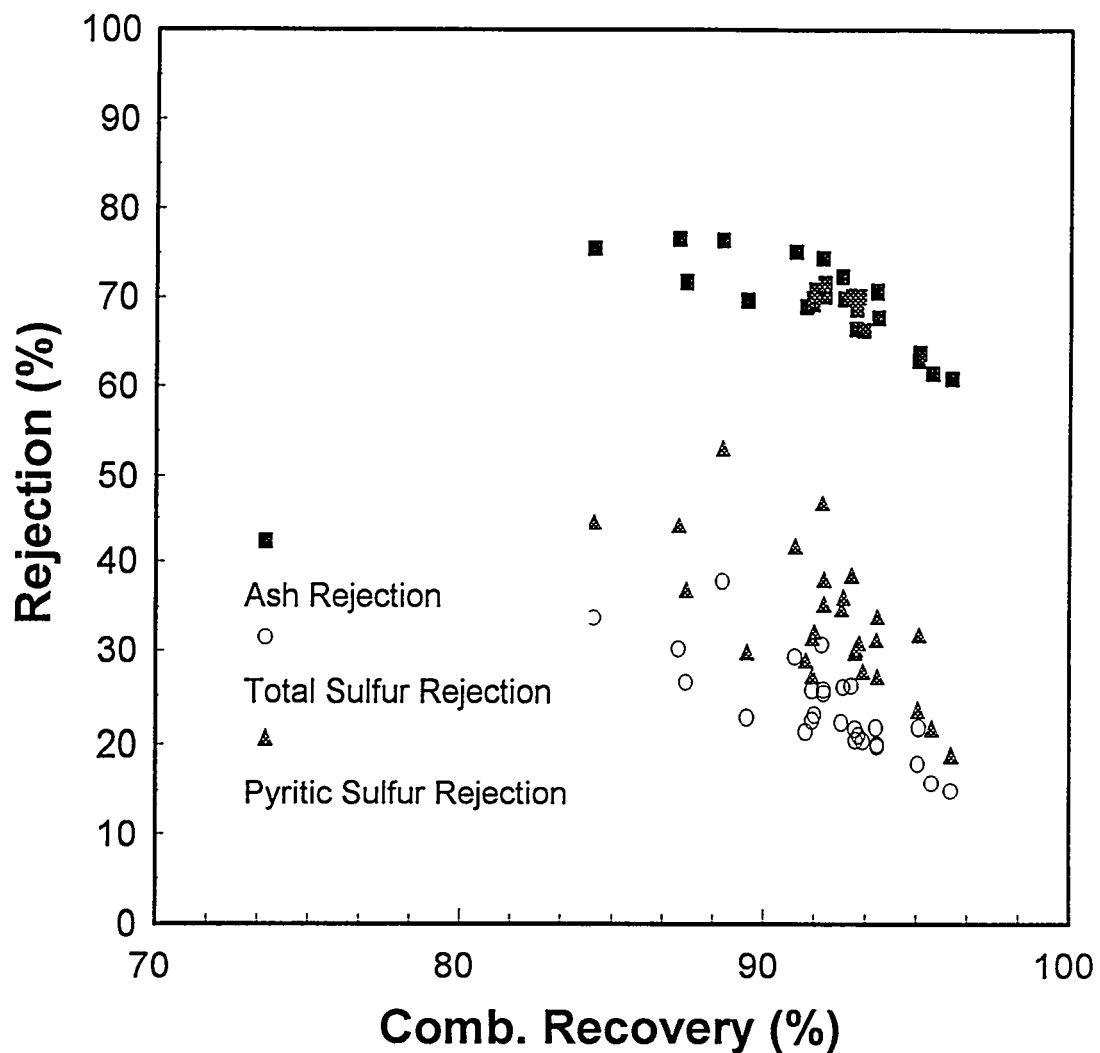
**MGS**

Percent Solids (w/w):	18 - 22
Shake Frequency (cps):	5
Shake Amplitude (mm):	15
Tilt Angle (degrees):	6

**MGS Variables**

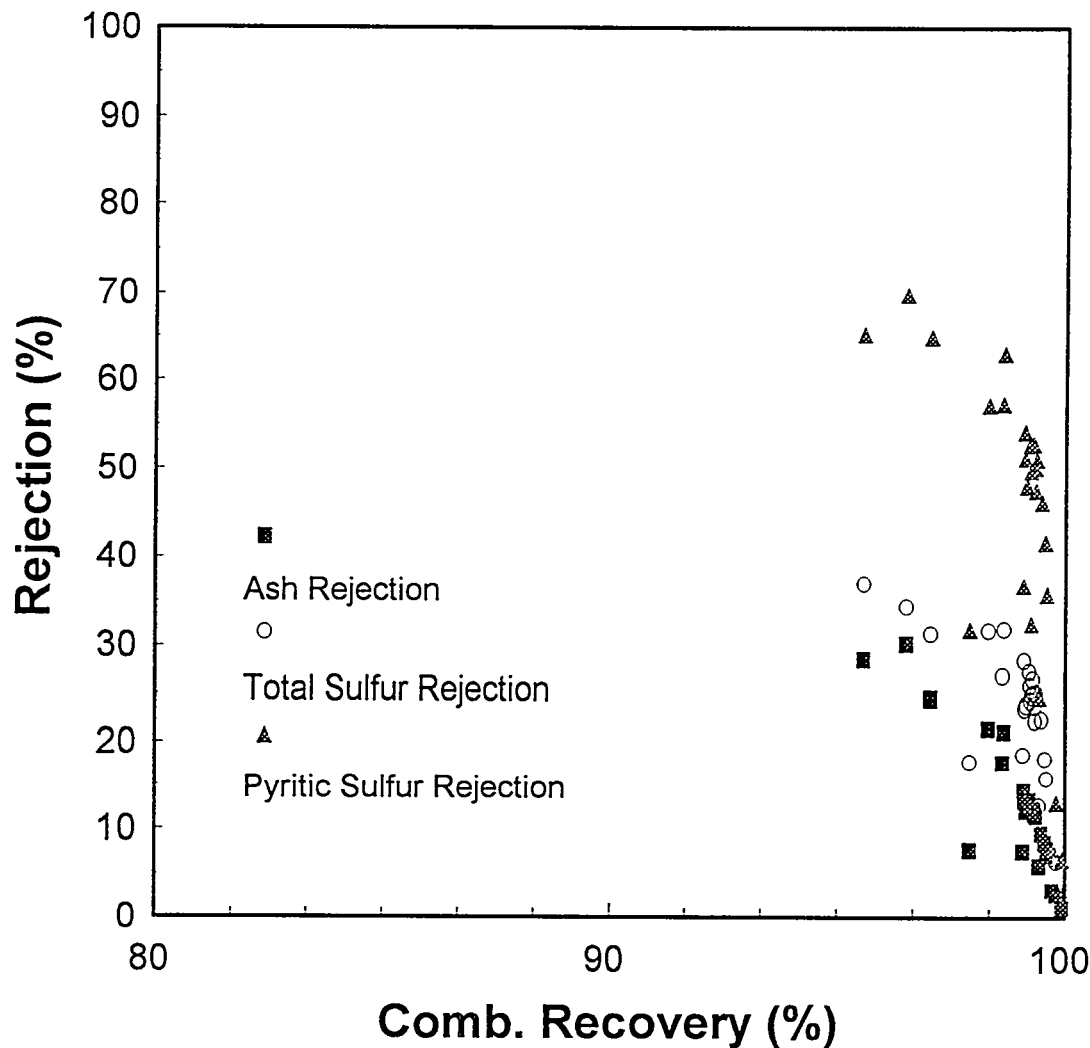
Test Number	Column Feed (lbs/hr)	Drum Speed rpm	Wash Water lpm	MGS Feed lbs/hr
301	512	282	0.51	249
302	527	283	1.02	378
303	415	241	1.51	259
304	392	242	0.98	373
305	414	280	0.49	381
306	427	282	1.06	260
307	420	322	1.50	241
308	414	242	0.98	124
309	415	320	0.98	351
310	391	280	0.49	135
311	397	280	1.51	393
312	410	280	1.55	134
313	458	280	0.95	259
314	302	280	0.98	160
315	333	241	1.00	267
316	529	281	0.98	141
317	474	241	0.98	276
318	491	320	0.98	267
319	491	282	1.55	285
320	444	242	0.49	325
321	383	280	0.95	313
322	427	320	0.51	297
323	393	320	0.97	170
324	311	281	0.51	268
325	318	281	1.55	285
326	294	280	0.95	474
327	324	320	0.98	328

Figures 23-25 show the recovery-rejection plots for the Microcel, MGS and combined Microcel/MGS units in the two-stage circuit. Once again, the Microcel column was found to be superior for ash rejection, while the MGS was better in rejecting pyritic sulfur. However, the combined results plotted in Figure 25 show that the best of both unit operations can be obtained by combining the Microcel and MGS units into a single circuit. In general, the combined circuit allowed excellent ash and pyrite rejections to be obtained while maintaining a high coal recovery. It is important to remember when viewing these plots, that the scatter in the data is due to intentionally varying several control parameters. Even with these variations, the performance remains within relatively close patterns. The synergy of combining the two units is well illustrated when comparing Figures 23-25. The test data suggest that the combined circuit is capable of achieving an energy recovery of approximately 90% at an ash rejection of 75-80%, total sulfur rejection of 50% and pyritic sulfur rejection of 70-75%.



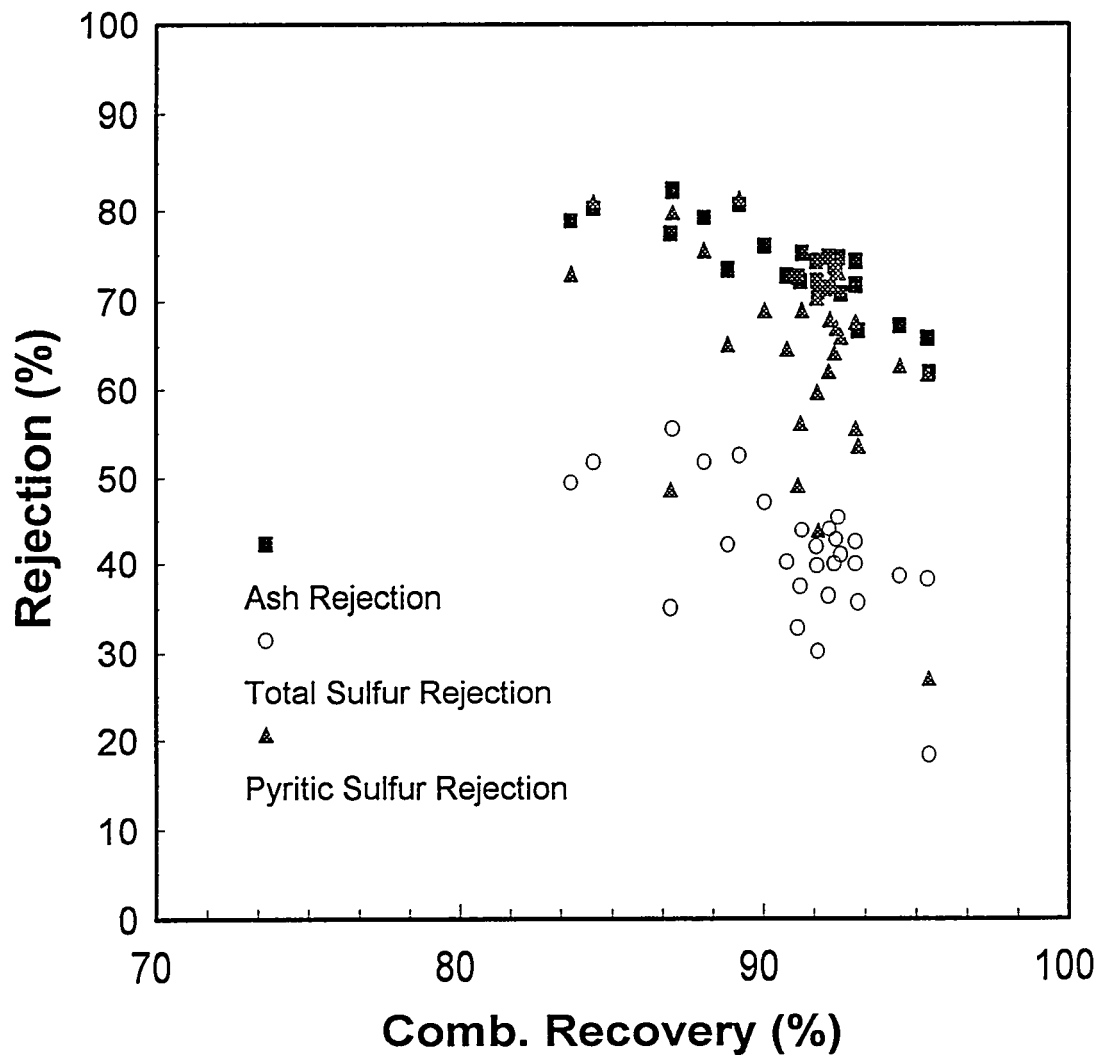
C\_COL\_REJ

Figure 23. Combustible recovery versus rejection plots obtained for the Microcel column during the parametric testing of the combined Microcel/MGS circuit using the Pittsburgh No. 8 seam coal.



C\_MGS\_REJ

Figure 24. Combustible recovery versus rejection plots obtained for the MGS unit during the parametric testing of the combined Microcel/MGS circuit using the Pittsburgh No. 8 seam coal.



C\_COM\_REJ

Figure 25. Combustible recovery versus rejection plots obtained for the combined Microcel/MGS circuit during the parametric testing of the Pittsburgh No. 8 seam coal.

Appendix 3-E provides a summary of the statistical analyses for the testing of the Pittsburgh No. 8 seam coal by the combined Microcel/MGS circuit. The correlation matrix for this series of tests is given in Table 18. According to these analyses, the most important operating parameter for the combined circuit was the MGS drum speed. As expected, an increase in drum speed tended to decrease the coal recovery and increase the rejections of ash, total sulfur and pyritic sulfur. The other operating parameters, i.e., Microcel feed rate, MGS feed rate and MGS wash water rate, were found to have a much smaller impact on circuit performance. In fact, drum speed was so dominant that the other operating parameters were found to be relatively insignificant by comparison. Nevertheless, the test data indicates that the coal recovery can be increased (and rejection of mineral matter decreased) by increasing the Microcel feed rate. Exactly the same trends were observed for the MGS feed rate and wash water rate. As with the independent unit testing, the improvement in coal recovery can be attributed to changes in the percentage of middlings particles reporting to either the clean-coal or reject streams.

Table 18. Correlation matrix for the testing of the Pittsburgh No. 8 seam coal using the combined Microcel/MGS circuit.

Process Response	Process Variable			
	Increasing Microcel Feed Rate	Increasing MGS Feed Rate	Increasing MGS Wash Water	Increasing MGS Drum Speed
Comb. Recovery	S↑	S↑	S↑	L↓
Energy Recovery	S↑	S↑	S↑	L↓
Ash Rejection	S↓	S↓	S↓	L↑
Sulfur Rejection	S↓	S↓	S↓	L↑
Pyritic Rejection	S↓	S↓	S↓	L↑
Efficiency	S↓	S↓	S↓	L↑
lb SO <sub>2</sub> /MM Btu	S↓	S↑	S↑	L↓

Correlation: L=Large, M=Medium, S=Small

The response surface plots and calculations for the combined Microcel/MGS tests conducted using the Pittsburgh No. 8 seam coal are provided in Appendix 4-E. In this case, a strong interaction was found to exist between Microcel feed rate and MGS drum speed. Typically, a decrease in the Microcel feed rate resulted in a larger proportion of middlings particles reporting to the MGS feed. Due to the larger particle population, a larger proportion of these middlings reported to the clean-coal product from the MGS. This resulted in an improved

coal recovery and lower rejection of mineral matter (see Table 18). Therefore, in order to maintain the same level of performance, the MGS must be operated at a higher speed to remove the additional middlings particles not rejected by the by flotation when the column operates at a lower feed rate.

#### *10.3.2 Testing of Illinois No. 6 Coal*

In order to examine addition operating variables for the MGS unit, all of the Microcel operating parameters were held constant for the combined Microcel/MGS testing of the Illinois No. 6 seam coal. This allowed the shake amplitude of the MGS unit to be added to the four-parameter Box-Behnken test matrix (see Table 19). The test data and performance calculations obtained for this series of tests are summarized in Appendix 2-F.

Table 19. Parametric test matrix used to investigate the performance of the combined Microcel/MGS circuit for the Illinois No. 6 seam coal.

**Microcel**

Feed Rate (lbs/ton):	550.00
Wash Water (lpm):	40.1
Percent Solids (w/w):	11-12
Grind Size (d80 (microns)	200
Air Flow Rate (SCFM):	8.89
Diesel dosage (lbs/ton):	1
Frother Dosage (ml/min):	1.5 - 1.6

**MGS Conditions Held Constant**

Shake Amplitude (mm):	15
Shake Frequency (cps):	5
Tilt Angle (degrees):	6
Grind Size (d80 (microns)	200
Percent Solids (w/w):	21 - 22

**MGS Variables**

Test Number	Drum Speed rpm	Wash Water lpm	Shake Amplitude mm	Feed Rate lbs/hr
601	283	1.51	10	269.00
602	283	0.95	15	269.00
603	280	0.47	20	257.08
604	239	1.06	15	341.50
605	239	0.95	20	276.02
606	280	0.95	15	267.90
607	240	1.51	15	272.84
608	280	1.51	15	160.99
609	323	1.10	10	306.12
610	239	0.45	15	259.45
611	322	0.91	20	281.57
612	322	0.98	15	148.13
613	280	1.59	20	241.03
614	282	0.95	15	299.91
615	280	0.45	15	147.53
616	321	1.06	15	342.89
617	282	0.45	15	355.58
618	282	0.93	20	377.79
619	240	0.95	15	163.11
620	282	1.51	15	352.70
621	283	0.53	10	287.10
622	241	1.06	10	219.17
623	322	1.55	15	238.37
624	281	1.10	10	160.41
625	320	0.53	15	305.49
626	280	0.96	20	134.70
627	281	1.10	10	376.77

Figures 26-28 show the recovery-rejection plots obtained from the combined Microcel/MGS tests conducted using the Illinois No. 6 seam coal. As with the Pittsburgh No. 8 seam coal, the results obtained for the Illinois No. 6 seam coal show that the combination of Microcel flotation and MGS provide the best overall rejection of both ash-containing mineral matter and pyrite. According to the data given in Figure 28, the combined circuit achieved ash and pyritic sulfur rejections of 85-90% at an overall combustible recovery of approximately 80%. A total sulfur rejection approaching 70% was achieved during many of the test runs.

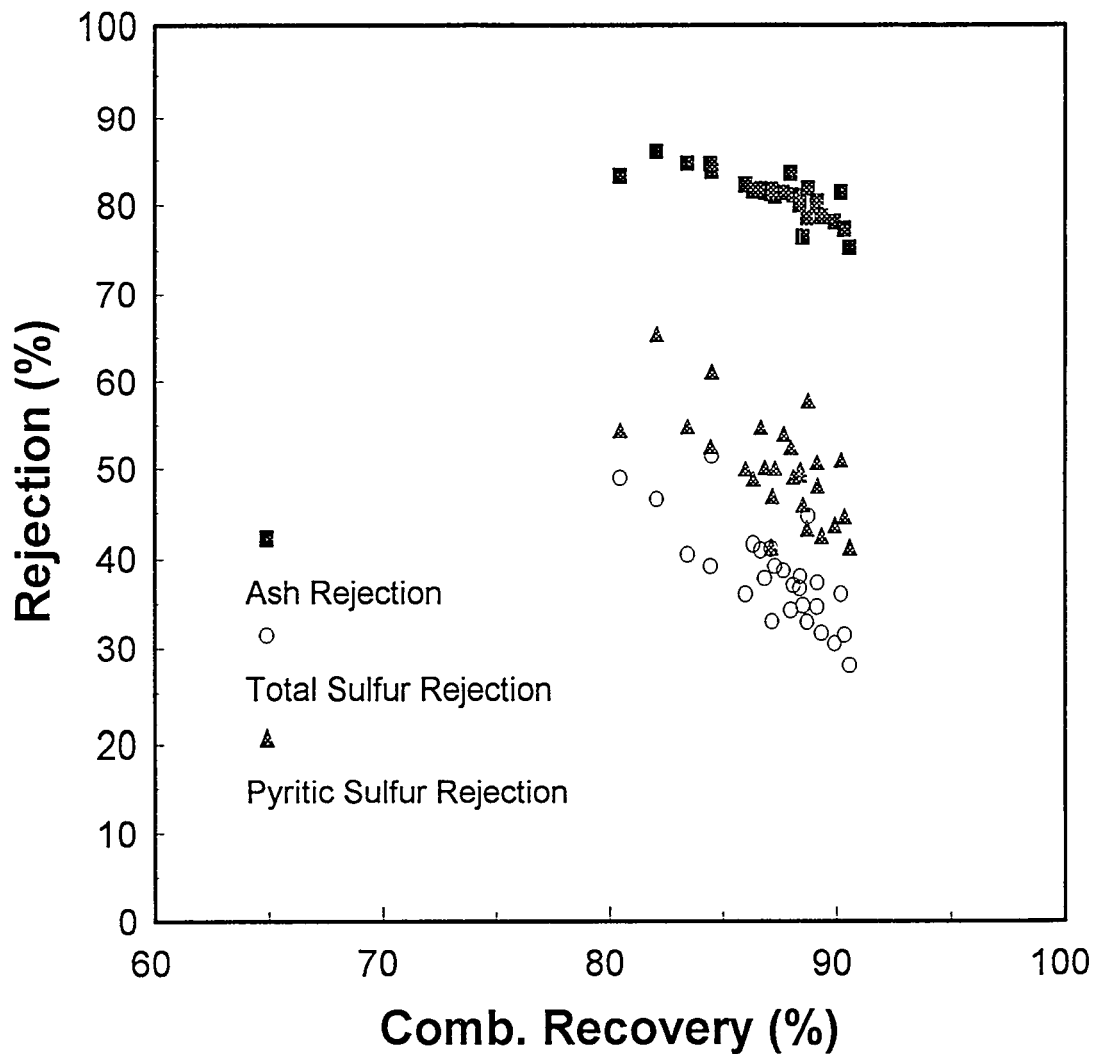


Figure 26. Combustible recovery versus rejection plots obtained for the Microcel column during the parametric testing of the combined Microcel/MGS circuit using the Illinois No. 6 seam coal.

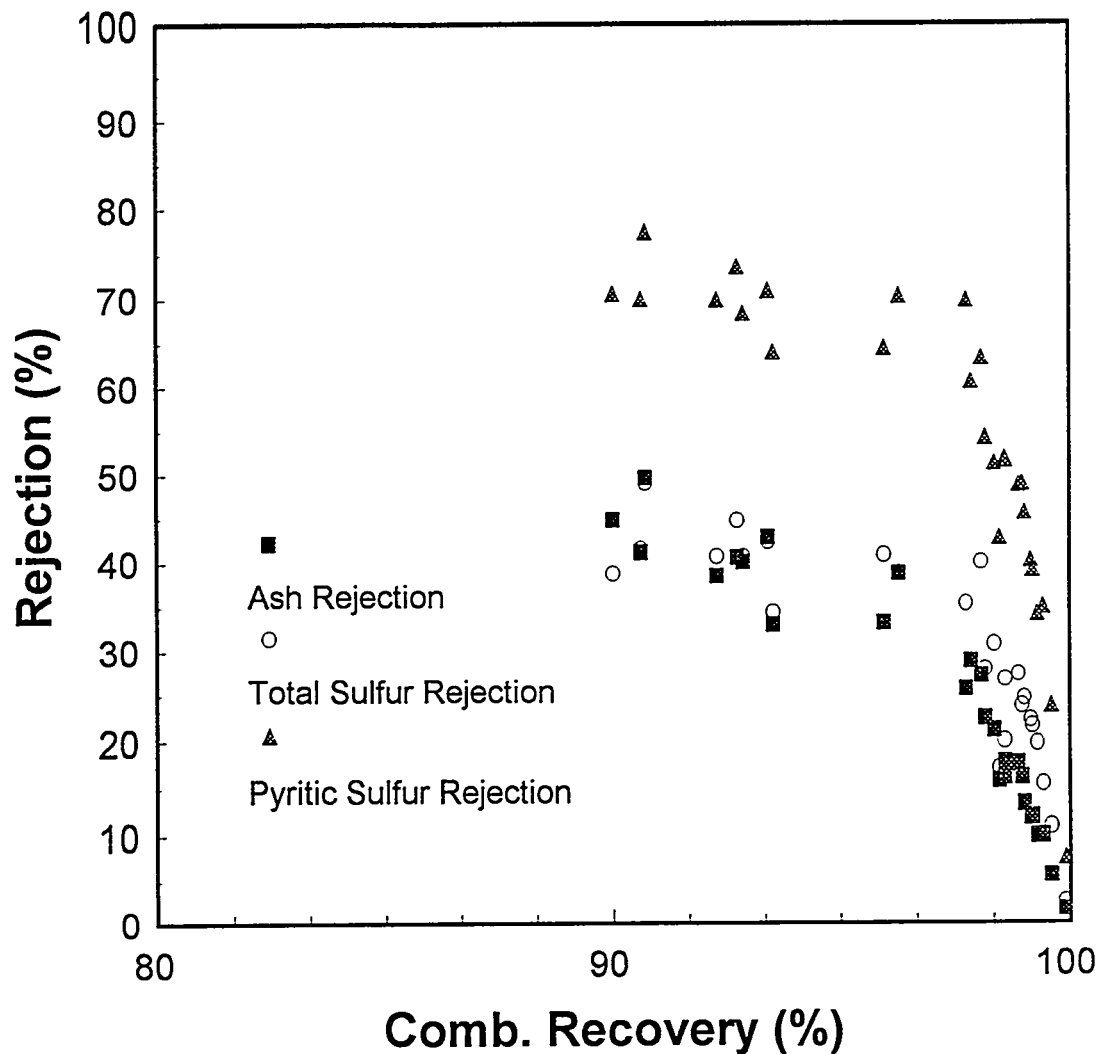
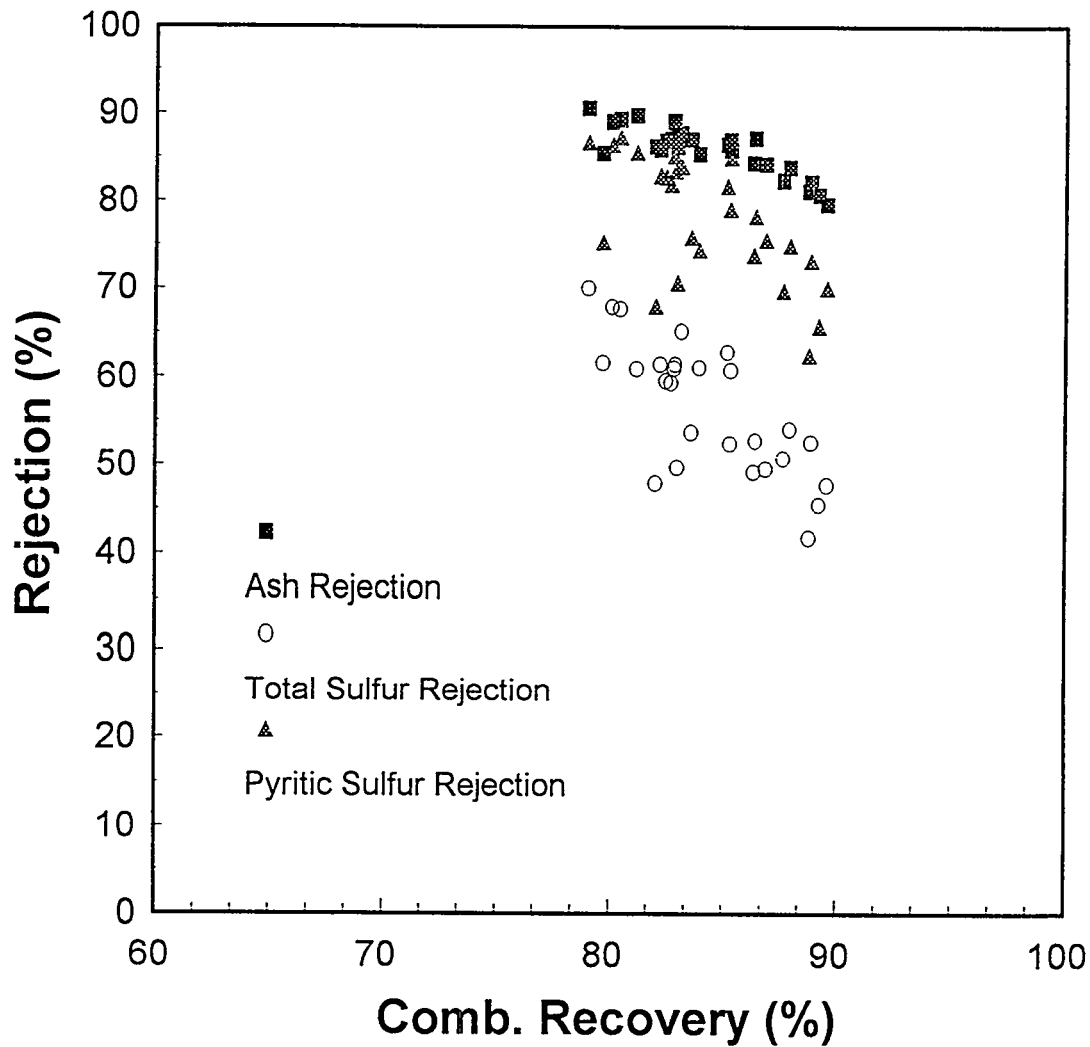


Figure 27. Combustible recovery versus rejection plots obtained for the MGS unit during the parametric testing of the combined Microcel/MGS circuit using the Illinois No. 6 seam coal.



C\_COM\_REJ

Figure 28. Combustible recovery versus rejection plots obtained for the combined Microcel/MGS circuit during the parametric testing of the Illinois No. 6 seam coal

Appendix 3-F summarizes the statistical analyses performed for the testing of the Illinois No. 6 seam coal by the combined Microcel/MGS circuit. The correlation matrix for this series of tests is given in Table 20. As shown, the correlation matrix for the Illinois No. 6 seam coal is essentially identical to that obtained for the Pittsburgh No. 8 seam. Drum speed was again found to be the dominant operating parameter, while the MGS wash water rate and feed rate had only a minor influence. The effect of MGS shake amplitude was also relatively small, although an increase in this parameter did produce a moderate improvement in coal recovery (and a correspondingly small decrease in the rejection of mineral matter). The improved recovery can probably be attributed to enhanced stratification of the particle bed which occurs within the MGS unit at the high shaking amplitudes.

Table 20. Correlation matrix for the testing of the Illinois No. 6 seam coal using the combined Microcel/MGS circuit.

Process Response	Process Variable			
	Increasing MGS Drum Speed	Increasing MGS Wash Water	Increasing MGS Shake Amplitude	Increasing MGS Feed Rate
Comb. Recovery	L↓	S↑	M↑	S↓
	L↓	S↑	M↑	S↓
Ash Rejection	L↑	S↓	S↓	S↑
Sulfur Rejection	L↑	M↓	S↓	S↑
Pyritic Rejection	L↑	S↓	S↓	S↑
Efficiency lb SO <sub>2</sub> /MM Btu	L↑	S↓	S↓	S↑
	L↓	M↑	S↑	S↑

Correlation: L=Large, M=Medium, S=Small

The response surface plots and calculations for the combined Microcel/MGS tests conducted using the Illinois No. 6 seam coal are summarized in Appendix 4-F. The most significant interaction was found to occur between MGS drum speed and feed rate. This can be explained by the fact that higher drum speeds are required to overcome the increased drag force imparted on the pinned particles by the faster flow of slurry passing through the MGS. The test data also indicated that a moderate interaction was found to exist between wash water rate and shake amplitude. At present, this particular interaction is not well understood.

#### **10.4 Combined Microcel/MGS/WOC with WOC Testing**

A limited number of tests were performed to determine whether a water-only cyclone (WOC) can be used to reduce the amount of feed that must be passed to the MGS unit. Since the incremental cost of treating coal by the MGS is significantly higher than for the WOC, any material that can by-pass the MGS will reduce the processing costs and improve the overall attractiveness of the proposed circuitry.

Three tests were conducted with a small water-only cyclone included in the combined circuit. In this configuration, the froth concentrate from the Microcel was pumped to the cyclone from which the overflow was taken as a final product and the underflow was fed to the MGS for pyrite removal. The low-density products from the MGS and WOC are combined to form the final clean-coal product from the circuit, while the column underflow and the high-density fraction from the MGS forms the reject. The importance of including the WOC in this circuit is to reduce the load on the MGS, to increase the percent solids in the MGS feed and to reduce the percentage of slimes (-400 mesh) reporting to MGS. The total circuit quality is maintained by operating the WOC to produce an overflow product of low ash. However, this produces a very low overflow yield from the WOC and necessitates additional processing of the WOC underflow by the MGS to recover misplaced coal.

The results of testing with the WOC are given in Table 21. Supporting data for these calculations are provided in Appendix 5. As expected, this data demonstrates that the pyritic sulfur rejections for the WOC are not as good as those obtained using the MGS. The overall circuit performance, however, is comparable to that of the combined Microcel/MGS circuit, while having the advantage of reducing the throughput to the MGS by 30-40%. Since the incremental cost of treating coal by the MGS is significantly higher than by the WOC, this circuit should be investigated further as a means of reducing the processing cost and improving the overall attractiveness of the proposed circuitry.

Table 21. Results obtained from the testing of the combined Microcel/WOC/MGS circuit.

## Ash Performance

Test Number	Microcel			WOC			MGS			Total Circuit		
	Comb. Recovery	Ash Rejection	Ash Separatio Efficiency %	Comb. Recovery	Ash Rejection	Ash Separatio Efficiency %	Comb. Recovery	Ash Rejection	Ash Separatio Efficiency %	Comb. Recovery	Ash Rejection	Ash Separatio Efficiency %
701	87.98	72.36	60.34	35.45	69.15	4.60	90.27	40.34	30.61	82.45	80.07	62.52
702	89.06	72.28	61.34	26.88	76.81	3.69	92.38	34.04	26.42	84.09	79.53	63.62
703	88.73	74.02	62.76	48.73	56.30	5.03	93.00	33.85	26.85	85.55	78.97	64.52

## Total Sulfur Performance

Test Number	Microcel			WOC			MGS			Total Circuit		
	Comb. Recovery	T. Sulfur Rejection	T. Sulfur Separatio Efficiency %	Comb. Recovery	T. Sulfur Rejection	T. Sulfur Separatio Efficiency %	Comb. Recovery	T. Sulfur Rejection	T. Sulfur Separatio Efficiency %	Comb. Recovery	T. Sulfur Rejection	T. Sulfur Separatio Efficiency %
701	87.98	27.95	15.93	35.45	72.00	7.45	90.27	44.57	34.84	82.45	51.09	33.54
702	89.06	30.08	19.13	26.88	78.25	5.13	92.38	37.87	30.25	84.09	50.68	34.77
703	88.73	29.56	18.30	48.73	57.91	6.63	93.00	40.83	33.83	85.55	46.12	31.67

## Pyritic Sulfur Performance

Test Number	Microcel			WOC			MGS			Total Circuit		
	Comb. Recovery	Pyritic S Rejection	Pyritic S Separatio Efficiency %	Comb. Recovery	Pyritic S Rejection	Pyritic S Separatio Efficiency %	Comb. Recovery	Pyritic S Rejection	Pyritic S Separatio Efficiency %	Comb. Recovery	T. Sulfur Rejection	T. Sulfur Separatio Efficiency %
701	87.98	38.76	26.74	35.45	77.28	12.73	89.50	72.38	61.88	82.45	72.99	55.45
702	89.06	41.84	30.90	26.88	82.79	9.67	91.90	69.31	61.21	84.09	75.17	59.26
703	88.73	42.89	31.63	48.73	67.07	15.80	93.25	69.58	62.83	85.55	69.60	55.15

## 10.5 Long-Duration Testing

In this subtask, two series of long-duration tests were performed under the optimized test conditions established on the basis of previous test work carried out under Task 10. These tests were used to establish the steady-state variability and operability of the proposed circuit over a period of at least 10 hours of continuous operation. Long-duration tests were conducted using both of the base coal samples.

### 10.5.1 *Testing of Pittsburgh No. 8 Coal*

The test results and performance calculations for the long-duration test run conducted using the Pittsburgh No. 8 seam coal are provided in Appendix 6-A. The specific operating conditions for this test was chosen on the basis of ash and pyrite rejections obtained in the parametric studies discussed previously. Long-duration testing involved holding all control parameters constant for a continuous run of over 10 hours. These operating parameters are given in Table 22.

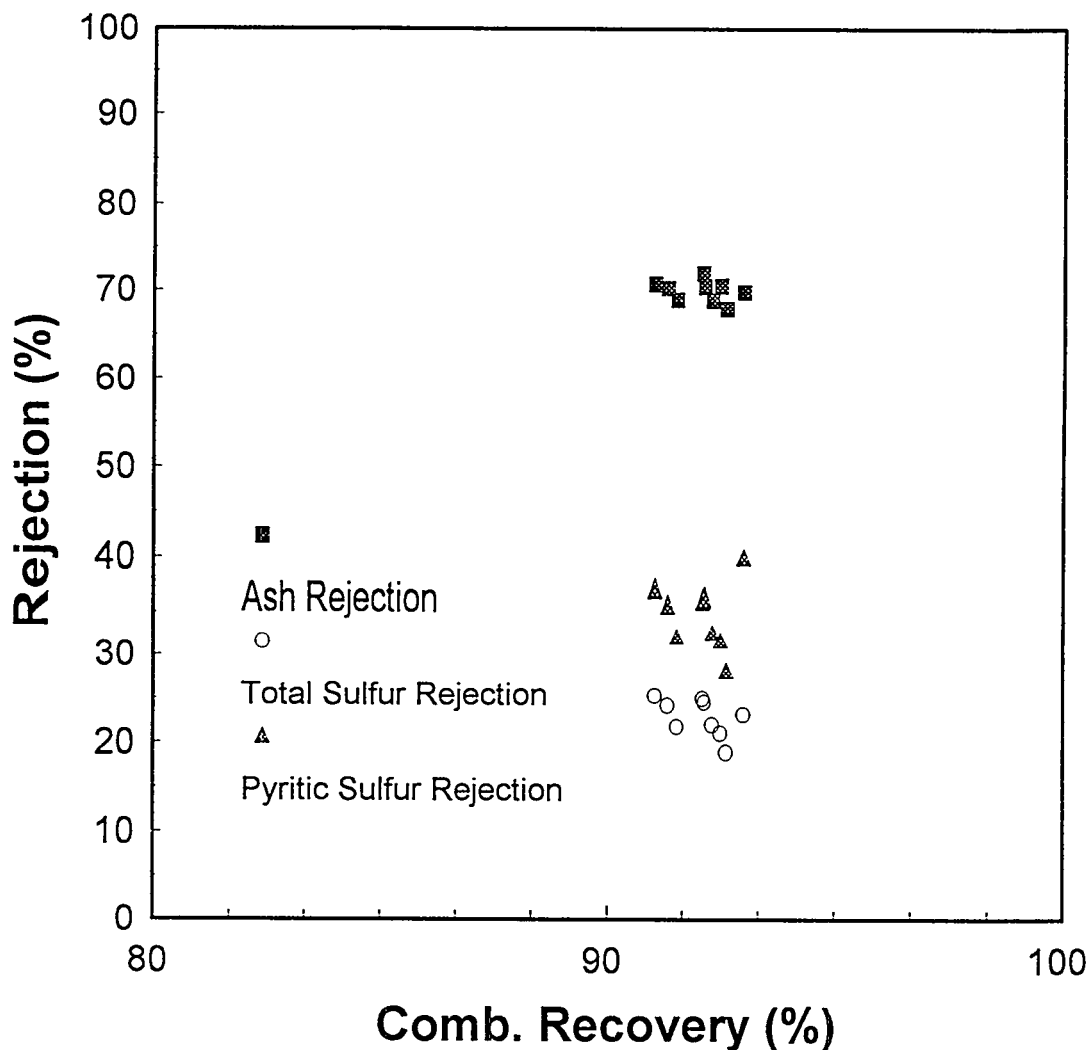
Table 22. Operating conditions examined in the long-duration testing of the Pittsburgh No. 8 seam coal.

<b>Microcel</b>	
Feed Rate (lbs/ton):	500
Wash Water (lpm):	39
Percent Solids (w/w):	12-14
Grind Size (d <sub>80</sub> (microns)): 200	200
Air Flow Rate (SCFM):	8.89
Diesel dosage (lbs/ton):	1.00
Frother Dosage (ml/min):	0.80

<b>MGS</b>	
Feed Rate (lbs/hr):	273
Drum Speed (rpm):	320
Wash water (lpm):	0.50 - 0.56
Percent Solids (w/w):	19 - 20
Shake Amplitude (mm):	15
Shake Frequency (cps):	5
Tilt Angle (degrees):	6

The results obtained during the long-duration test run are plotted in Figures 29-31. These graphs show the energy recoveries and rejections of ash, total sulfur and pyritic sulfur obtained for the Microcel, MGS and combined Microcel/MGS circuit. The results were found to be in good agreement with those obtained during the parametric test programs. On average, the combined circuit achieved ash and pyritic sulfur rejections of over 75% at a combustible recovery of approximately 90%. Figure 32 shows the stability of the combined circuit during the long duration run. The consistent performance over time indicates the operating robustness of the equipment.



LD\_COL\_REJ

Figure 29. Combustible recovery versus rejection plots obtained for the Microcel column during the long-duration testing of the combined Microcel/MGS circuit using the Pittsburgh No. 8 seam coal.

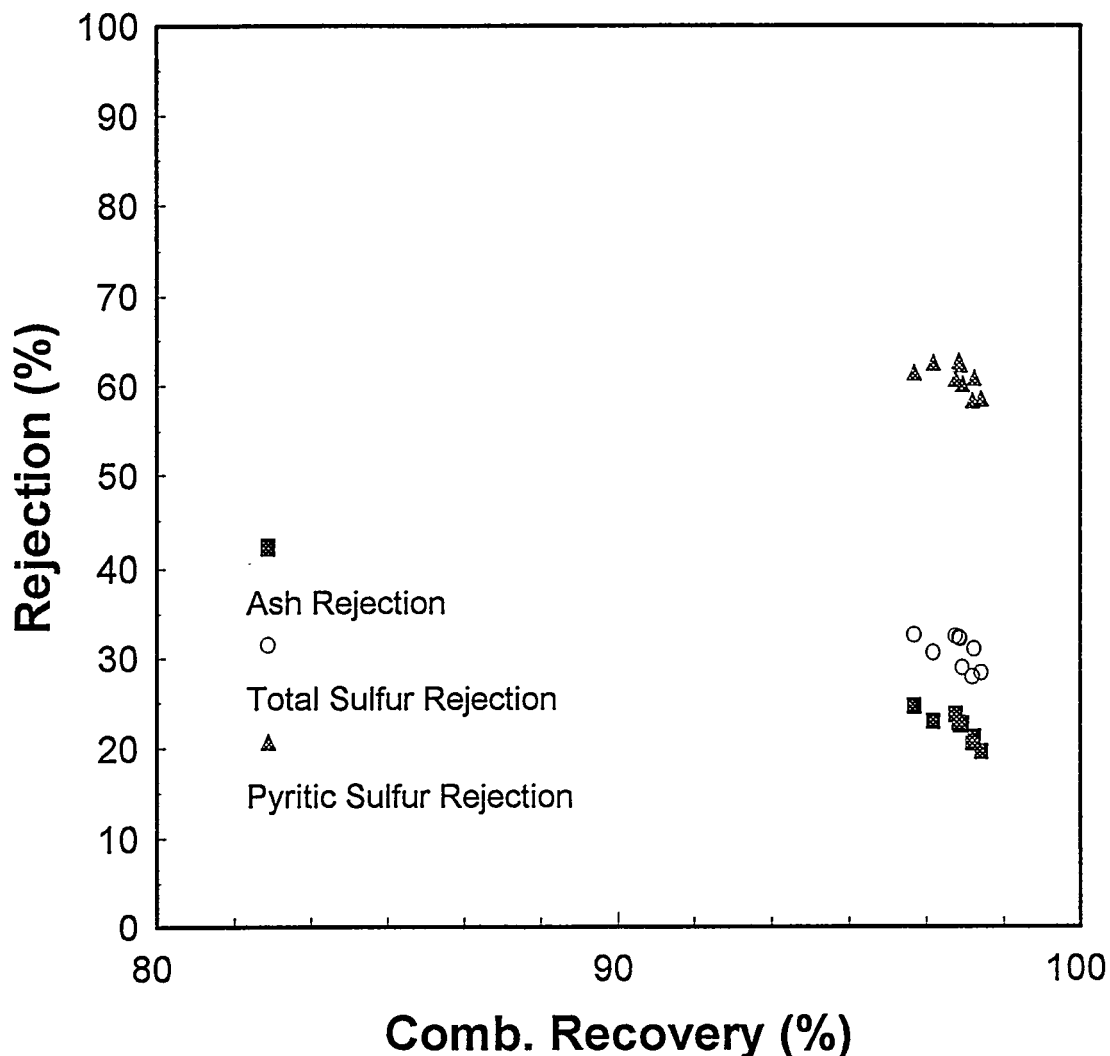
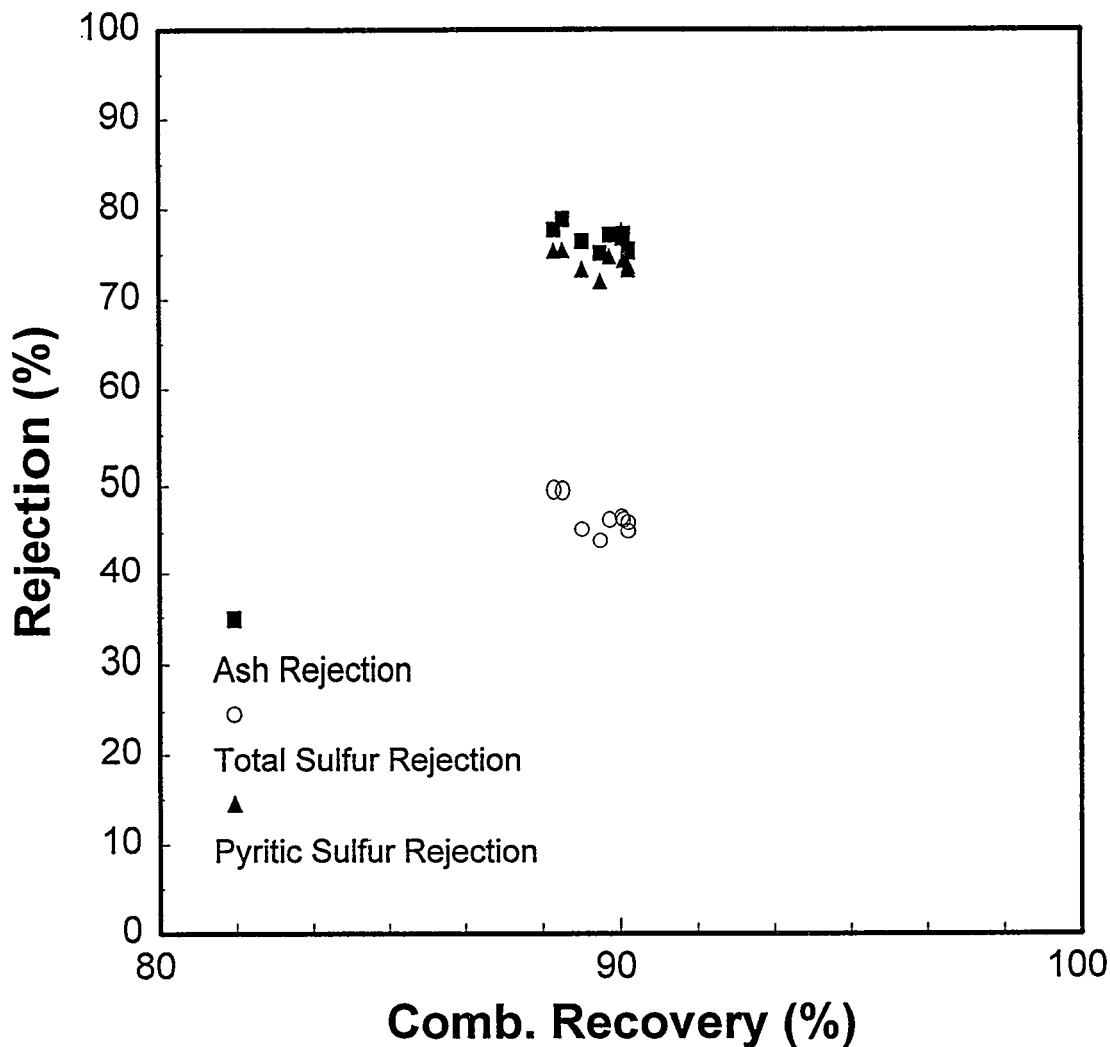


Figure 30. Combustible recovery versus rejection plots obtained for the MGS unit during the long-duration testing of the combined Microcel/MGS circuit using the Pittsburgh No. 8 seam coal.



LD\_COM\_REJ

Figure 31. Combustible recovery versus rejection plots obtained for the combined Microcel/MGS circuit during the long-duration testing of the Pittsburgh No. 8 seam coal.

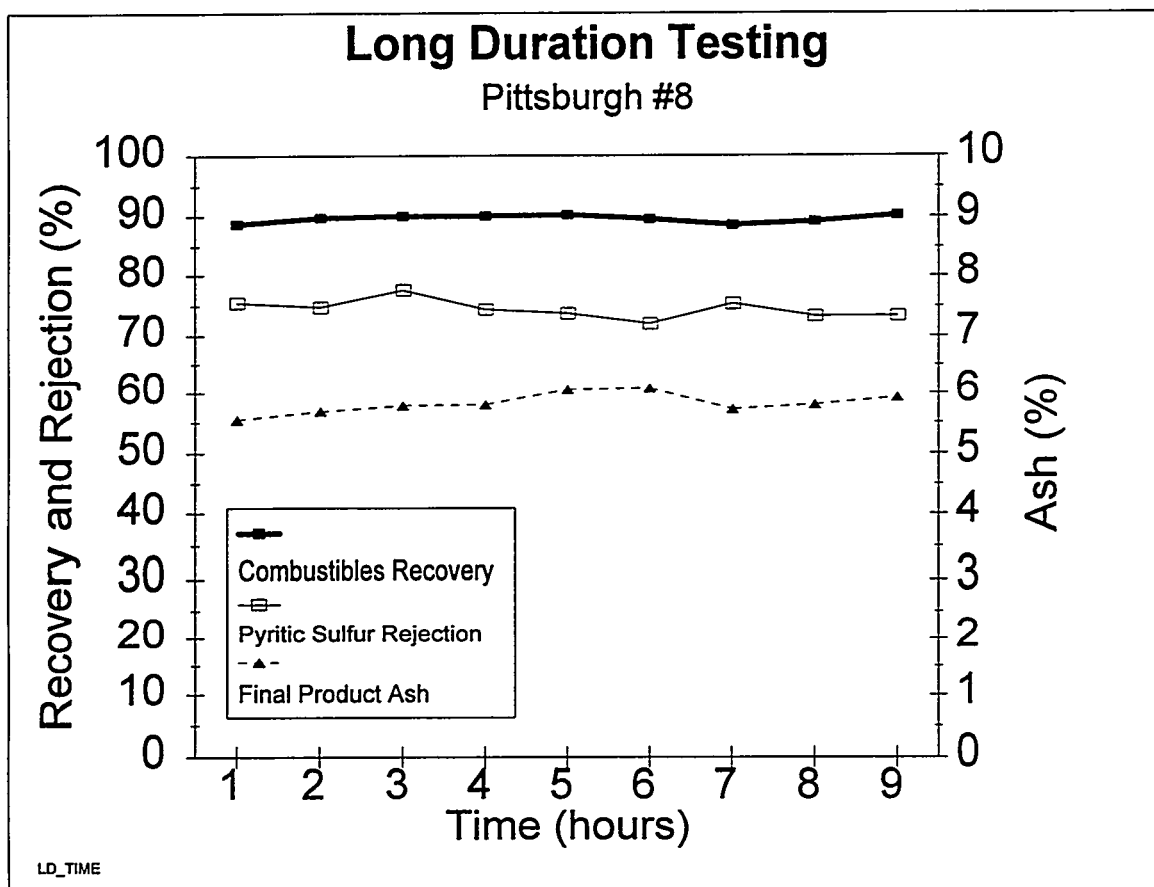


Figure 32. Long Duration results per hour during Pittsburgh #8 seam test.

*10.5.2 Testing of Illinois No. 6 Coal*

As discussed above, the best results of the combined testing were also used to select the operating parameters to be held constant during the long-duration testing of the Illinois No. 6 coal. The operating parameters selected for this series of tests are summarized in Table 23. The corresponding test data and performance calculation for these runs are summarized in Appendix 6-B.

Table 23. Operating conditions examined in the long-duration testing of the Illinois No. 6 seam coal.

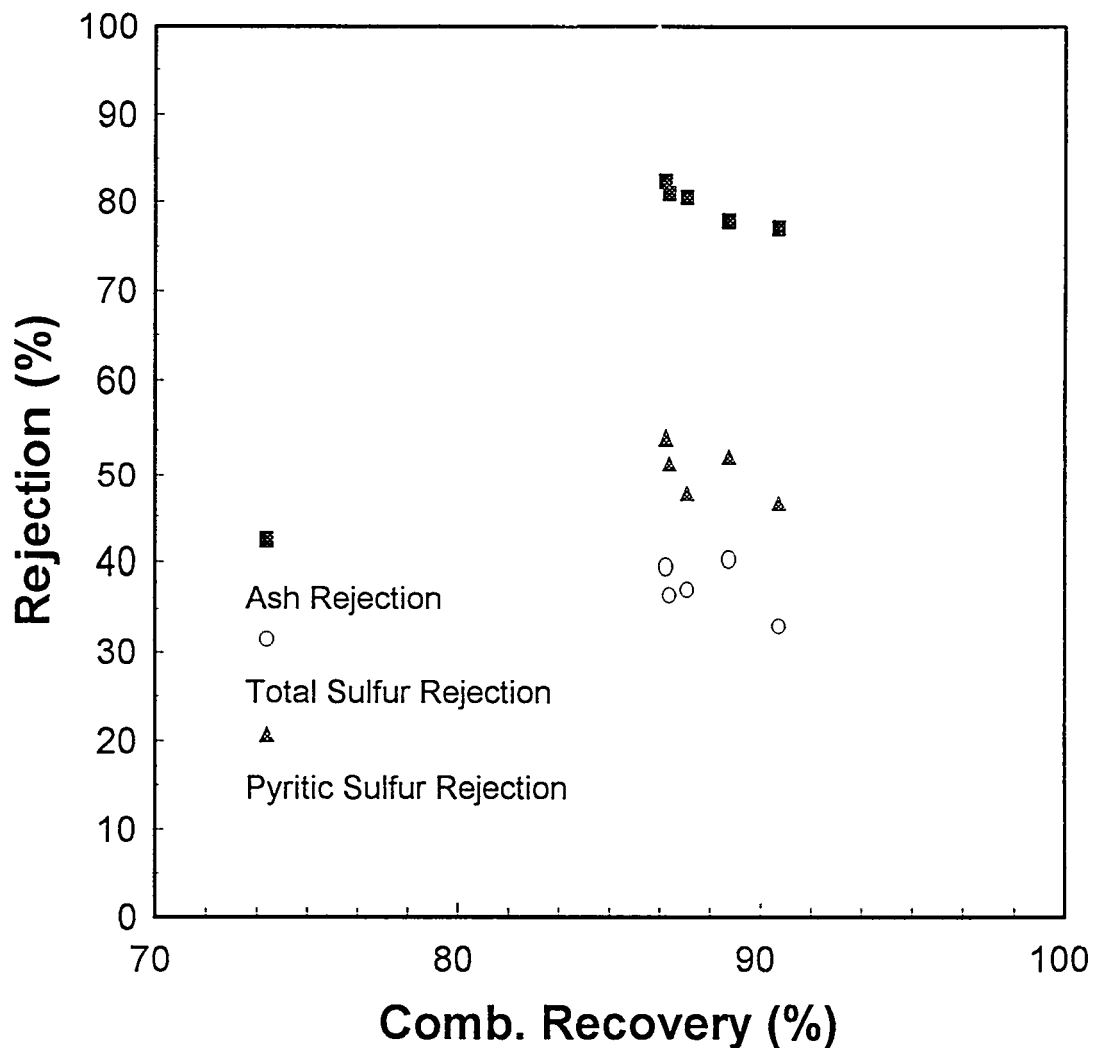
**Microcel**

Feed Rate (lbs/ton):	600
Wash Water (lpm):	40.1
Percent Solids (w/w):	11-12
Grind Size (d <sub>80</sub> (microns)): 200	200
Air Flow Rate (SCFM):	8.89
Diesel dosage (lbs/ton):	1
Frother Dosage (ml/min):	1.7

**MGS**

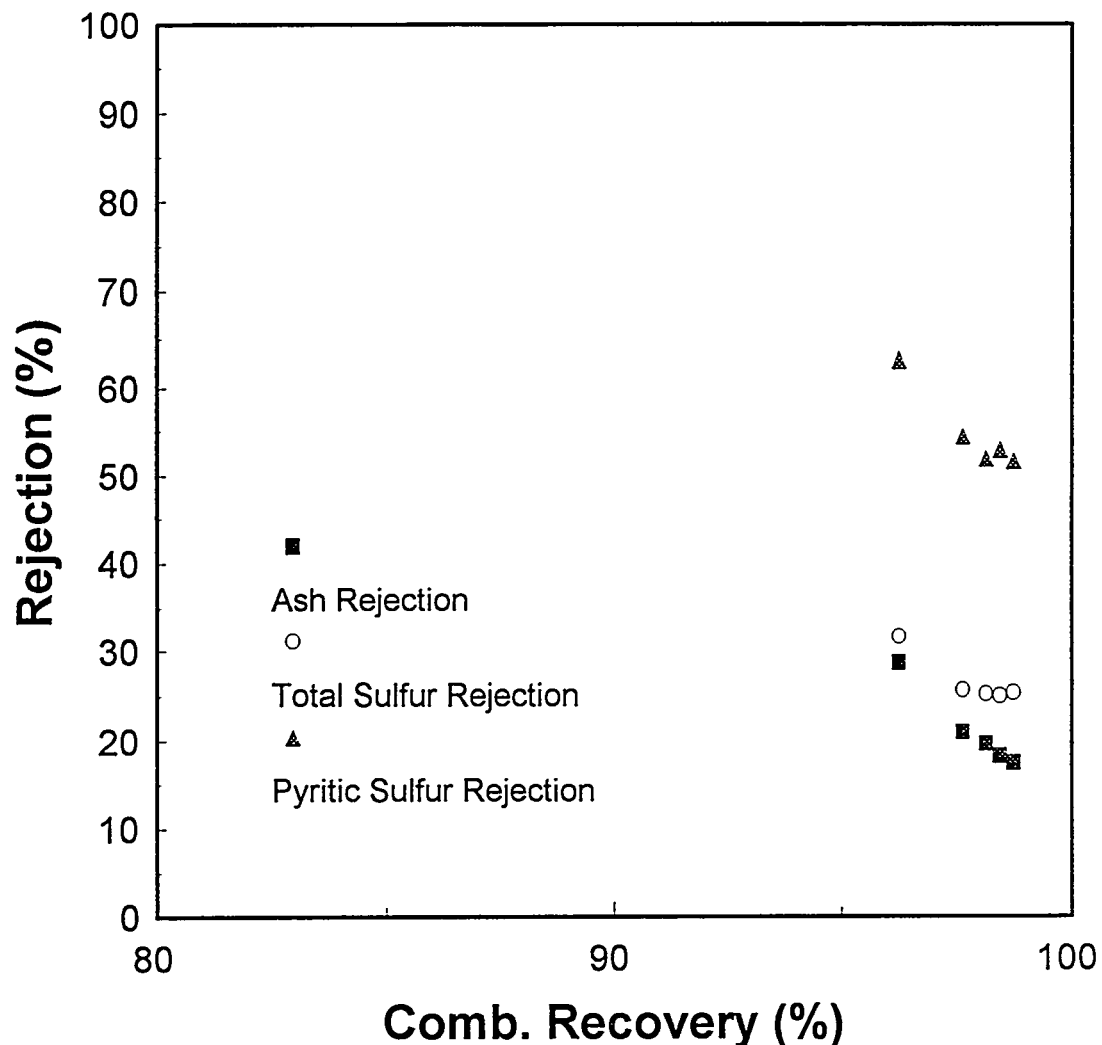
Feed Rate (lbs/hr):	340
Drum Speed (rpm):	283
Wash water (lpm):	0.49
Percent Solids (w/w):	23 - 24
Shake Amplitude (mm):	15
Shake Frequency (cps):	5
Tilt Angle (degrees):	6

Figures 33-35 show graphically the ash, total sulfur and pyritic sulfur rejections obtained using the Microcel, MGS and combined Microcel/MGS circuit. The synergistic effect is again evident in the performance graphs. For the overall circuit, ash and pyrite rejections of over 75% were obtained at a combustible recovery of over 85%. Although the Illinois No. 6 seam coal had a much higher feed ash than the Pittsburgh No. 8 seam coal (and tended to be more difficult to clean), the test results were in very good agreement with those obtained using the Pittsburgh No. 8 seam coal. Figure 36 shows the stability of the combined circuit during the long duration run.



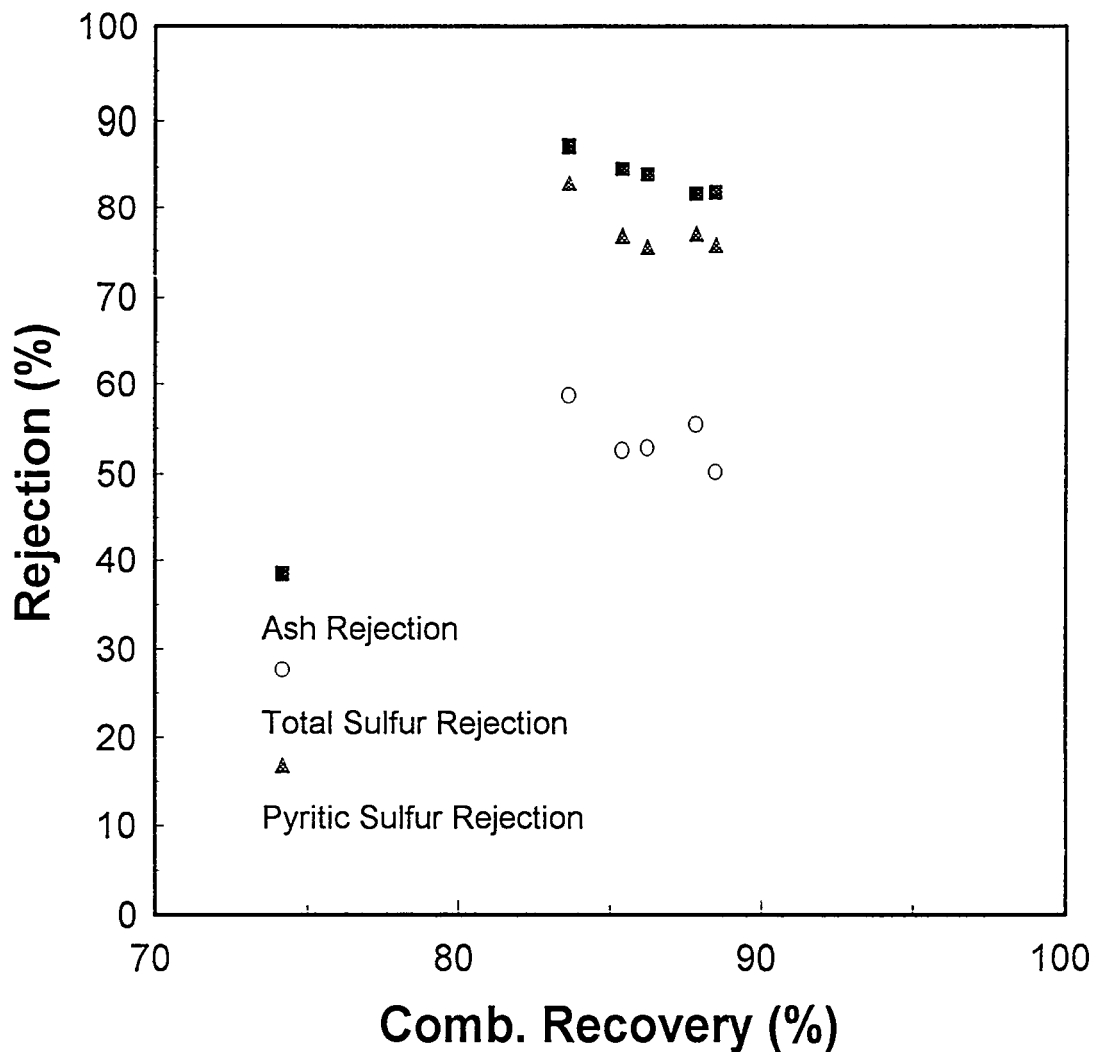
LD\_COL\_REJ

Figure 33. Combustible recovery versus rejection plots obtained for the Microcel column during the long-duration testing of the combined Microcel/MGS circuit using the Illinois No. 6 seam coal.



LD\_MGS\_REJ

Figure 34. Combustible recovery versus rejection plots obtained for the MGS unit during the long-duration testing of the combined Microcel/MGS circuit using the Illinois No. 6 seam coal.



LD\_COM\_REJ

Figure 35. Combustible recovery versus rejection plots obtained for the combined Microcel/MGS circuit during the long-duration testing of the Illinois No. 6 seam coal.

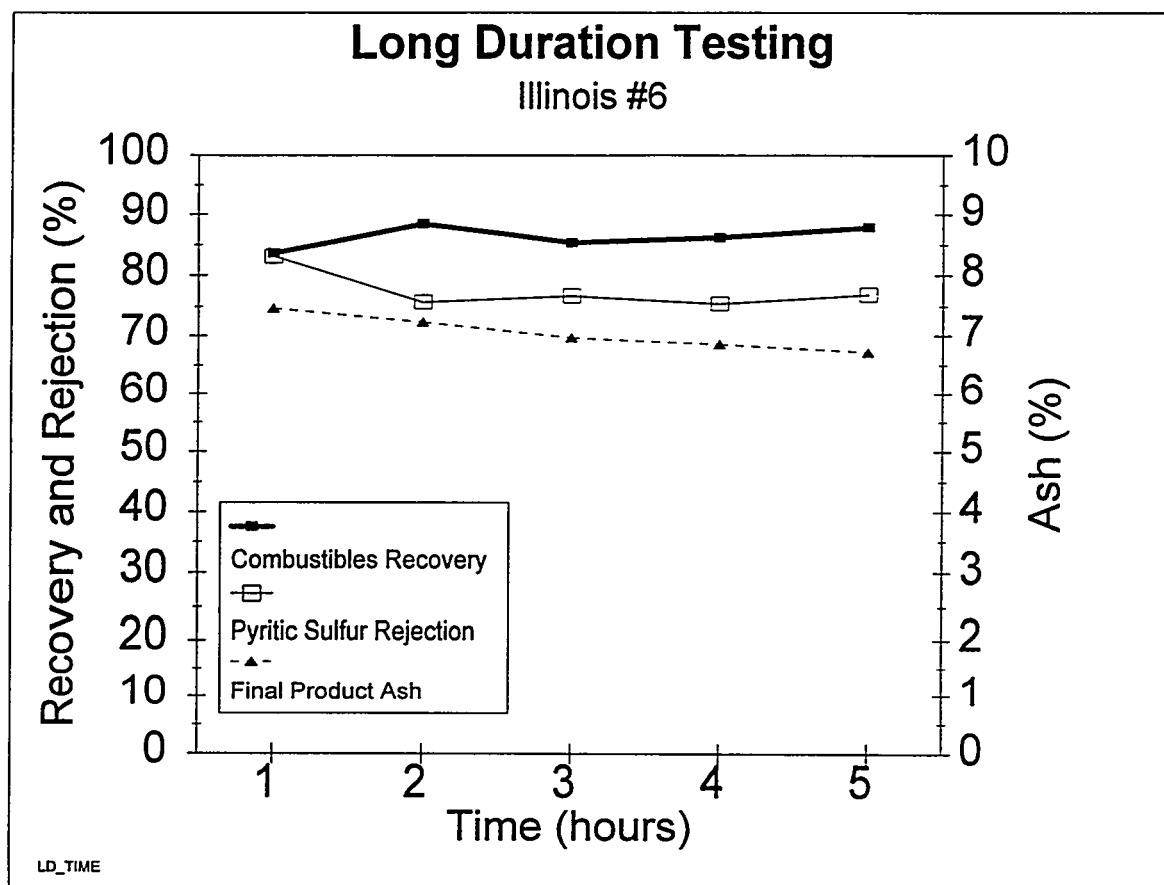


Figure 36. Long Duration results per hour during Illinois #6 seam test.

### *10.5.3 Partition Curves for the MGS*

Distribution curves (i.e., partition curves) were constructed using samples collected from the MGS during the middle segment of the long-duration test runs. The fine-coal washability analyses were performed by Process Tech, Inc., of Calumet, Michigan. This organization is well known for their expertise in conducting fine-coal washability tests. Organic heavy liquids were used in place of zinc chloride solutions in this series of analyses in order to avoid the coal dispersion problems that were encountered during the washability analyses conducted in Subtask 4.2 (Washability Characterization).

Figures 37 and 38 show the distribution curves obtained for the Pittsburgh No. 8 and Illinois No. 6 coal seams, respectively. For convenience, the cut-point ( $SG_{50}$ ) and probable error ( $E_p$ ) values have been summarized in Table 24. In general, the MGS provided cut-points higher than approximately 1.9 SG. Since pyrite has a very high density (SG=5.1), composite particles containing this mineral can be effectively rejected by the MGS at this high cut-point. Unfortunately, composite particles containing ash-forming minerals of lower density (i.e., 2.2-2.6 SG) would be rejected less effectively at this high cut-point. This finding helps to explain why the MGS achieves a lower rejection of ash than pyritic sulfur.

The test data obtained using the Illinois No. 6 seam coal shows that the  $E_p$  values ranged from 0.110 for the +100 mesh size fraction to 0.155 for the -400 mesh size fraction. The sharpest separations were achieved between 100 mesh and 400 mesh, in which  $E_p$  values of approximately 0.085-0.087 were achieved. The  $E_p$  values obtained for the Pittsburgh No. 8 seam were slightly poorer and varied from 0.156 to 0.205 for the +100 mesh and -400 mesh fractions, respectively. The sharpest separations were again achieved for the intermediate sizes (i.e., 100 x 400 mesh) which gave  $E_p$  values in the range of 0.125 to 0.155. For comparison, the average  $E_p$  values obtained with the MGS are plotted along with those reported by Osborne (1988) for conventional coal cleaning processes. This plot illustrates that the MGS is capable of significantly extending the particle size range over which density-based separations are effective.

Table 24. Overview of the MGS performance during the long-duration tests.

Particle Size (Mesh)	Pittsburgh No. 8 Seam		Illinois No. 6 Seam	
	SG <sub>50</sub>	E <sub>p</sub>	SG <sub>50</sub>	E <sub>p</sub>
+100	2.28	0.156	2.00	0.110
100 x 200	1.90	0.126	1.95	0.085
200 x 400	1.94	0.155	2.19	0.087
-400	1.97	0.205	2.71	0.155

Performance area for various coal cleaning devices

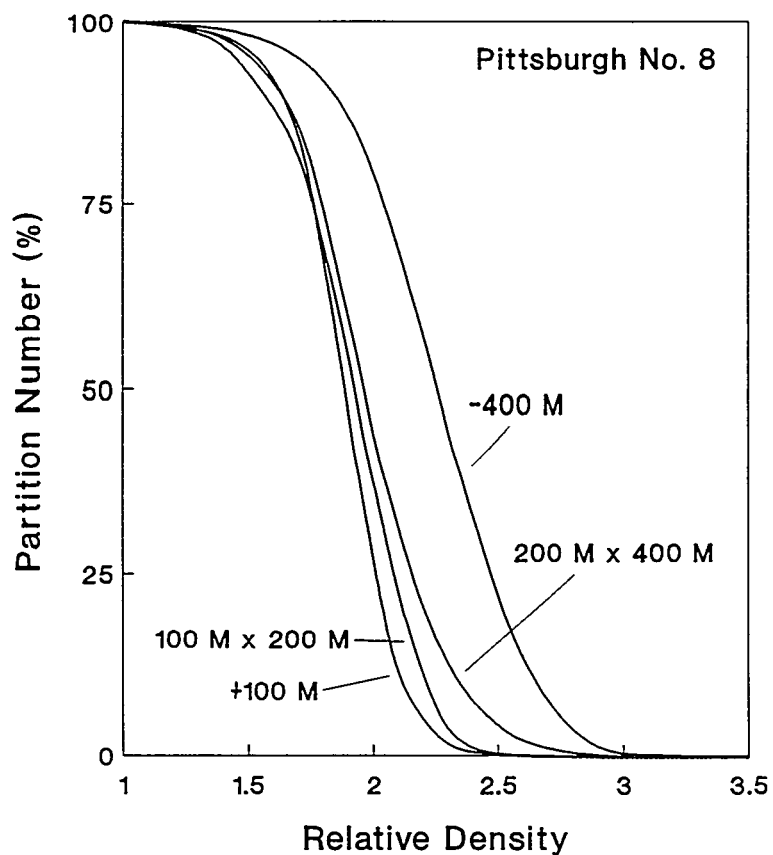


Figure 37. Effect of particle size on the partition curves for the MGS unit obtained during the long-duration testing of the Pittsburgh No. 8 seam coal.

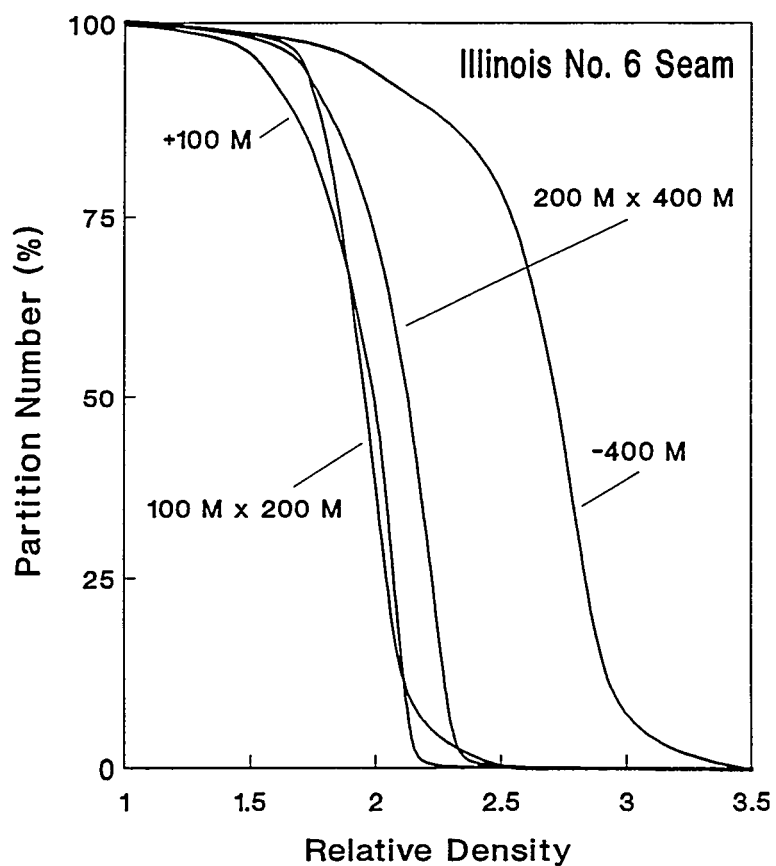


Figure 38. Effect of particle size on the partition curves for the MGS unit obtained during the long-duration testing of the Illinois No. 6 seam coal.

## 10.6 Near-Term Applications

In order to further evaluate the commercialization potential of the proposed circuit, tests were conducted near the end of the detailed test program using other coal samples supplied by the two participating coal companies. Time did not permit the selection of coal from any other sources.

### *10.6.1 Testing of Pittsburgh No. 8 Coal*

For this test, one of the participating coal companies sent a large volume of slurry collected directly from an operating coal preparation plant. The sample was nominal 0.5 mm x 0 material that had been partially deslimed in a small cyclone. This feed slurry was screened at 1 mm to remove any gross oversize material and then fed directly to the MGS circuit. The purpose of this series of testing was to determine the possible performance of the MGS as a stand alone unit on a natural feed. The benefit of this would be the possible replacement of other cleaning devices in the minus 0.5 mm range.

The test data and performance calculations for the near-term testing of the Pittsburgh No. 8 seam coal are provided in Appendix 8-A. The test data is summarized in Table 25. As shown, the MGS performed very well down to a particle size of minus 325 mesh. This is much finer than can typically be achieved using any other conventional water-based separation device used by the coal preparation industry.

Table 25. Test results obtained during the near-term testing of the Pittsburgh No. 8 seam coal.

Test no. 901

Size (mesh)	Yield (%)	Comb. Recovery (%)	Ash Rejection (%)	T. Sulfur Rejection (%)	Pyritic S Rejection (%)	Ash Separation Efficiency (%)	T. Sulfur Separation Efficiency (%)	Pyritic S Separation Efficiency (%)
+ 48	85.81	91.83	58.13	24.04	34.75	49.96	15.87	26.58
48 x 100	63.63	78.59	79.72	62.83	74.21	58.31	41.42	52.80
100 x 200	68.59	80.31	79.99	69.47	84.06	60.31	49.79	64.38
200 x 325	67.20	78.44	81.92	74.49	84.70	60.36	52.94	63.14
- 325	84.82	91.00	22.62	56.29	76.76	13.62	47.29	67.75
Cum.	79.28	87.83	54.01	47.69	64.00	41.85	35.52	51.83

Test no. 902

Size (mesh)	Yield (%)	Comb. Recovery (%)	Ash Rejection (%)	T. Sulfur Rejection (%)	Pyritic S Rejection (%)	Ash Separation Efficiency (%)	T. Sulfur Separation Efficiency (%)	Pyritic S Separation Efficiency (%)
+ 48	92.12	97.22	46.51	17.84	35.04	43.73	15.06	32.26
48 x 100	75.10	87.20	69.25	55.39	68.10	56.45	42.59	55.30
100 x 200	70.42	83.00	78.74	70.47	81.04	61.74	53.47	64.04
200 x 325	78.69	87.79	71.28	67.67	83.52	59.07	55.46	71.31
- 325	91.29	95.35	13.64	44.71	72.61	8.99	40.07	67.97
Cum.	86.13	93.39	43.55	41.26	63.20	36.93	34.65	56.59

Test no. 903

Size (mesh)	Yield (%)	Comb. Recovery (%)	Ash Rejection (%)	T. Sulfur Rejection (%)	Pyritic S Rejection (%)	Ash Separation Efficiency (%)	T. Sulfur Separation Efficiency (%)	Pyritic S Separation Efficiency (%)
+ 48	93.68	97.20	43.68	19.47	38.00	40.88	16.67	35.20
48 x 100	81.37	87.72	58.31	52.42	60.97	46.03	40.13	48.69
100 x 200	85.74	91.78	69.53	55.71	74.60	61.31	47.49	66.37
200 x 325	86.07	94.16	70.21	59.72	83.96	64.38	53.89	78.13
- 325	99.12	99.61	1.48	27.72	64.48	1.08	27.32	64.08
Cum.	91.89	95.46	22.27	35.30	60.49	17.73	30.77	55.96

Test no. 904

Size (mesh)	Yield (%)	Comb. Recovery (%)	Ash Rejection (%)	T. Sulfur Rejection (%)	Pyritic S Rejection (%)	Ash Separation Efficiency (%)	T. Sulfur Separation Efficiency (%)	Pyritic S Separation Efficiency (%)
+ 48	88.96	94.23	53.86	21.98	41.84	48.09	16.22	36.07
48 x 100	79.43	88.26	70.42	50.71	65.40	58.68	38.97	53.65
100 x 200	88.99	93.80	55.60	47.28	67.47	49.40	41.08	61.27
200 x 325	69.92	78.74	78.79	67.85	86.43	57.53	46.59	65.17
- 325	89.96	94.33	15.16	48.53	66.64	9.49	42.86	60.97
Cum.	85.79	91.70	38.95	41.16	61.73	30.66	32.86	53.43

Test no. 905

Size (mesh)	Yield (%)	Comb. Recovery (%)	Ash Rejection (%)	T. Sulfur Rejection (%)	Pyritic S Rejection (%)	Ash Separation Efficiency (%)	T. Sulfur Separation Efficiency (%)	Pyritic S Separation Efficiency (%)
+ 48	93.06	95.89	47.48	16.36	25.55	43.36	12.24	21.44
48 x 100	89.04	93.20	49.30	37.41	27.81	42.51	30.61	21.01
100 x 200	94.71	97.35	32.75	27.90	50.58	30.10	25.26	47.94
200 x 325	83.64	90.73	63.35	60.75	79.78	54.08	51.48	70.51
- 325	95.45	97.63	7.05	28.82	55.37	4.68	26.45	53.00
Cum.	92.35	95.35	21.03	30.47	45.96	16.38	25.82	41.32

### *10.6.2 Testing of Illinois No. 6 Coal*

The testing of the Illinois No. 6 coal was only partially successful due to the problems with stabilizing the overall circuit. In addition, much of the feed sample was discarded as oversize when pre-sized for circuit feed. Therefore, only a limited amount of this particular coal sample was available for the near-term test program. In fact, most of the remaining coal was consumed trying to stabilize the circuit. Therefore, no reliable data was collected for this particular series of near-term tests. The test data that was collected is summarized in Appendix 8-B.

## **Task 11 - Decommissioning**

### **11.1 Circuit Decommissioning**

Prior to dismantling the circuit, a Decommissioning Plan was prepared by CCMP which described the orderly removal of all related process equipment from the CPPRF by Rizzo & Sons. Decommissioning began after the completion of Task 10 (Detailed Testing) and involved the dismantling of all unit operations, disassembly of all electrical and mechanical components, and the restoration of the CPPRF to its original condition. The prime contractor (CCMP) and participating A&E firm (Roberts & Schaefer) shared the responsibility for the supervision of Rizzo & Sons. This task was completed in approximately 4 days.

### **11.2 Equipment Disposition**

This subtask involved the cleaning, minor repair, packing and shipment of the decommissioned equipment to storage facilities specified by the DOE COR. DOE retained ownership to all components necessary for the operation of a complete Microcel column flotation circuit. Virginia Tech was assigned ownership of all other process equipment, including the Multi-Gravity Separator (MGS).

## **Task 12 - Sample Analysis**

### **12.1 Standard Analyses**

The following ASTM procedures and standards were employed for all determinations.

- D 121-91              Definition of Terms Relating to Coal and Coke
- D 311-84              Method of Sieve Analysis of Crushed Bituminous Coal
- D 410-84              Method of Sieve Analysis of Coal
- D 1857-87              Test Method for Fusibility of Coal and Coke Ash
- D 2013-86              Method of Preparing Coal Samples for Analysis
- D 2015-91              Test Method of Gross Calorific Value of Solid Fuel by Adiabatic Bomb Calorimeter

- D 2234-89      Method of Collection of a Gross Sample of Coal
- D 2492-90      Test Method for Forms of Sulfur in Coal
- D 3172-89      Methods for Proximate Analysis of Coal and Coke
- D 3173-87      Test Method for Moisture in the Analysis Sample of Coal and Coke
- D 3174-89      Test Method for Ash in the Analysis Sample of Coal and Coke from Coal
- D 3177-89      Test Methods for Total Sulfur in the Analysis Sample of Coal and Coke
- D 3180-89      Methods for Calculating Coal/Coke Analyses As Determined to Different Bases
- D 3302-91      Test Method of Total Moisture in Coal
- D 4371-91      Test Method for Determining the Washability Characteristics of Coal
- E 11-87          Specification for Wire Cloth Sieves for Testing Purposes
- E 323-80          Specification for Perforated-Plate Sieves for Testing Purposes

Details on the ASTM tests are available in the 1992 Annual Book of ASTM Standards (Volume 05.05, Gaseous Fuels; Coal and Coke). Unless otherwise specified, these analyses consisted of the determination of moisture, ash, total sulfur, pyritic sulfur, and heating value. Particle size analyses were also determined for selected samples. Particle size distributions were determined using standard wet-sieving techniques down to a minimum size of 400 mesh (37 microns), while sub-sieve analysis were conducted using an Elzone particle size analyzer. Results from the sub-sieve analysis will be blended with the sieve results to determine the overall particle size distribution. Additional details related to the laboratory analyses were provided in the Test, Sampling and Analytical Plan provided to DOE. In order to facilitate the timely completion of the sample analyses, small portions of the work effort were subcontracted to a commercial laboratory (Precision Testing, Beckley, West Virginia). All other analyses were conducted at CCMP.

The reliability of the experimental data was evaluated using the BILMAT material balance program. This program examines the overall circuit to determine whether the mass flow rate of each component entering and leaving each unit operation within the circuit is equivalent. If this criterion is not met, the program adjusts the measured values until all component mass flows are externally and internally consistent. Little or no adjustment suggests that the data set is reliable. This provides some degree of assurance that the sampling procedures and laboratory analysis techniques used throughout the test program were accurate.

## 12.2 Specialty Analyses

Additional analyses were conducted on selected samples. These included the measurement of particle size distributions and fine-coal washability. Other characterization analyses, include IPS/SEM studies, were conducted as necessary. In order to construct partition curves for some of the MGS tests, selected samples were shipped to an external laboratory (Process Tech, Inc., Calmulet, MI) for centrifugal float-sink testing. These analyses have been discussed in previous sections throughout this report.

### 12.3 Trace Element Analyses

A Cooperative Research and Development Agreement (CRADA) was established with DOE/PETC to permit personnel from CCMP to collect samples from the combined Microcel/MGS circuitry for trace element analyses. The sampling effort and associated analyses of trace elements were conducted under a separate project sponsored by the Electric Power Research Institute (EPRI Reference Number RP8022-07). The trace element analyses were conducted on representative samples collected during the long-duration testing of the Pittsburgh No. 8 and Illinois No. 6 seam coals.

The results of the various trace element analyses are summarized in Tables 26-27. Using these values, removal efficiencies of various trace elements after Microcel and MGS processing were calculated and plotted in Figures 39 and 40. Note that antimony, boron and molybdenum have been excluded from these plots since the concentration of these elements in the various clean coal products were below the detection limit of the analytical techniques used in the present work. For the Pittsburgh No. 8 seam coal, trace element removal efficiencies ranging from a low of 27% for vanadium to a high of 89% for copper were achieved using the combined circuit. Likewise, the removal efficiencies for the Illinois No. 6 seam coal ranged from a low of 46% for mercury to a high of 93% for manganese. In general, the overall removal efficiencies obtained using the Illinois No. 6 seam coal were typically higher than those obtained using the Pittsburgh No. 8 seam coal.

With the exception of mercury, the Microcel achieved good removal efficiencies of metals (i.e., 25-80%) for both coals. For the MGS, the best removal efficiencies were obtained for arsenic (Pittsburgh No. 8 at 32% and Illinois No. 6 at 29%) and mercury (Pittsburgh No. 8 at 25% and Illinois No. 6 at 38%). In addition, the MGS removed a significant amount of selenium (21%) from the Pittsburgh No. 8 seam coal and lead (35%) from the Illinois No. 6 seam coal. The incremental improvement in removal efficiency by the MGS is believed to be impressive in light of the high removals of trace elements achieved by the Microcel unit.

Table 26.

Trace element analysis of the samples collected during the long-duration testing of the Pittsburgh No. 8 seam coal (material balanced data).

Sample	Sample Description	Trace Element Analysis															
		Sb	As	Ba	Be	B	Cd	Cr	Co	Cu	Pb	Mn	Hg	Mo	Ni	Se	V
1S	Circuit Feed Solids	ND	8.04	66.2	4.47	ND	0.14	31	7.47	5.93	7.03	49	0.12	ND	11.8	2.2	31.3
1F	Circuit Feed Filtrate																
2S	Microcel Feed Solids	ND	8.04	66.2	4.47	ND	0.14	31	7.47	5.93	7.03	49	0.12	ND	11.8	2.2	31.3
2F	Microcel Feed Filtrate																
3S	Microcel Reject Solids	ND	20.8	282	2.91	ND	0.35	119	19.9	31.2	23.9	236	0.24	ND	38.9	5.24	73.5
3F	Microcel Reject Filtrate																
4S	MGS Feed Solids	ND	5.72	27	4.75	ND	0.1	15.1	5.21	1.34	3.97	15	0.1	ND	6.83	1.65	23.6
4F	MGS Feed Filtrate																
5S	MGS Reject Solids	ND	69.3	67.7	1.16	ND	0.48	39.6	15.9	18.2	28	130	0.86	ND	28	13.1	46.2
5F	MGS Reject Filtrate																
6S	MGS Product Solids	ND	3.17	25.4	4.89	ND	0.08	14.1	4.78	0.67	3.01	10.4	0.07	ND	5.98	1.19	22.7
6F	MGS Product Filtrate																
7	Make-Up Water																
**	Analytical Technique	ICP	GF	ICP	ICP	GF	GF	GF	GF	GF	GF	DG	ICP	GF	GF	ICP	
**	Detection Limit (ug/L)	50	1	1	1	6	0.1	0.5	1	1	1	0.2	3E-04	5	1	1	1

ND = Not Detected, Solids in ug/g, Filtrate in ug/L

GF = Graphite Furnace Atomic Absorption Spectroscopy

ICP = Inductively Coupled Plasma Atomic Emission Spectroscopy

DG = Double-Gold Amalgam Mercury Vapor Method

Table 27. Trace element analysis of the samples collected during the long-duration testing of the Illinois No. 6 seam coal (material balanced data).

Sample	Sample Description	Trace Element Analysis															
		Sb	As	Ba	Be	B	Cd	Cr	Co	Cu	Pb	Mn	Hg	Mo	Ni	Se	V
1S	Circuit Feed Solids	ND	10.2	103	1.7	ND	2.19	107	12.2	22.7	29.6	210	0.13	ND	39.8	12.1	96.6
1F	Circuit Feed Filtrate																
2S	Microcel Feed Solids	ND	10.2	103	1.7	ND	2.19	107	12.2	22.7	29.6	210	0.13	ND	39.8	12.1	96.6
2F	Microcel Feed Filtrate																
3S	Microcel Reject Solids	ND	15.4	241	4.27	ND	5.03	239	21.6	46.5	46.4	501	0.15	ND	78.8	23.9	186
3F	Microcel Reject Filtrate																
4S	MGS Feed Solids	ND	7.02	21.2	0.17	ND	0.49	27.9	6.57	8.44	19.6	36.7	0.12	ND	16.6	5.09	43.5
4F	MGS Feed Filtrate																
5S	MGS Reject Solids	ND	96.8	51.3	0.97	ND	9.17	62	48.5	63.5	338	702	1.71	ND	62.7	34.3	101
5F	MGS Reject Filtrate																
6S	MGS Product Solids	ND	4.04	20.2	0.14	ND	0.2	26.7	5.18	6.61	9.04	14.7	0.07	ND	15	4.12	41.5
6F	MGS Product Filtrate																
7	Make-Up Water																
**	Analytical Technique	ICP	GF	ICP	ICP	GF	GF	GF	GF	GF	GF	DG	ICP	GF	GF	ICP	
**	Detection Limit (ug/L)	50	1	1	1	6	0.1	0.5	1	1	0.2	3E-04	5	1	1	1	

ND = Not Detected, Solids in ug/g, Filtrate in ug/L

GF = Graphite Furnace Atomic Absorption Spectroscopy

ICP = Inductively Coupled Plasma Atomic Emission Spectroscopy

DG = Double-Gold Amalgam Mercury Vapor Method

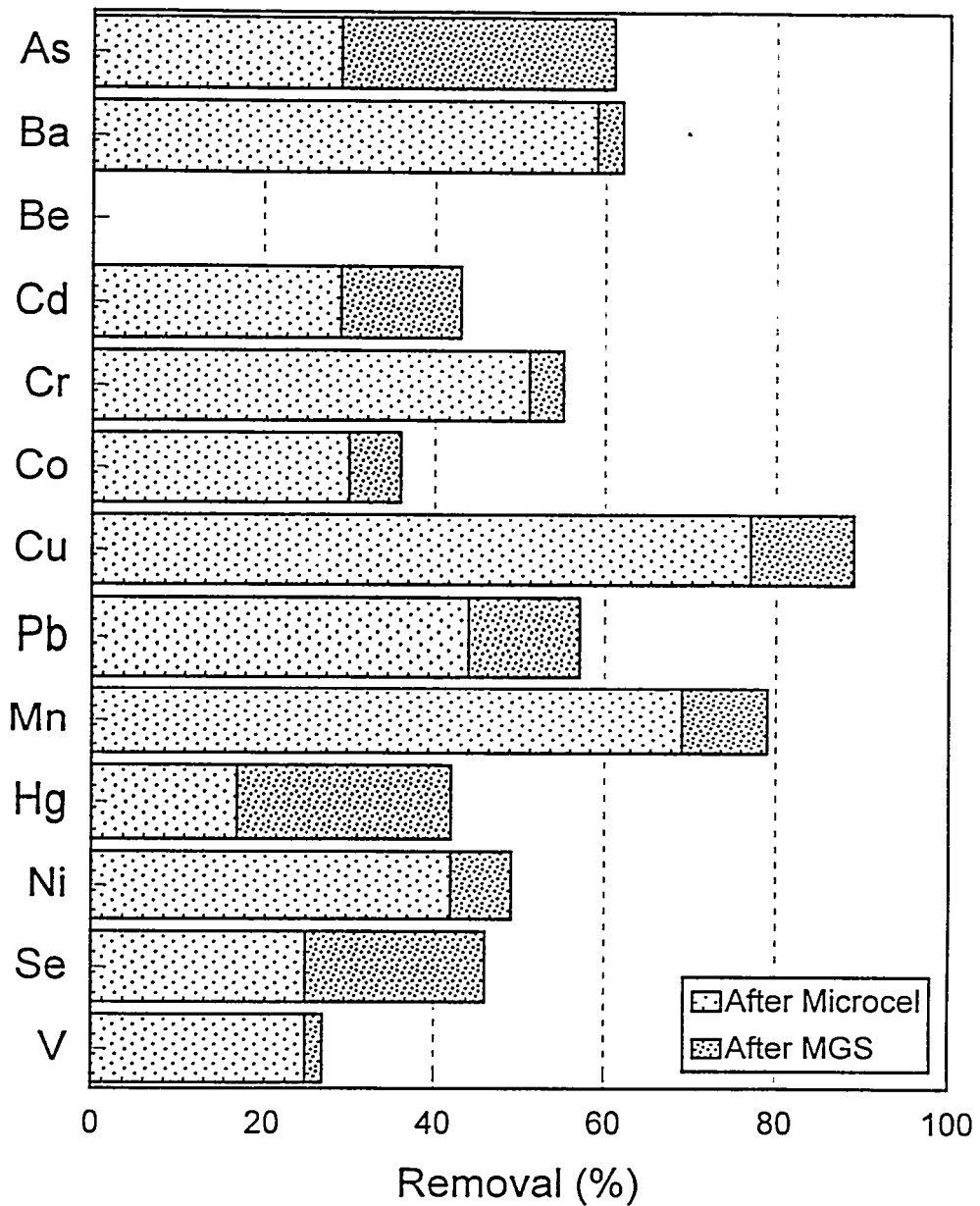


Figure 39. Percent removals of trace elements after Microcel and MGS processing for the Pittsburgh No. 8 seam coal

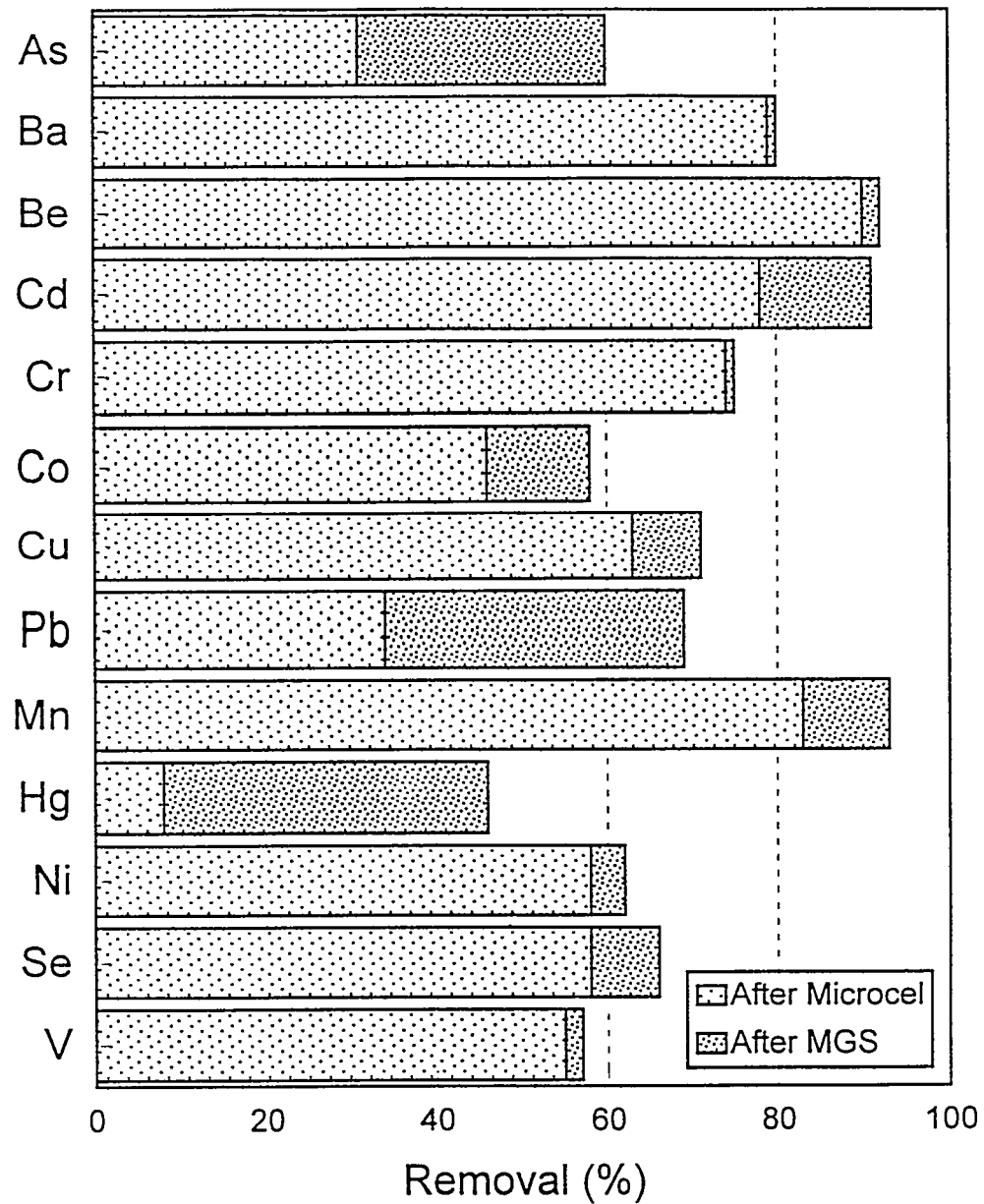


Figure 40. Percent removals of trace elements after Microcel and MGS processing for the Illinois No. 6 seam coal

## Task 13 - Final Report

### 13.1 Technical Evaluation

The results obtained from the parametric testing of the Pittsburgh No. 8 and Illinois No. 6 seam coals are summarized in Figures 41-58. Although the data points are the same as those plotted in Subtasks 10.1-10.3, the values have been replotted so that the performance of the Microcel, MGS and combined Microcel/MGS circuits can be easily compared. These figures give an excellent summary of the parametric and long duration testing for each of the two seams. Although combustible recovery is plotted, this is essentially equal to energy recovery for these two coals. As shown, the experimental data points obtained for each circuit fall along distinct grade-recovery curves. This trend was surprising in light of the fact that the test runs were conducted over a wide range of operating conditions. Data obtained using the run-of-mine Pittsburgh No. 8 seam (Figures 41-43) indicate that the MGS achieved an ash rejection of 40% and pyritic sulfur rejection of 70% at an energy recovery that approached 95%. Similar rejections of ash and pyritic sulfur were obtained for the Illinois No. 6 seam coal (Figures 50-52), but at a slightly lower energy recovery of 90%. These results suggest that the MGS is very effective in separating high-density pyrite from low-density coal. On the other hand, the MGS appears to be less effective in removing ash-forming mineral matter from the feed coal.

The relatively poor ash rejections obtained using the MGS can be largely attributed to the presence of clay minerals in the run-of-mine feed coals. Because of their ultrafine size, these particles lack sufficient mass to be pinned to the drum surface and are readily entrained with the flowing-film into the clean coal product. To overcome this problem, each of the run-of-mine coals were precleaned using the Microcel flotation column to remove ultrafine clays. As shown in Figures 44-46 for the Pittsburgh #8 seam, the removal of ash-forming minerals by the Microcel column allowed the MGS to achieve a much higher level of performance in terms of ash removal. Figures 53-55 indicate similar results for the Illinois #6 seam. By combining the two unit operations, the two-stage circuit provided high rejections (75%-85%) of both ash and pyritic sulfur with minimal losses in overall energy recovery (<5-10%). The previous comments are also shown in Figures 47-49 (Pittsburgh #8) and Figures 56-58 (Illinois #6) which indicate the consistent equipment performance of the combined testing during the long duration runs.

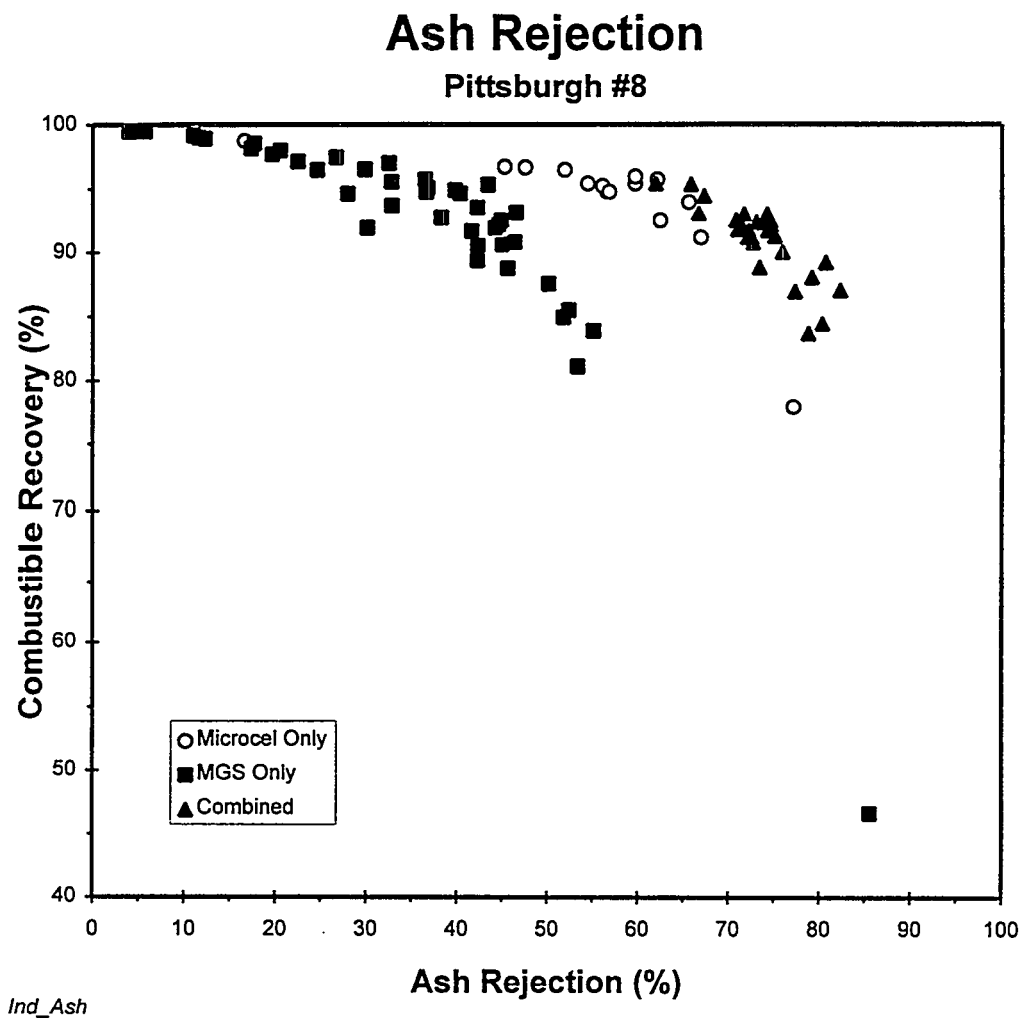


Figure 41. Combustible recovery versus ash rejection for run-of-mine Pittsburgh #8 seam coal.

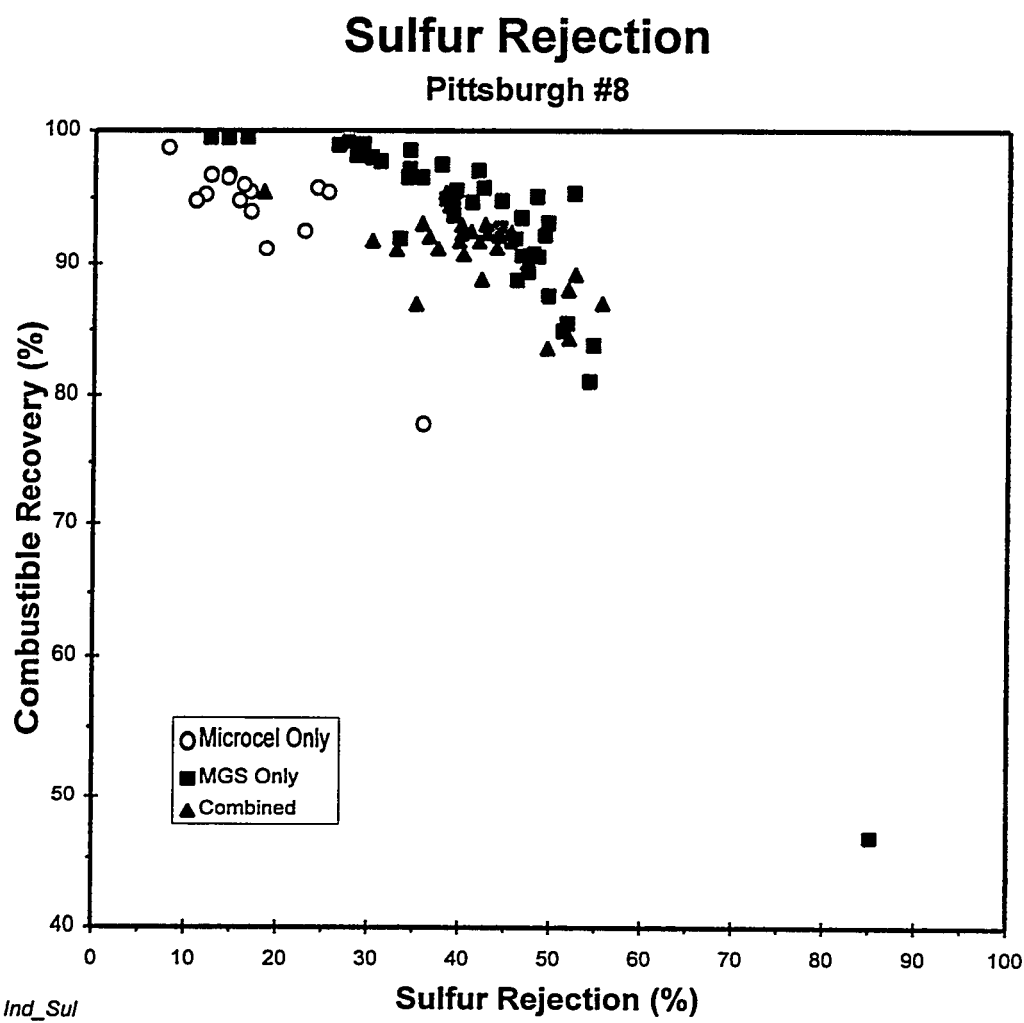


Figure 42. Combustible recovery versus total sulfur rejection for run-of-mine Pittsburgh #8 seam coal.

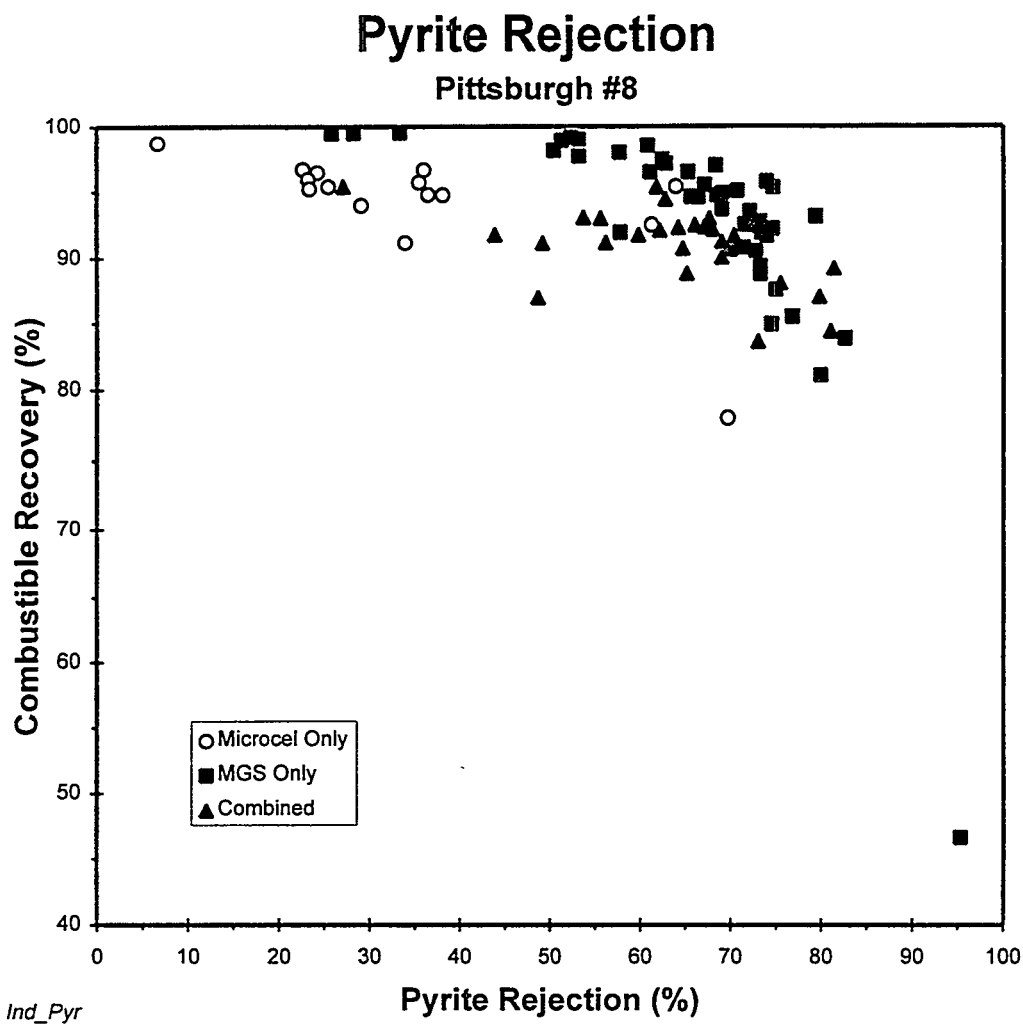


Figure 43. Combustible recovery versus pyrite rejection for run-of-mine Pittsburgh #8 seam coal.

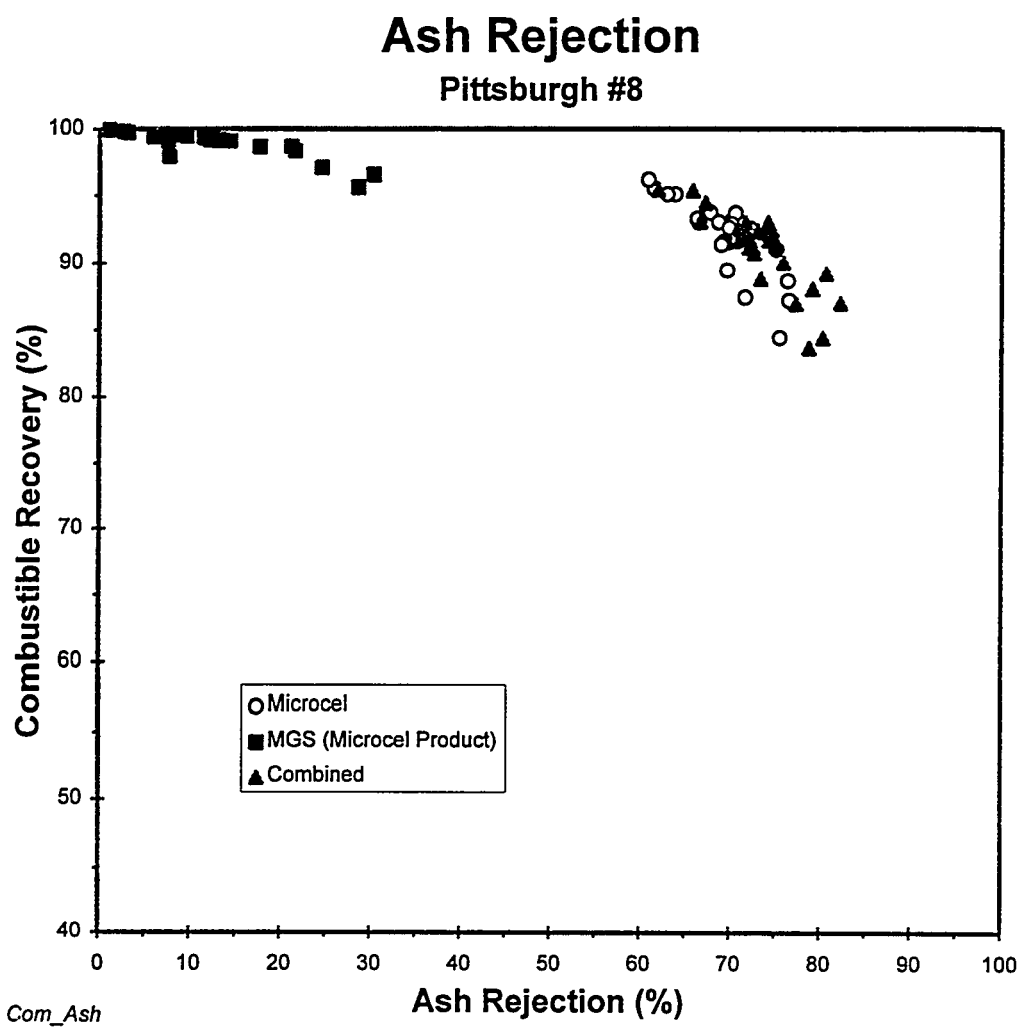


Figure 44. Combustible recovery versus ash rejection for each unit of the combined circuit.

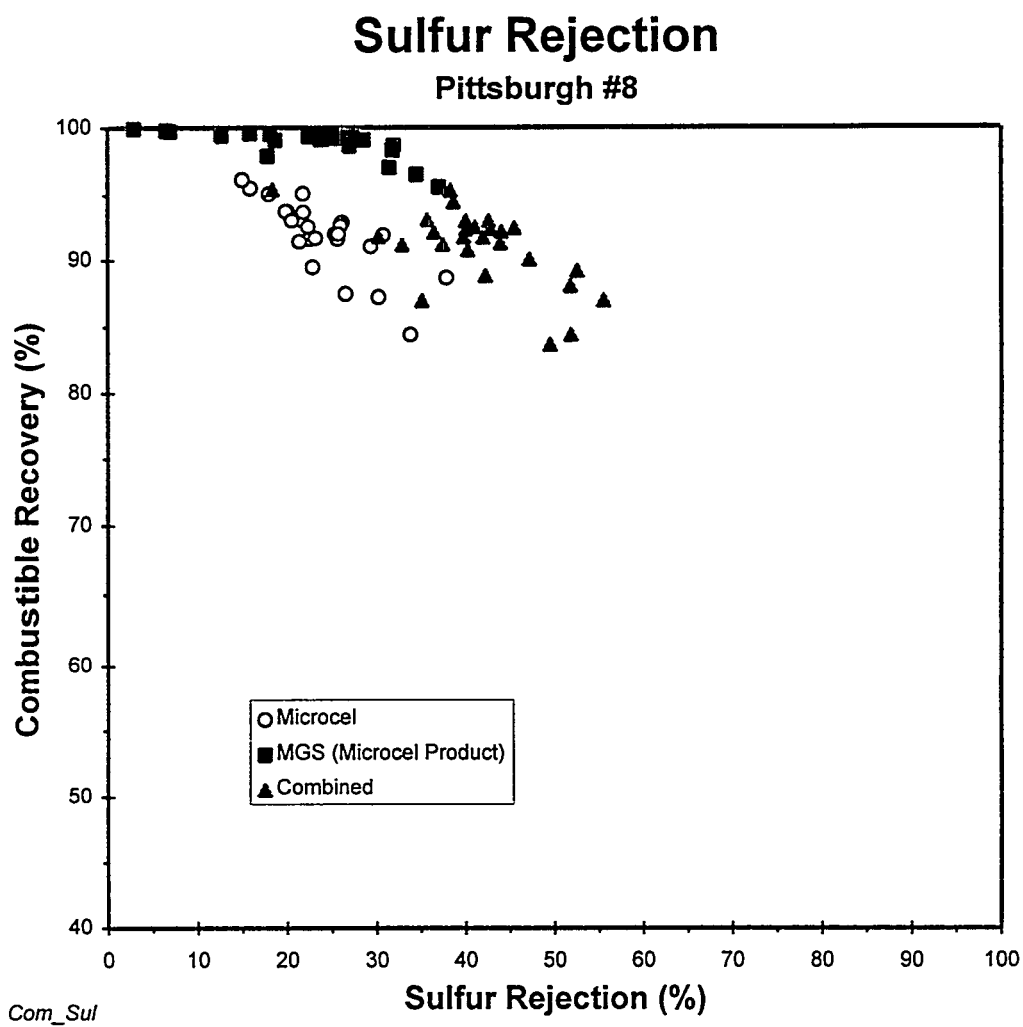


Figure 45. Combustible recovery versus total sulfur rejection for each unit of the combined circuit.

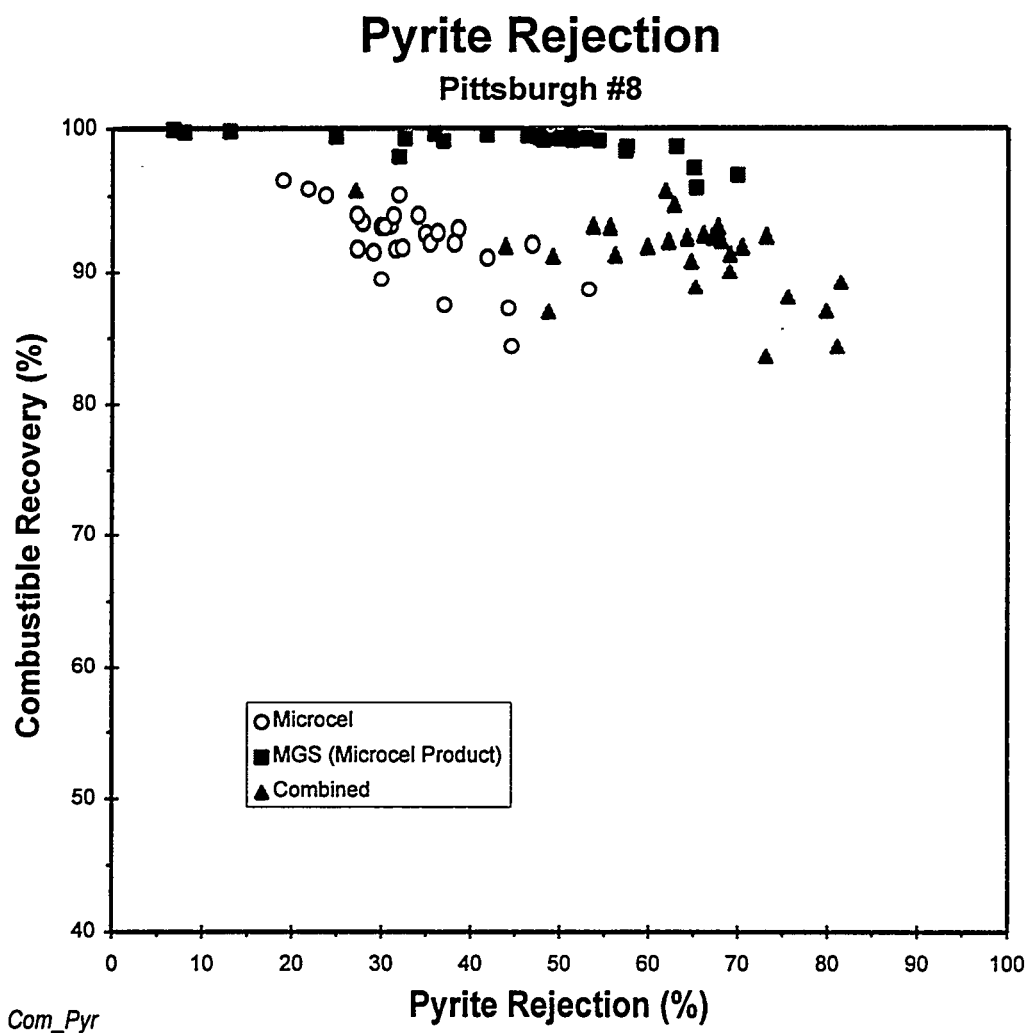


Figure 46. Combustible recovery versus pyritic sulfur rejection for each unit of the combined circuit

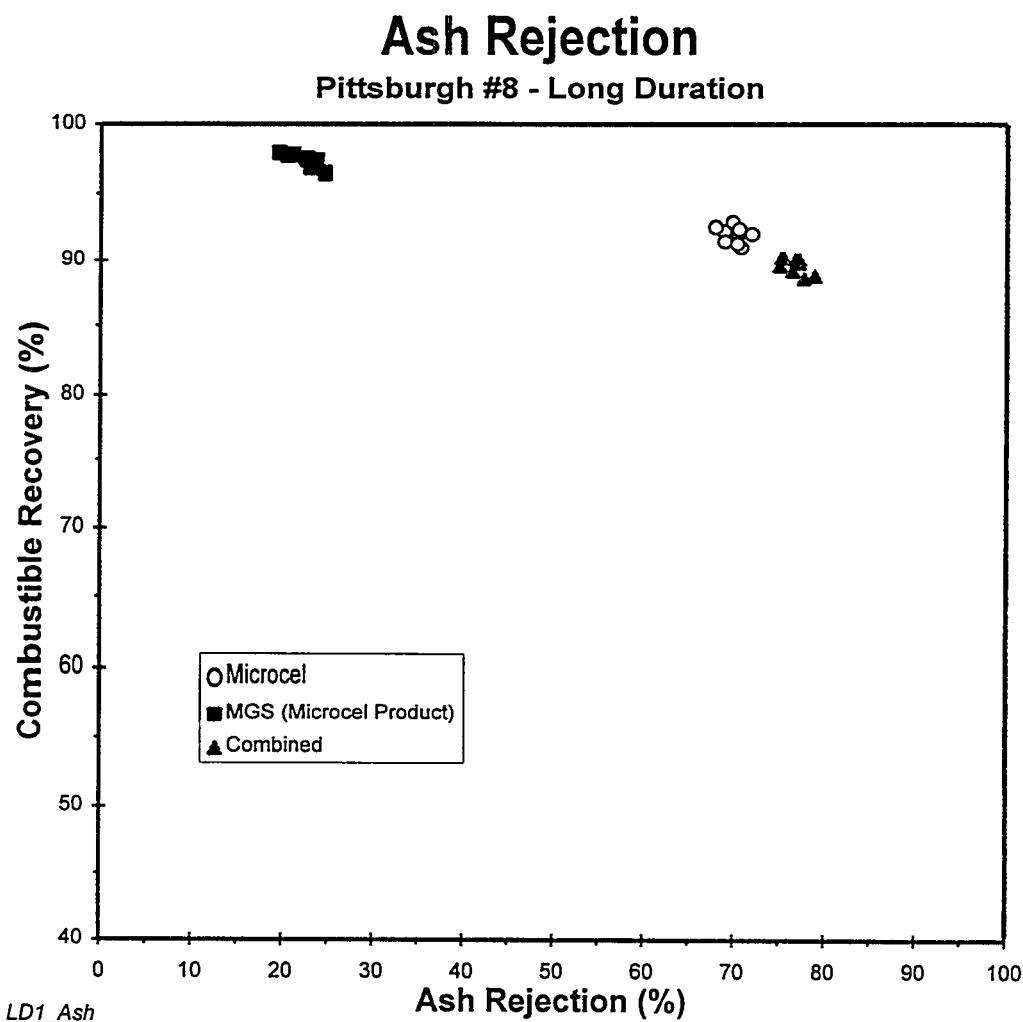


Figure 47. Combustible recovery versus ash rejection for each unit of the combined circuit during long duration testing.

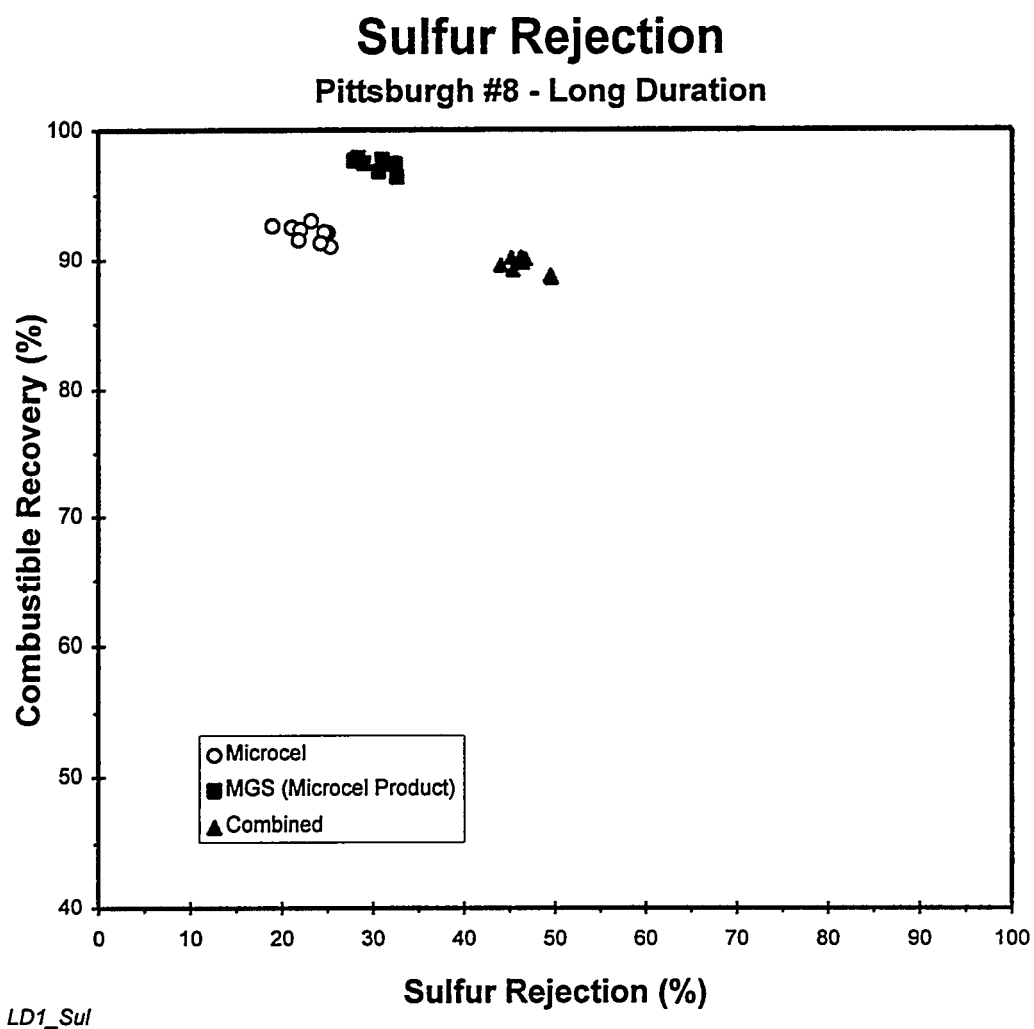


Figure 48. Combustible recovery versus total sulfur rejection for each unit of the combined circuit during long duration testing.

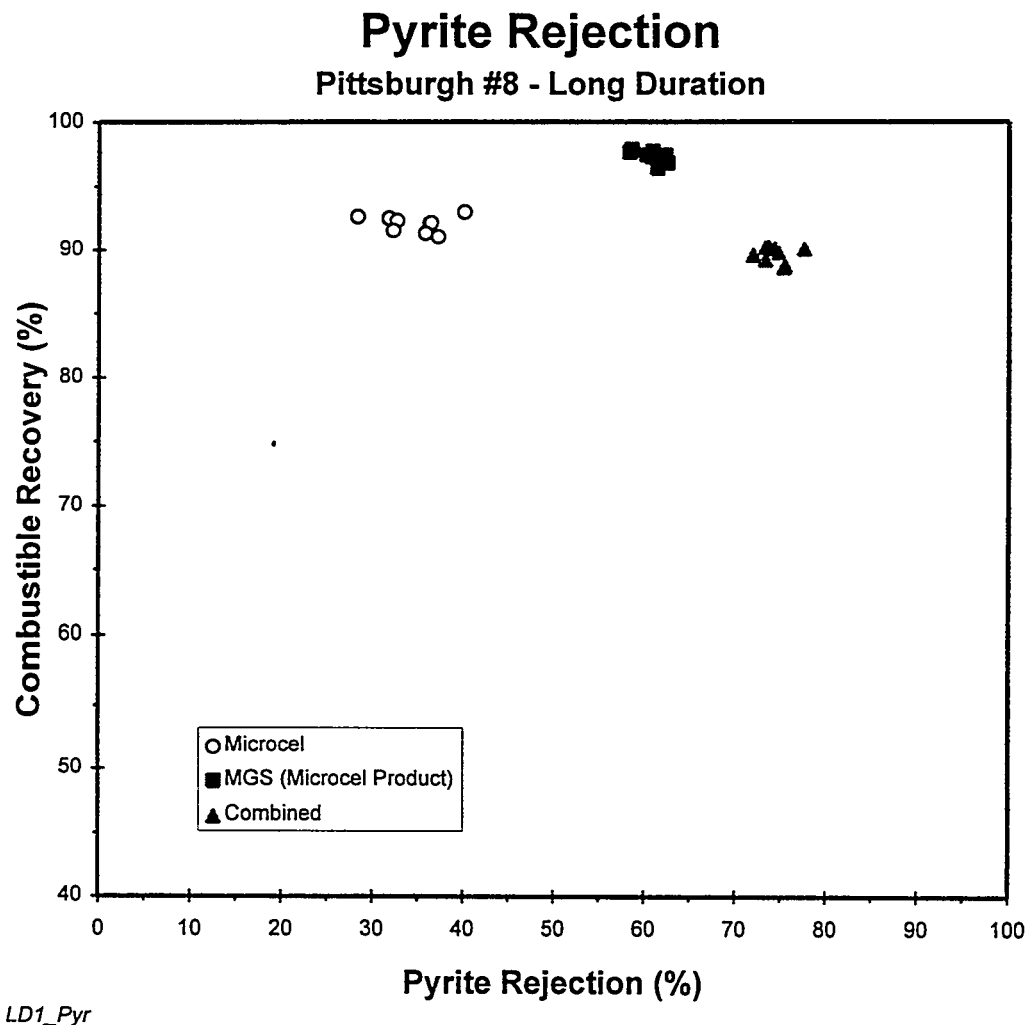


Figure 49. Combustible recovery versus pyritic sulfur rejection for each unit of the combined circuit during long duration testing.

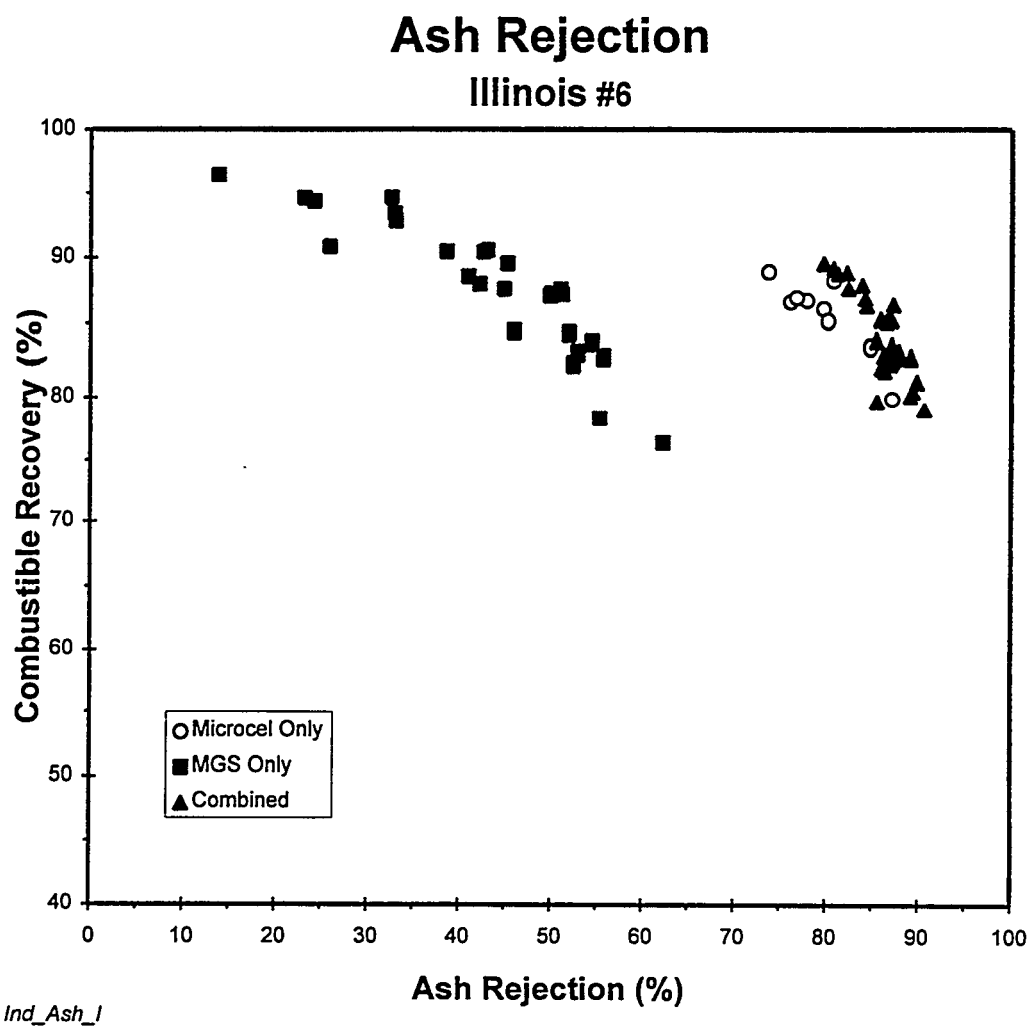


Figure 50. Combustible recovery versus ash rejection for run-of-mine Illinois #6 seam coal.

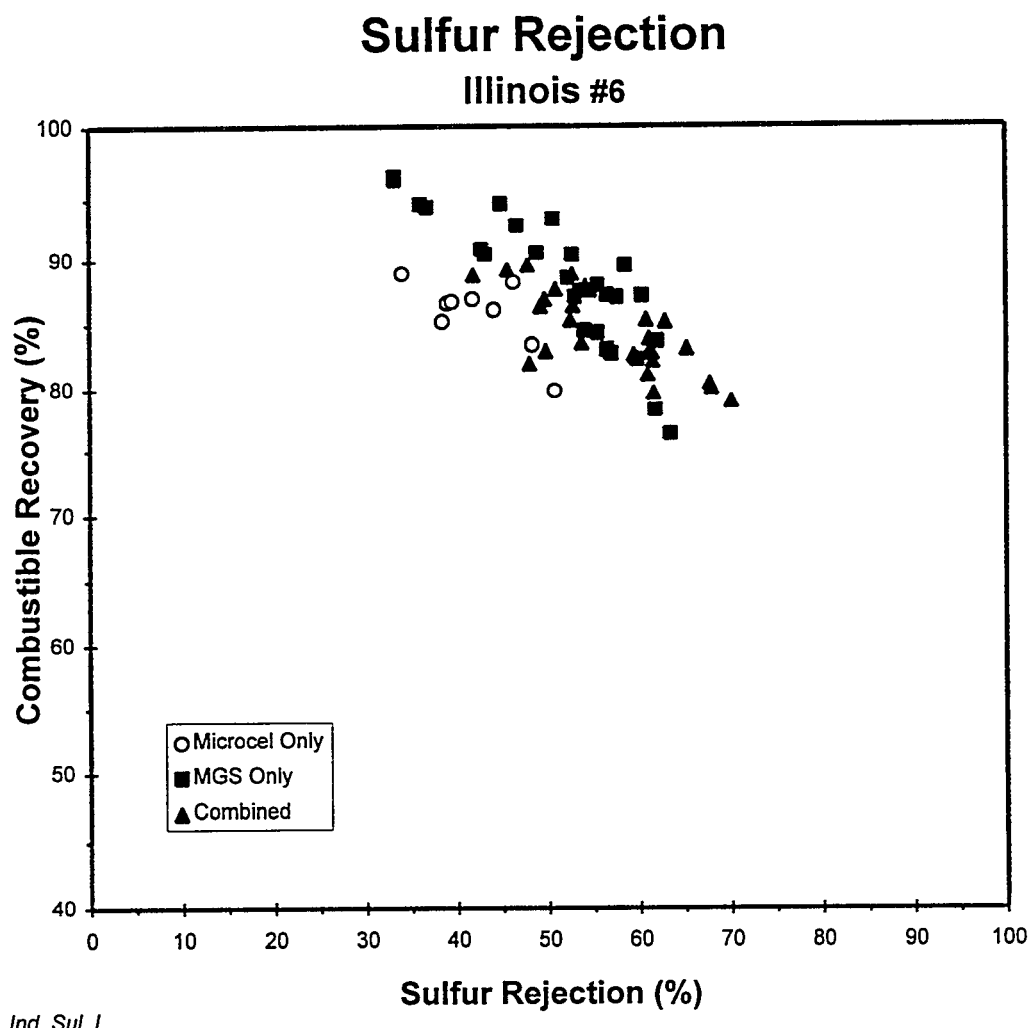


Figure 51. Combustible recovery versus total sulfur rejection for run-of-mine Illinois #6 seam coal.

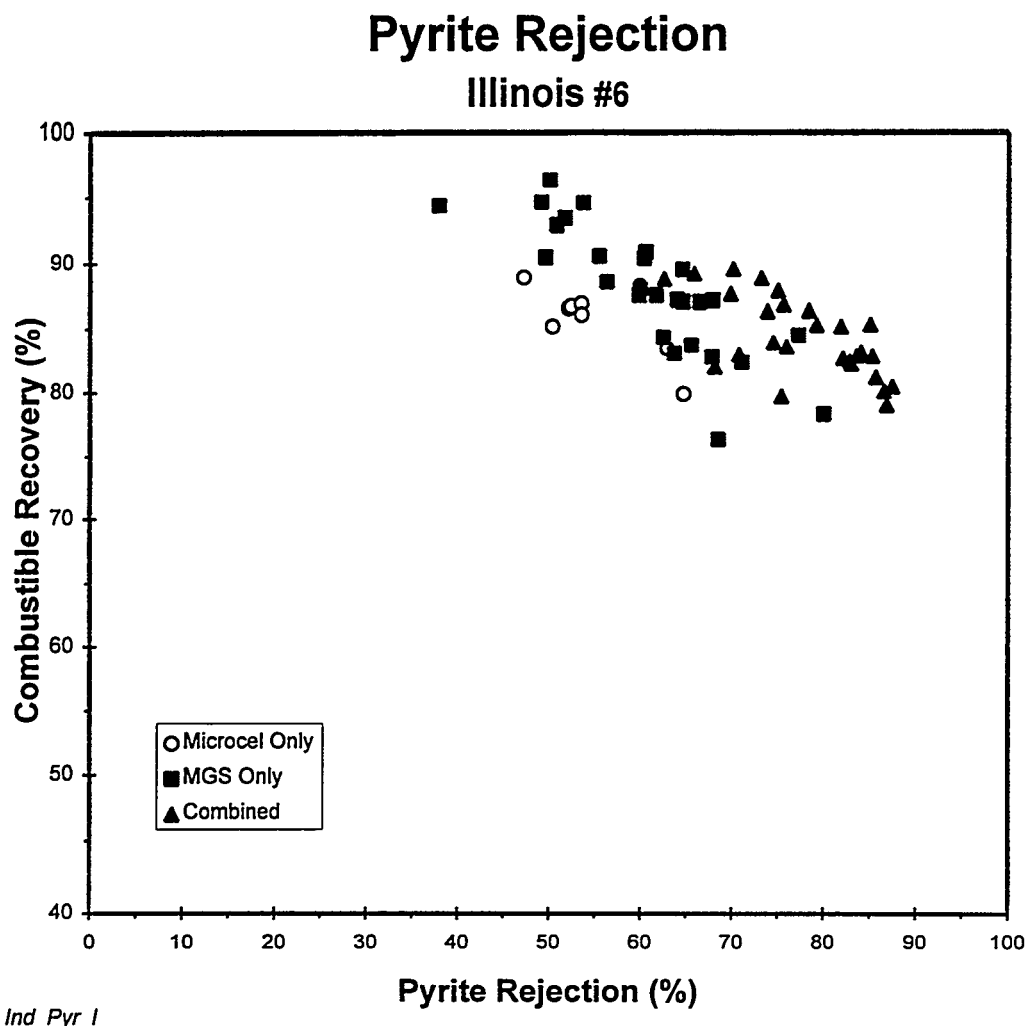


Figure 52. Combustible recovery versus pyritic sulfur rejection for run-of-mine Illinois #6 seam coal.

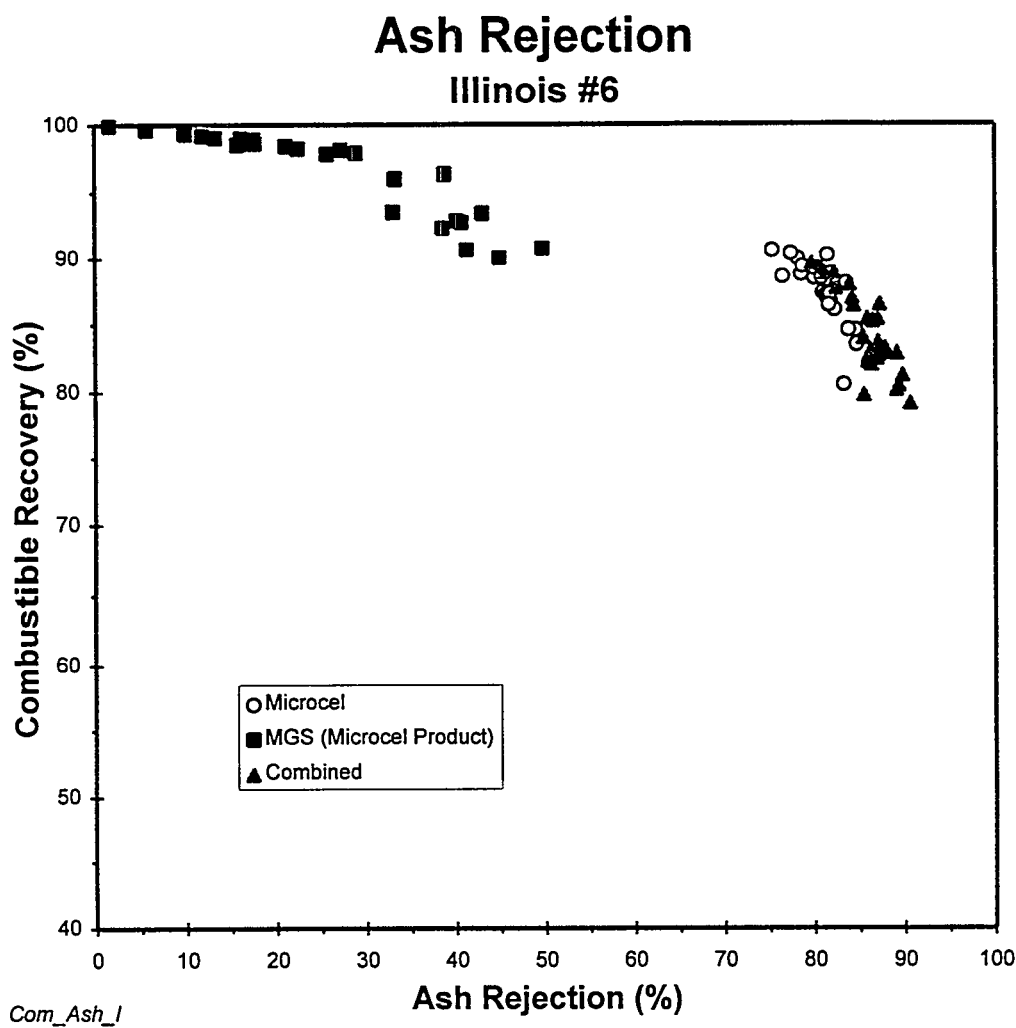


Figure 53. Combustible recovery versus ash rejection for each unit of the combined circuit.

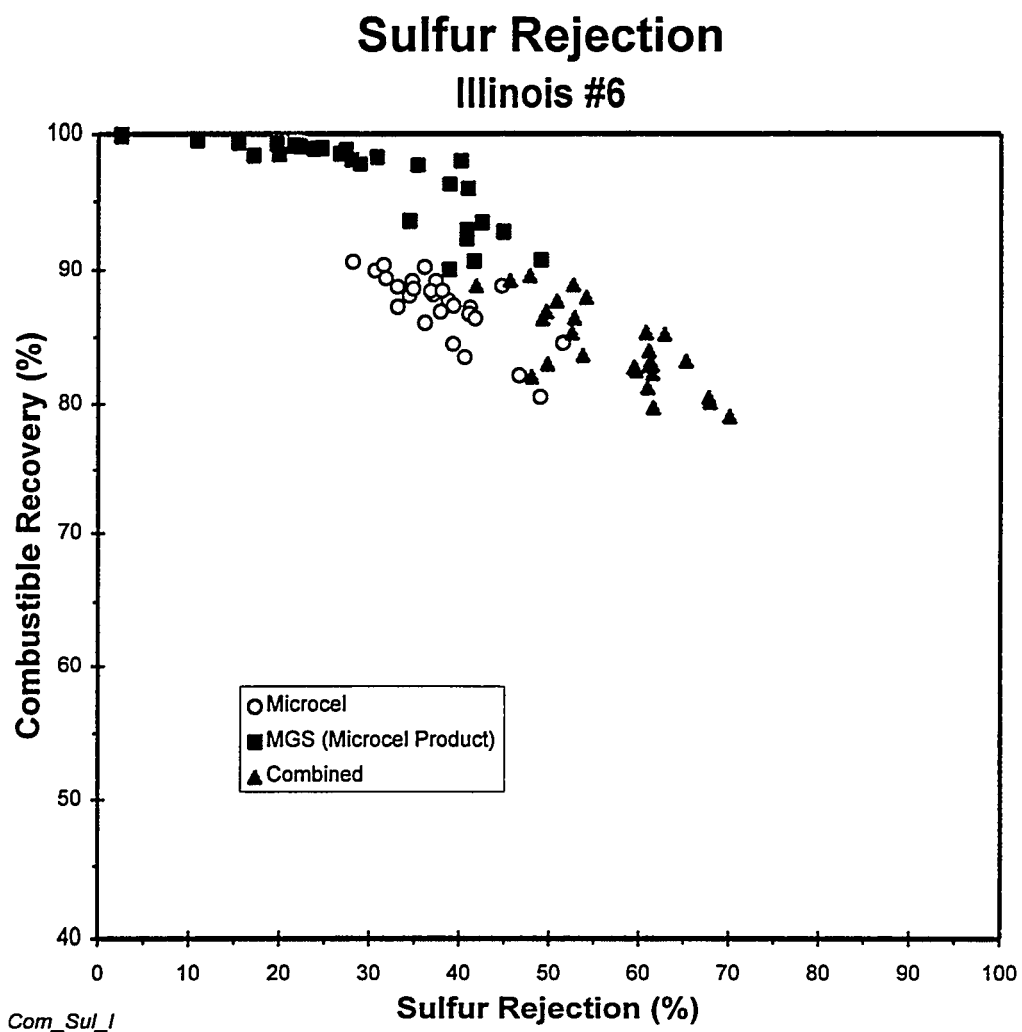


Figure 54. Combustible recovery versus total sulfur rejection for each unit of the combined circuit.

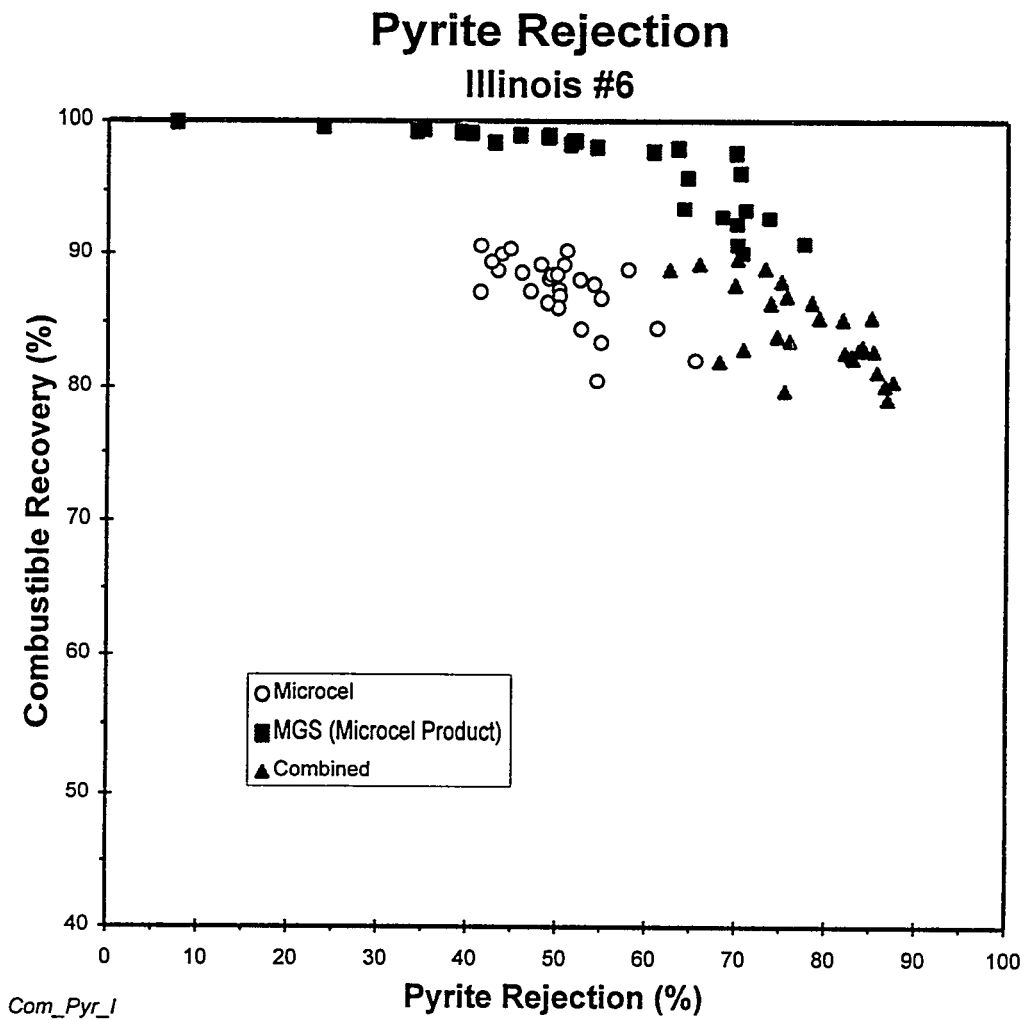


Figure 55. Combustible recovery versus pyritic sulfur rejection for each unit of the combined circuit

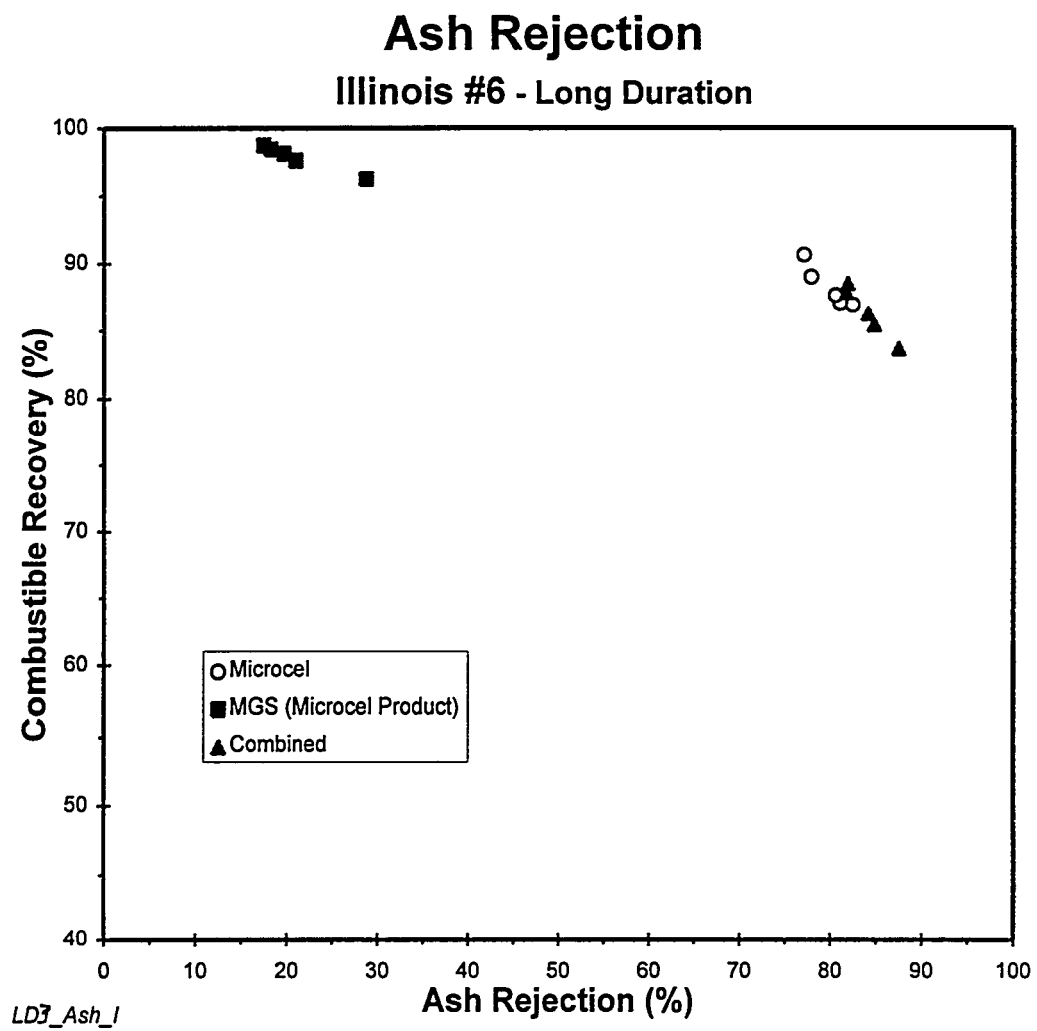


Figure 56. Combustible recovery versus ash rejection for each unit of the combined circuit during long duration testing.

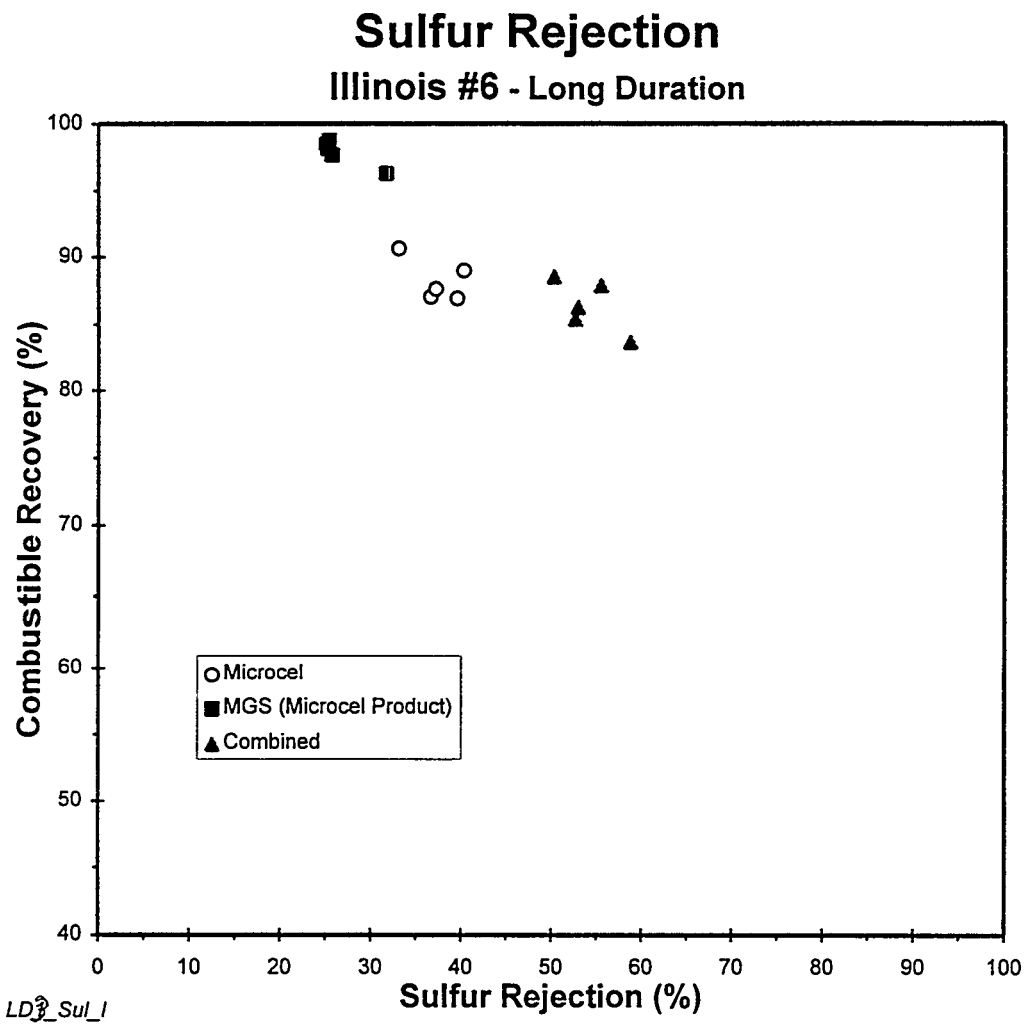


Figure 57. Combustible recovery versus total sulfur rejection for each unit of the combined circuit during long duration testing.

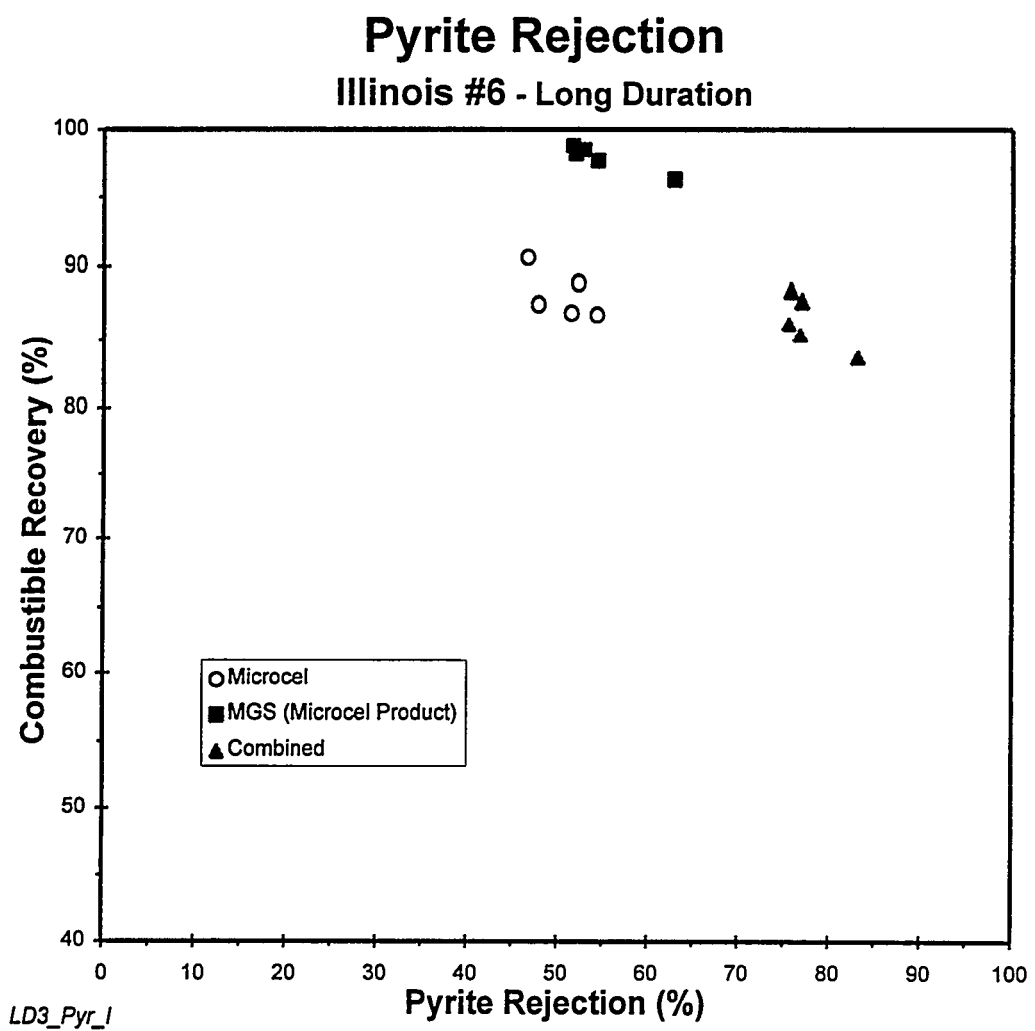


Figure 58. Combustible recovery versus pyritic sulfur rejection for each unit of the combined circuit during long duration testing.

The capabilities of the MGS are best illustrated by the data shown in Figures 59 and 60. These plots show the pyritic sulfur and ash contents of the clean coal products obtained during the parametric test programs. As shown, the test data obtained using froth flotation fall into the low-ash/high pyritic sulfur region of the plots. This indicates a preferential removal of ash-forming minerals using the surface-based separation technique. On the other hand, the data obtained using the MGS (i.e., density-based separation process) fall in the high-ash/low-pyritic sulfur region of the plots. This suggests that the MGS removes high-density pyrite in preference to other ash-forming minerals. Pyrite may also be difficult to reject by surface-based processes because of the formation of hydrophobic oxidation products which makes the mineral floatable. However, the data shown in Figures 59 and 60 suggest that it is possible to take advantage of the benefits of both surface- and density-based separation techniques by precleaning the MGS feed coal using froth flotation. As shown, this two-stage processing strategy can provide a low-ash/low-sulfur coal product without micronizing the feed coal to ultrafine sizes.

No major technical deficiencies were noted as a result of the integration of the Microcel and MGS units. Excessive frother dosages in the Microcel did not have an adverse impact on the performance of the MGS as originally feared since any residual coal-laden froth which remained stable when fed to the MGS floated on the surface of the flowing film and reported to the clean-coal product. Also, no technical deficiencies are expected upon the transfer of this MGS technology into the commercial sector. Although relatively small in size compared to full-scale industrial units, all of the unit operations used in this project were commercial-scale equipment, i.e., no prototype devices were used. The Microcel and MGS units, as well as ancillary equipment, are readily available and currently operating in larger sizes. The capacity of the pilot-scale MGS unit was also found to be adequate to handle the desired flow rate of clean-coal slurry from the Microcel unit. However, additional demonstration tests using full-scale MGS units may be warranted to ensure that the industrial units are capable of achieving the desired production capacity without diminishing the separation efficiency.

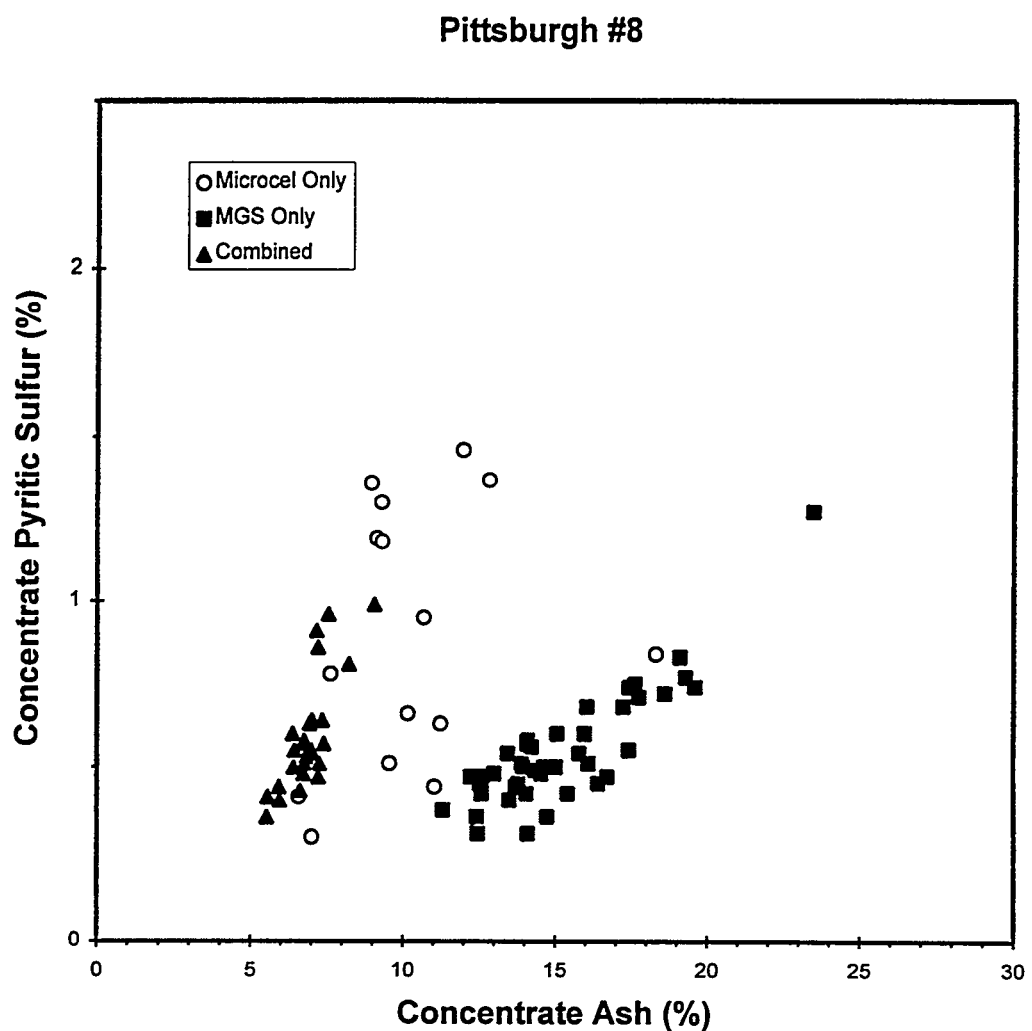


Figure 59. Concentrate sulfur versus ash content obtained during the parametric testing of the Pittsburgh No. 8 seam coal.

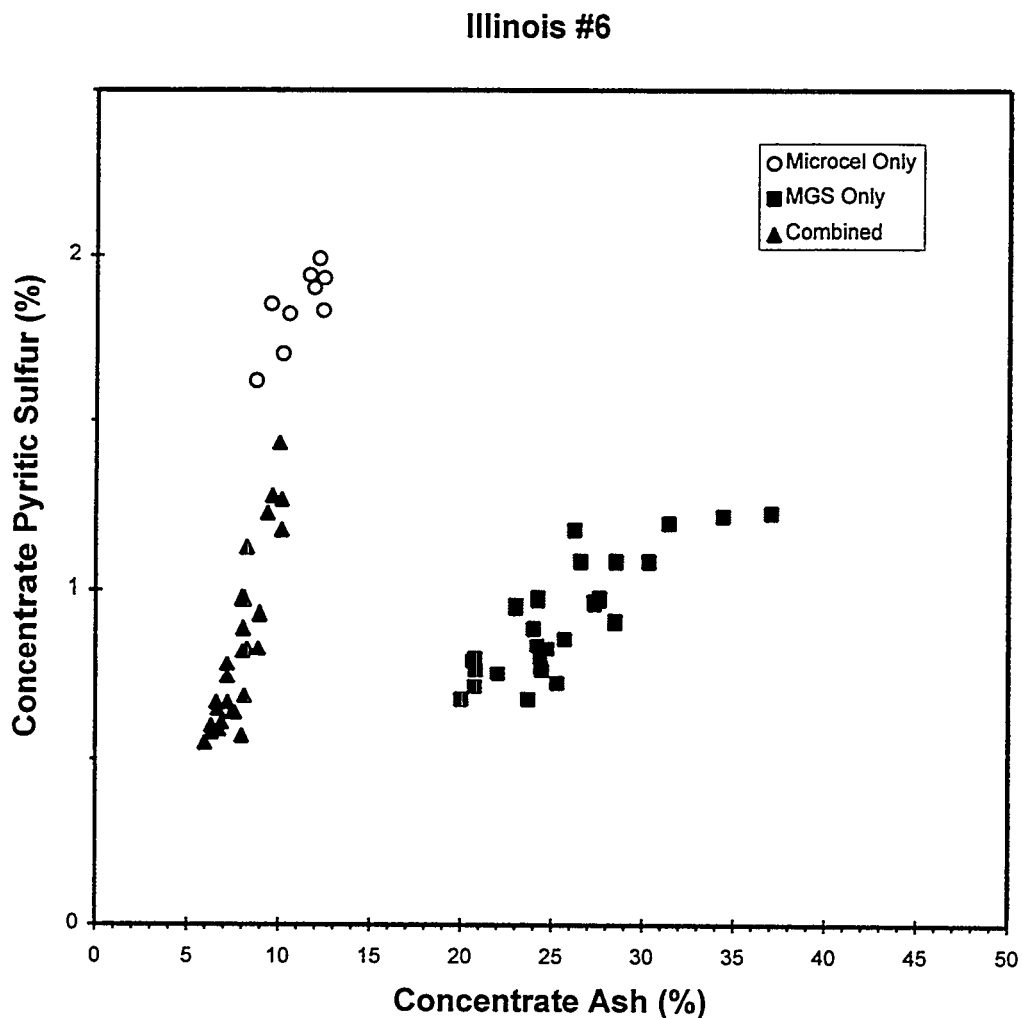


Figure 60. Concentrate sulfur versus ash content obtained during the parametric testing of the Illinois No. 6 seam coal.

## 13.2 Economic Evaluation

The technical evaluation demonstrates that the cleanability of fine-coal streams can be significantly improved through the use of circuit configurations which incorporate the Microcel and MGS technologies. However, an economic evaluation must be carried out in conjunction with the technical evaluation in order to establish the near-term commercialization potential of the various circuit configurations.

The economic evaluation conducted in the present work assumes that the Microcel and/or MGS units have been installed to upgrade fine coal at an existing preparation plant. This scenario is believed to be the most promising near-term application of these technologies. The analyses assume that the Microcel and MGS circuits would be added to an existing plant in which the fine coal is currently being discarded. Experimental data obtained from the testing of the Pittsburgh No. 8 and Illinois No. 6 seam coals has been used to provide the necessary input data for the economic analyses. For each coal, cost-benefit analyses were performed for full-scale circuits incorporating the Microcel alone, the MGS alone and the combined Microcel/MGS circuit. For the purpose of this study, the feed rate to the fine coal circuit has been assumed to be 75 tph. The fine coal circuit has been assumed to operate two 8-hour shifts per day for 250 days per year, i.e., 3600 hr/yr, with an on-line availability of 90%. The relevant performance data and associated economic calculations for each of the two base coals are summarized in Appendices 9-A and 9-B.

### *13.2.1 Estimation of Capital Costs*

In order to estimate the capital costs of the proposed circuits, preliminary scale-up projections were made for the Microcel and MGS units. These calculations indicated that four 10-ft diameter Microcel columns and four 5-ft diameter MGS units would be required to achieve the desired production rates. The cost of each Microcel unit, including associated instrumentation and controls, has been estimated to be \$110,000. Likewise, the cost of each MGS unit has been assumed to be \$120,000. These estimates are believed to be very conservative. In addition to these coal cleaning units, several ancillary operations were also included in the listing of capital costs. These included a single 1000 scfm air compressor (\$90,000), two screen-bowl centrifuges (\$175,000 each), and miscellaneous sumps and pumps (<\$45,500). An additional capital outlay of \$10,000 was allocated to cover heat/lighting. Total installed cost was estimated by multiplying the total equipment cost by a factor of two. This estimation procedure is routinely used by local fabricators located in the coal fields. Other costs considered in the capital estimation included a 10% fee for engineering/permitting and an overhead rate of 20%.

### *13.2.2 Estimation of Operating Costs*

Annual operating costs were estimated for power consumption, equipment maintenance, personnel and miscellaneous consumables (i.e., reagents, lubricants, etc.). Electrical power consumption was estimated for the Microcel columns (4 @ 60 HP), MGS units (4 @ 10 HP), air compressor (150 HP), screen-bowl centrifuges (2 @ 250 HP), feed pumps (40 HP), product pumps, (30 HP), reagent feeders (<0.5 HP) and heat/light (60 HP). For primary unit operations, a power load factor of 80% was used to estimate actual power requirements, while a power factor of 15% was used for heat/light and small reagent pumps. Power costs were estimated at an industrial rate of \$0.05/kW-hr.

The various plant circuits were assumed to require a part-time operator (\$35,000/yr) and part-time mechanic/electrician (\$45,000/yr) for each working shift. Personnel benefits were estimated as 50% of the base salary. The utilization of manpower required for operation and maintenance of the fine coal circuitry was adjusted between 10%-50% depending on the complexity of the circuit configuration.

The major consumable items included in the annual operating costs were the flotation reagents (i.e., frother @ \$0.86/lb and fuel oil collector @ \$0.11/lb). An additional \$0.05/ton of feed was also allocated to account for incremental increases in water clarification costs that may be associated with the operation of the proposed circuits (i.e., 300 gpm for each column and 10 gpm for each MGS). Annual equipment maintenance costs were estimated as 10% of the total capital cost of the proposed circuitry.

### *13.2.3 Cost-Benefit Analysis*

Cost-benefit analyses were conducted for each circuit over an effective life span of 20 years. An inflation rate of 4% was assumed and that no debt was carried forward after the first year of operation (i.e., no loan was necessary to cover the capital expenditure). Tax payments were estimated using a 20 year depreciation period and 38% corporate tax rate. In addition, additional payments were made at a rate of 6.5% for coal royalties and 6.7% for miscellaneous taxes/fees (4.5% severance tax, 1% black lung tax and 1.2% reclamation fees). A straight-line depreciation schedule was assumed in each case. A discount rate of 10% was assumed in calculating the rate-of-return on the capital investment.

The value of the various coal products was calculated by pro-rating a base market value of \$1.30/MM Btu at 10-12% ash and 0.75 % sulfur. Significant differences in ash or sulfur resulted in changes to the base value (i.e. higher sulfur or ash meant lower value per MM BTU). In addition, the total heating value of the shipped products was also reduced to account for differences in final product moisture contents. Shipping costs were estimated to be \$10/ton of clean coal for this particular case study. Mining costs (i.e., the cost of fine feed coal) were not considered in the economic analysis since the fines were assumed to be discarded at present.

The results of the cost-benefit analysis for the Pittsburgh No. 8 seam coal are summarized in Table 28. Details related to the economic analyses are provided in Appendix 9-A. As shown, the MGS unit had the lowest overall costs in terms of cost per ton of ash and SO<sub>2</sub> removed (i.e., \$15.26 and \$44.23, respectively). Unfortunately, the ash content of the MGS product was higher (i.e., 14.1%) than that normally desired by electric utilities. As a result, the product from the MGS carried a substantial coal quality penalty which made it less marketable under existing coal pricing structures. The anticipated market premium for the reduced sulfur content obtained using the MGS circuitry has not been realized in the current coal pricing structure. On the other hand, the froth product from the Microcel had an ash content of only half that of the MGS (6.98% versus 14.1%). In addition, the Microcel was reasonably good at reducing the sulfur content of this particular coal. The improved marketability of the coal produced by the Microcel resulted in this unit having the best overall return on the capital investment. In this particular case study, the Microcel installation offered a 77% internal rate of return and a corresponding payback period of less than 17 months (1.37 years). Because of the high capital costs associated with the installation of two-stage circuits, the combined Microcel/MGS configuration had the lowest overall return on investment.

Table 29 provides a summary of the cost-benefit analysis for the Illinois No. 6 seam coal. Details related to the economic analyses are provided in Appendix 9-B. As expected, the MGS unit again had the lowest overall costs in terms of cost per ton of ash and sulfur removed. However, despite the low cost of sulfur removal achieved by the MGS (i.e., \$36.54/ton of SO<sub>2</sub> removed), this particular circuit configuration was found to be uneconomical due to the inability of the MGS to lower the product ash below 25%. Of the two remaining alternatives, the Microcel circuit was found to be most attractive in terms of rate-of-return (36.7%) and payback period (<37 months). A slightly lower rate of return (29.9%) and longer payback period (45 months) was calculated for the combined Microcel/MGS circuit.

Various coal cleaning technologies are frequently compared with each other on the basis of \$/ton of SO<sub>2</sub> removed. Figure 61 shows a plot of \$/ton of SO<sub>2</sub> removed vs. % pyrite rejection for various coal cleaning processes. The conventional coal cleaning devices such as jigs and dense-medium separators show the lowest costs but the pyrite rejections are only 49 and 55%, respectively. These estimates were made for the Pittsburgh No. 8 coal based on the washability data reported by Cavallaro et al.<sup>1</sup> and the typical partition curves obtained for jigs and dense-medium separators. Advanced coal cleaning processes show significantly improved pyrite rejections over the conventional processes; however, the costs are in the \$243-327/ton range. These costs are comparable to those for flue-gas scrubbing, which are reported to be in the \$250-350/ton range. The advanced coal cleaning costs used in Figure 61 are listed as follows:

<sup>1</sup> Cavallaro, J.A., Deurbrouck, A.W., Killmeyer, R.P., Fuchs, W. and Jacobsen, P.S., 1990, Sulfur and Ash Reduction Potential and Selected Chemical and Physical Properties of United States Coals, Volume I - Eastern Region, U.S. Department of Energy Report No. DOE/PETC/TR-90/7 (DE91001737), 1226 pp.

- Pittsburgh No. 8 coal by oil agglomeration after ball mill grinding to 74  $\mu\text{m}$  top size; \$284/ton SO<sub>2</sub> removed; 200 TPH plant case (Feeley et al., 1994)<sup>2</sup>
- Illinois No. 5 coal by oil agglomeration after ball mill grinding to 150  $\mu\text{m}$  top size; \$243/ton SO<sub>2</sub> removed; 200 TPH plant case (Feeley et al., 1994)<sup>2</sup>
- Pittsburgh No. 8 coal by Microcel™ flotation column after ball mill grinding to 80% finer than 74  $\mu\text{m}$ ; \$327/ton SO<sub>2</sub> removed; 200 TPH plant case (Ferris et al., 1994)<sup>3</sup>
- Illinois No. 6 coal by Microcel™ flotation column after ball mill grinding to 80% finer than 74  $\mu\text{m}$ ; \$305/ton SO<sub>2</sub> removed; 200 TPH plant case (Ferris et al., 1994)<sup>3</sup>

These costs are compared in Figure 61 with those obtained in the present work for using the combined Microcel™/MGS circuit:

- Pittsburgh No. 8 coal; \$158/ton of SO<sub>2</sub> removed (Table 28)
- Illinois No. 6 coal; \$77/ton of SO<sub>2</sub> removed (Table 29)

These costs are substantially lower than those that result when coal is ground to a fine size in a ball mill (to achieve a higher degree of pyrite liberation) and then cleaned by advanced flotation or oil agglomeration. There are two major reasons for the cost savings. First, the combined circuit eliminated the cost associated with fine grinding. Second, because of its ability to remove pyrite at coarser sizes, the cost of dewatering is significantly reduced.

In summary, the cost-benefit analyses conducted in the present work indicate that all of the test circuits evaluated under this program have a very good rate-of-return (30-77%) and short payback period (16-46 months). The only apparent exception is the processing of the Illinois No. 6 seam coal by the MGS alone. Surprisingly, the most attractive circuit configuration in terms of return on investment was found to be the Microcel column. The advantage of this technology is its ability to achieve high ash reductions which provide the largest market premiums. In fact, the MGS was superior to the Microcel in terms of desulfurization performance, although current coal pricing structures made this technology somewhat less attractive in terms of return on investment. The combined Microcel/MGS circuit was also financially attractive, yielding internal rates of return on the order of 30-50%. These margins are expected to improve as additional market premiums are realized for low-ash and low-sulfur coal products.

<sup>2</sup> Feeley, T.J., Barnett, W. P. and Hucko, R.E., 1994, Advanced Physical Coal Cleaning for Controlling Acid Rain Emissions, 12th International Coal Preparation Congress, May 23-27, Cracow, Poland, pp. 369-378.

<sup>3</sup> Ferris, D.D., Bencho, J.R. and Torak, E.R., 1995, Engineering Development of Advanced Froth Flotation, Executive Summary - Final Report for Contract DE-AC22-88PC88881 (U.S. Dept. of Energy), ICF Kaiser Engineers, Inc., Pittsburgh, Pennsylvania.

Table 28. Cost-Benefit Analysis for the Pittsburgh No. 8 Seam Coal.

Cost Indicator	Microcel Only	MGS Only	Microcel/MGS Combined
Production Cost: (\$/ton clean coal)	\$4.04	\$1.88	\$5.15
Removal Cost: (\$/ton ash) (\$/ton sulfur) (\$/ton SO <sub>2</sub> )	\$22.50 \$517.95 \$259.97	\$15.26 \$88.46 \$44.23	\$24.88 \$407.87 \$158.16
Economic Indicators:			
Rate of Return	77.0%	55.1%	50.2%
Payback Period	1.37 yrs	1.95 yrs	2.16 yrs

Table 29. Cost-Benefit Analysis for the Illinois No. 6 Seam Coal.

Cost Indicator	Microcel Only	MGS Only	Microcel/MGS Combined
Production Cost: (\$/ton clean coal)	\$4.97	\$2.14	\$6.61
Removal Cost: (\$/ton ash) (\$/ton sulfur) (\$/ton SO <sub>2</sub> )	\$11.56 \$161.51 \$80.76	\$9.92 \$73.08 \$36.54	\$12.66 \$153.64 \$76.82
Economic Indicators:			
Rate of Return	36.7%	NA	29.9%
Payback Period	3.03 yrs	NA	3.78 yrs

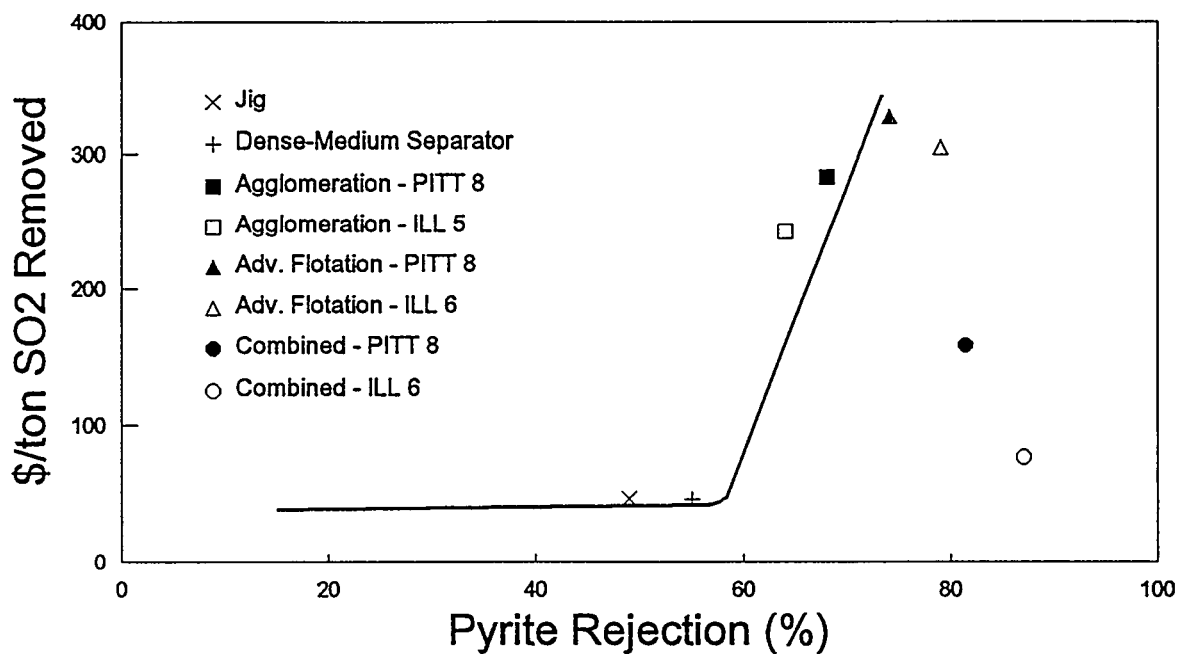


Figure 61. Cost of SO<sub>2</sub> removed versus pyrite rejection for several traditional and advanced cleaning circuits.

### 13.3 Final Report

After completing the primary project work elements, a draft final report was prepared and submitted to the DOE COR. Following review by DOE, the draft report was revised and submitted as the final project report. This document is the product of this effort.

## CONCLUSIONS

This project consisted of combining the Microcel flotation column with the Multi-Gravity Separator (MGS) for high ash and pyritic sulfur rejection. This concept proved very successful since overall ash and pyritic sulfur rejections of 75%, and a 90% combustible recovery, were consistently achieved on the Pittsburgh No. 8 seam coal. On the Illinois No. 6 coal, pyritic sulfur rejections over 75% and combustible recoveries of over 85% were achieved. The consistency of the long-duration results indicate the ease and reliability of the operation of the combined Microcel/MGS circuit.

Based on the success of this project the combined circuit can be considered ready for a larger-scale demonstration and possibly commercial application. Its success elsewhere would obviously be dependent upon the liberation and nature of the pyritic sulfur. If flotation release analysis testing yields significant pyritic sulfur in the concentrate then gravity separation for the concentrate should be investigated. In-plant testing at existing coal preparation plants should be the next step considered. Several small- or medium-sized column and gravity separator units are available and could be utilized for determining applicability and performance at specific preparation plants. The relative portability of these units allows for actual plant testing without major installation expense.

Combining a column flotation device with a fine-particle gravity separator is now ready to be evaluated in the commercial sector. The units tested were not laboratory prototypes but were small versions of commercially available machines. The Microcel is currently producing coal in several coal preparation plants as are other brands of flotation columns. Several mineral sands processing plants are currently operating MGS units and a large unit for coal (i.e., 20-25 tph) is currently available. There are at least three other brands of centrifugal fine-particle gravity separators also available, although at this writing none are currently in full-scale production on coal. Pilot size units can be tested at minimal cost within a coal preparation plant to verify performance results for specific coals.

Due to the inefficiencies of most gravity separators in the near 100 mesh (150 micron) range, the success of column flotation should cause coarser sizes than 100 mesh to be considered for flotation. Sizing at 48 mesh would make desliming ahead of spirals or heavy media much more efficient. Pushing more of the slimes to the column and utilizing its wash water would decrease the plant product ash without a significant effect on yield. When high pyritic sulfur is encountered then the fine gravity separator could be considered to remove the high density pyrite.

In summary, the testing of the Microcel/MGS circuit was very successful and demonstrated the potential to remove ash and pyritic sulfur while maintaining a high energy recovery. Thus, the primary objective of the project, i.e., to demonstrate the synergistic advantages of this circuit at a continuous-scale, was successfully met. In addition, the secondary

objectives of the project were all achieved. The performance of each unit operation, individually and combined, was optimized by conducting parametric studies. This work allowed operating conditions to be identified that maximized the rejections of pyritic sulfur and ash while maintaining a high energy recovery. In addition, the steady-state performance of the optimized processing circuit was evaluated by conducting two different series of long-duration test runs with the Pittsburgh No. 8 and Illinois No. 6 seam coals. Finally, detailed technical and economic evaluations were conducted to examine the feasibility of the proposed concept for fine-coal cleaning on an industrial scale. This analysis suggests that the proposed circuit is technically feasible for commercial application and economically attractive in today's coal market.